Technical Report

440

Design of Transmission Lines and Waveguide Structures Using the Maximum Principle

J. Burchfiel

5 June 1968

Lincoln Laboratory

MASSACHUSETTS INSTITUTE OF TECHNOLOGY

Lexington, Massachusetts

MASSACHUSETTS INSTITUTE OF TECHNOLOGY

LINCOLN LABORATORY

DESIGN OF TRANSMISSION LINES AND WAVEGUIDE STRUCTURES USING THE MAXIMUM PRINCIPLE

J. BURCHFIEL

Group 42

TECHNICAL REPORT 440

5 JUNE 1968

LEXINGTON MASSACHUSETTS

DESIGN OF TRANSMISSION LINES AND WAVEGUIDE STRUCTURES USING THE MAXIMUM PRINCIPLE*

ABSTRACT

A distributed parameter maximum principle provides the basis for design of optimal lossless impedance matching structures. Given an arbitrary (wide-band) source at $z = -\ell$ and an arbitrary load at $z = 0$, the optimization procedure synthesizes a uniform cross section, dielectric loaded waveguide or transmission line of length ℓ which maximizes the real power delivered to the load.

This optimization is performed subject to constraints on the filler material: $\mu(z) \equiv \mu_0$ and $\epsilon(z)$ is in $\{\epsilon_1, \epsilon_2, \ldots \epsilon_n\}$. The solution is easily implemented, as the filler consists of successive intervals of readily available dielectric materials.

An iterative numerical procedure for solving the (split-boundary function) necessary conditions is given, and a number of typical solutions for transmission line and waveguide couplers are presented. In the examples studied, the performance obtained using only ϵ_{MIN} and ϵ_{MAX} was within 0.2 percent of that obtained using a continuum of dielectric constants $[\epsilon_{MIN}, \epsilon_{MAX}]$.

Accepted for the Air Force
Franklin C. Hudson
Chief, Lincoln Laboratory Office

---

*This report is based on a thesis of the same title submitted to the Department of Electrical Engineering at the Massachusetts Institute of Technology on 19 February 1968 in partial fulfillment of the requirements for the degree of Doctor of Science.

CONTENTS

SUMMARY

This research is based on the application of the results of the maximum principle to the design of optimal transmission line and waveguide structures.

The systems considered are a lossless TEM (transmission line) structure and a lossless TE (waveguide) structure. The solution sought for the transmission line is the optimal distribution along the line for the capacity per unit length, $C(z)$, $z \in [-\ell, 0]$, when the inductance $L(z) \equiv L_o$ is constant. This solution may be implemented by filling a uniform TEM structure with a dielectric material having a varying $\epsilon(z)$. In the waveguide, we seek the optimal dielectric filler material, i.e., the permittivity $\epsilon(z)$ for $\mu(z) \equiv \mu_o$.

The cost functional, to be minimized in this process of optimal design, measures how effective a "match" the electromagnetic structure provides between an arbitrary (wide-band) source at $z = -\ell$ and an arbitrary load at $z = 0$. This cost is the total power reflected due to impedance mismatch; since the structures are lossless, minimizing this reflected power maximizes the power delivered to the load.

This minimization process is performed subject to the constraint that $C(z) \in \{C_1, C_2, \ldots C_n\}$, or $\epsilon(z) \in \{\epsilon_1, \epsilon_2, \ldots \epsilon_n\}$. This constraint insures that the solution is practical to implement, as it only requires successive intervals of dielectric filler material having readily available dielectric constants.

Necessary conditions for optimality of the solution [$C(z)$ or $\epsilon(z)$] are stated in the form of a distributed parameter maximum principle. (The systems of interest are distributed over both spatial and frequency domains.) Application of this principle to the TEM or TE system yields a pair of coupled partial differential equations with split boundary-function conditions. An iterative numerical procedure for solving these equations is given, and a number of typical solutions for transmission line and waveguide couplers are presented.

A practical design example was selected to demonstrate the use of this technique: an impedance match is desired between narrow slots forming a phased array receiving antenna and stripline receivers inserted in the waveguides which connect to the slots.

The small height of the waveguides and their slot openings (chosen to fit the stripline) results in a severe mismatch between the characteristic impedance of the wave guided in the waveguide and the free space wave beyond the surface of the phased array; the VSWR is greater than 20:1 across the band at boresight for the slot pattern under consideration, leaving room for over 7 db of improvement by effective impedance matching.

The method used in this investigation is an iterative, numerical technique based on the Maximum Principle of Pontryagin, and coded in FORTRAN for execution on a digital computer.

The results were as follows: filling the waveguide as indicated with successive intervals of quartz ($\epsilon = 3.78\,\epsilon_o$) and alumina ($\epsilon = 9\,\epsilon_o$) over a distance of 1.15 inches, reduced the VSWR (power-averaged across the band) from 20:1 to 5.4:1, reducing reflection losses from 7.5 to 2.7 db.

When the available dielectrics range between ϵ_{MIN} and ϵ_{MAX} the reflected power cost showed negligible improvement with the addition of more available intermediate dielectric values: the performance using only $\{\epsilon_{MIN}, \epsilon_{MAX}\}$ was within 0.2 percent of that obtained using a continuum of dielectric constants $\{[\epsilon_{MIN}, \epsilon_{MAX}]\}$.

This iterative solution required about 10 minutes of run time on an IBM 360/65, showing very poor convergence from a simple-minded initial guess because of the Newton-Raphson iterative technique employed. Attempts to obtain a better match using higher-ϵ materials and a longer length of waveguide failed to converge in a reasonable length of time.

Changing from a Newton-Raphson iterative technique to a steepest descent gradient method will considerably improve the convergence properties of the iteration. Once the procedure is appropriately recoded, it is predicted that a fairly good impedance match solution (VSWR < 1.5) can be obtained using reasonable lengths of waveguide ($\approx$3 inches) and reasonable dielectric materials (e.g., $\epsilon \sim 16\,\epsilon_o$).

DESIGN OF TRANSMISSION LINES AND WAVEGUIDE STRUCTURES USING THE MAXIMUM PRINCIPLE

I. INTRODUCTION

A. PROBLEM STATEMENT

The goal of this research is to apply the results of the maximum principle of Pontryagin to the design of optimal lossless transmission line and waveguide coupling structures.

The systems to be considered are a lossless TEM (transverse electro-magnetic, i.e., transmission line) structure and a lossless TE (transverse electric, i.e., waveguide) structure. The solution sought for the transmission line is the optimal distribution along the line for the inductance $L(z)$ and capacity $C(z)$ per unit length. In the waveguide, we seek the optimal choice of materials filling the waveguide, i.e., the permeability $\mu(z)$ and the permittivity $\epsilon(z)$ for $z\epsilon\ [-\ell, 0]$.

The results of the maximum principle are generally stated in the context of an optimal control problem where time is the independent variable and an optimal control vector u is sought (as a function of time) which minimizes a cost functional dependent on $u(t)$ and $x(t)$, the state of the controlled system for $t\epsilon\ [t_o, T]$.

We will, instead, choose a one-dimensional space variable $z\epsilon\ [-\ell, 0]$ as the independent variable, and seek an optimal parameter vector u as a function of position z which minimizes a functional on the $u(z)$ and the system state $x(z)$.

The cost functional to be minimized in each example will measure how effective a "match" the electromagnetic structure provides between an arbitrary source at $z = -\ell$ and an arbitrary load at $z = 0$ for a given signal. Specifically, let the source be a transmitter with impedance $Z_s(\omega)$ with spectral power density $S(\omega)$ as the "available" power density (power per unit frequency which could be delivered into a perfectly matched load), let the load at $z = 0$ be an arbitrary impedance $Z(\omega)$ (viz., an antenna) and let the reflection coefficient[1] looking into the electromagnetic coupler at $z = -\ell$ be called $\rho(\omega, -\ell)$. Of course, this reflection coefficient is a function of both the impedance of the source and the impedance presented by the coupler. Then the total power reflected back into the source (not transmitted from the antenna) is

$$J = \int S(\omega)\left|\rho(\omega, -\ell)\right|^2 d\omega \quad . \tag{1-1}$$

If we normalize the source to 1 watt ($\int S(\omega)\, d\omega = 1$), J is also a direct measure of the fractional power lost (reflected back into the source) when a particular structure is used to match between the source and an arbitrary load. This is the functional on the $L(z)$, $C(z)$, $[u(z), \epsilon(z)]$ parameters which we wish to minimize by finding the optimal parameter distribution $L^*(z)$, $C^*(z)$ $[u^*(z), \epsilon^*(z)]$ for $z\epsilon\ [-\ell, 0]$.

The design example considered during this research involves a phased array receiving antenna consisting of narrow slots distributed in a uniform pattern over a plane surface. Each slot forms the mouth of a waveguide which terminates in a coupling to a stripline having the same height and width as the waveguide; integrated circuit receiving electronics is embedded in the stripline receiving structure.

This antenna operates over the band 5 to 5.5 Gc, using waveguide 0.125 × 0.9 inch in cross section. The small height (chosen to fit the stripline) results in a severe mismatch between the characteristic impedance of the wave guided in the waveguide and the free space wave beyond the surface of the phased array; the VSWR is greater than 20:1 across the band at boresight for the slot pattern under consideration, leaving room for over 7 db of improvement by effective impedance matching.

The method used in this investigation is an iterative, numerical technique based on the Maximum Principle of Pontryagin, and coded in FORTRAN for execution on a digital computer.

The solution obtained lies in the choice of dielectric materials which fill successive intervals of the waveguide in order to maximize the total (wide-band) power delivered to the stripline receiver.

B. BACKGROUND

1. Theoretical Limitations on Impedance Matching

A great deal of effort has been devoted to the problem of wide-band impedance matching in the last 20 years; we will attempt to survey some of the most important results available in the literature.

The problem under consideration is shown in Fig. 1-1: given an arbitrary load impedance Z_L and a 1-ohm resistive source, we want to find a lossless coupling network which maximizes the real power delivered from the source into the load. It can easily be shown that this power is maximized when the impedance Z of Fig. 1-1 (the impedance seen "looking into" the lossless network) is equal to 1 ohm, hence the expression "matching" impedances. Unfortunately, it is in general impossible to obtain the perfect match Z = 1 ohm over a band of frequencies; we can only make Z approximate 1 ohm over a band, with perhaps Z exactly equal to 1 ohm at a finite number of distinct frequencies within the band.

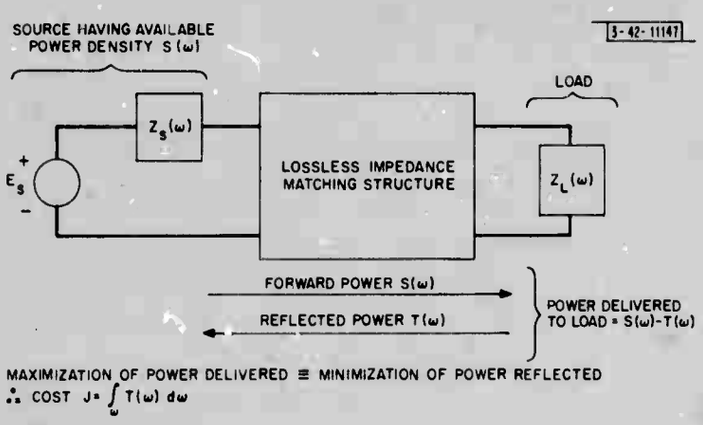

Fig. 1-1. Basic impedance matching problem.

A precise measurement of the quality of our "approximate match" over the frequency band is needed: the quality measurement we choose is the fractional power reflected:

$$1 - P_L/P_o = |\rho|^2 \tag{1-2}$$

where P_L is the actual power delivered into the load and P_o is the available power of the source, i.e., the power which could be delivered into an ideal 1-ohm load.

ρ is the reflection coefficient defined by

$$\rho = (Z - 1)/(Z + 1) \quad (-1 < \rho < 1) \quad . \tag{1-3}$$

To minimize the reflected power, we want to keep $|\rho|^2$ small over the frequency band of interest.

The first general theoretical results for such a problem were obtained by H. W. Bode[2] when he dealt with the problem of impedance matching between a parallel R-C circuit (load) and a resistive source by means of a lossless coupling network. The fundamental limitation on the performance of such a coupling network was shown to be

$$\int_0^\infty \ln \frac{1}{|\rho|} \, d\omega < \frac{\pi}{RC} \tag{1-4}$$

where ρ is the reflection coefficient corresponding to the impedance Z in Fig. 1-1.

If $|\rho|$ is kept constant and equal to $|\rho|_{max}$ over a frequency bandwidth of W radians/second, and is made unity over the rest of the frequency spectrum (total power reflection) then Bode's integral constraint reduces to

$$W \ln \frac{1}{|\rho|_{max}} < \frac{\pi}{RC} \tag{1-5}$$

i.e., the fractional power in the frequency band lost through mismatch (reflection back into the source) is greater than, or equal to, $\exp -(2\pi/WRC)$. Clearly, this loss can be reduced to zero when the bandwidth W is reduced to zero, but for a nonzero bandwidth it is impossible to obtain a perfect match.

R. M. Fano[3] extended the analysis of theoretical limitations on broadband matching to arbitrary load impedances specified in terms of their complex poles and zeros. He obtained integral constraints of the form:

$$\int_0^\infty P(\omega) \ln \frac{1}{|\rho|} \, d\omega = F(s_1, s_2, \ldots s_n) \tag{1-6}$$

where $P(\omega)$ is a ratio of polynomials in ω, ρ is again the reflection coefficient corresponding to Z of Fig. 1-1, and s_i ($i = 1, 2, \ldots n$) are the complex poles and zeros of the load impedance. These integral equations express the conditions of physical realizability of the matching network, and, like Bode's integral constraint, yield useful information on the tolerance and bandwidth of possible match.

Fano next made the point that when we are equally concerned about power transfer at every frequency in a band W, and not at all concerned about matching outside this band, the best choice for $|\rho(\omega)|$, subject to the integral constraint on $\ln 1/|\rho|$, is

$$|\rho(\omega)| = \begin{cases} \rho_{max} & \text{for } \omega \epsilon W \\ 1 & \text{for } \omega \notin W \end{cases} . \qquad (1\text{-}7)$$

This means that to achieve the best power match over the band subject to the above-mentioned integral constraint, we want a uniformly good match within the band and total reflection outside the band. This reflection coefficient behavior is shown in Fig. 1-2. Note that with this strategy,

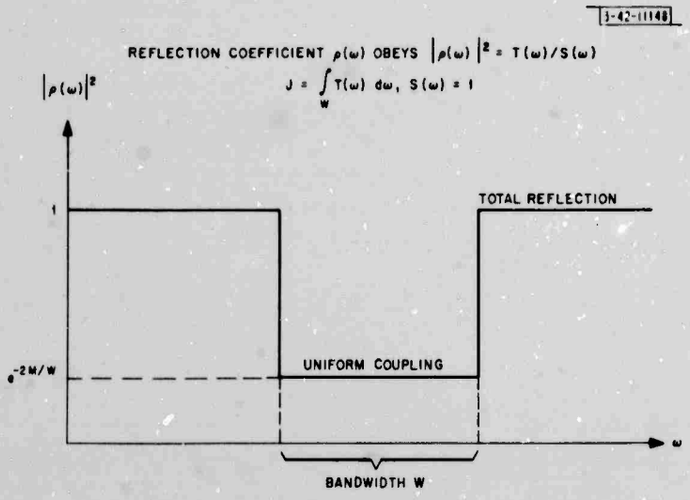

Fig. 1-2. Optimal choice of $|\rho(\omega)|$ subject to $\int_0^\infty \ln 1/|\rho|\, d\omega \leq M$.

there is no point where a perfect match is achieved; a perfect match at $\omega = c$ would mean

$$\lim_{\omega \to c} \ln \frac{1}{|\rho(\omega)|} = \infty \qquad (1\text{-}8)$$

which is a very inefficient choice of a distribution for ρ, since

$$\int_0^\infty \ln \frac{1}{|\rho(\omega)|}\, d\omega \qquad (1\text{-}9)$$

is strictly bounded.

It is not very difficult to confirm that the choice of uniform $|\rho(\omega)|$ for $\omega \epsilon W$ yields a local minimum of

$$\int_W |\rho(\omega)|^2\, d\omega$$

subject to the constraint that the previous integral is bounded (see Appendix A).

Unfortunately, if we want to synthesize a matching network with a small number of elements, it is impossible to obtain the perfectly square $|\rho(\omega)|$ characteristic as shown in Fig. 1-2; we can only obtain an approximation to it. The approximation recommended by Fano is derived from the Tchebycheff polynomial $T_n(\omega/\omega_c)$.

$$|\rho(\omega)|^2 = 1 - [(1 + r^2) + \epsilon^2 T_n(\omega/\omega_c)]^{-1} . \qquad (1\text{-}10)$$

This is the low pass filter characteristic shown in Fig. 1-3; the reflection coefficient ρ oscillates between two given values in the pass band, and asymptotically approaches unity in the attenuation band. For a bandpass filter, the argument ω/ω_c would be replaced by

$$[(\omega/\omega_o - \omega_o/\omega)]$$

where ω_o is the center frequency. If the coupling network is to be realized with k lossless lumped (LC) elements, the Tchebycheff polynomial is of order k; by increasing k to infinity we can approach the square $|\rho(\omega)|$ characteristic, and, as Fano demonstrates in an example,

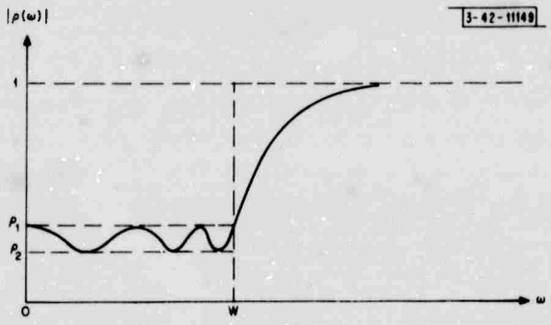

Fig. 1-3. Tchebycheff approximation to optimal (low pass) $|\rho(\omega)|$ characteristic.

$$\int \ln \frac{1}{|\rho(\omega)|}\, d\omega$$

can approach its theoretical bound, i.e., the integral inequality constraint can become an equality.

Assuming that we have decided to realize a (suboptimal) Tchebycheff match with a finite number of elements, we need to find the element values which correspond to such a match. In order to do this, the load is expressed as a Darlington realization, consisting of a lossless network terminated in a 1-ohm resistor. The coupling network plus load will then consist of two lossless networks in cascade terminated in the resistor, as shown in Fig. 1-4. The transfer matrix of the second lossless network is known, and the desired Tchebycheff transfer matrix for the two cascaded lossless networks is known, so determination of the required transfer matrix of the coupling network becomes a problem in matrix inversion. Now that we have the transfer matrix of the coupling network, standard synthesis methods lead us to the element values.

This approach is examined in great detail by Schoeffler[4] who establishes sets of conditions under which the matching network obtained in this fashion will be physically realizable, and conditions for uniqueness of the realization.

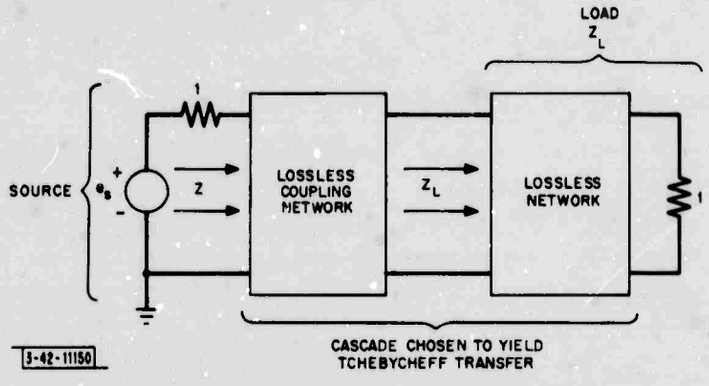

Fig. 1-4. Darlington realization of Tchebycheff transfer.

2. Practical Approximations to Lossless Optimal Match

Various approximations to the optimal square $|\rho(\omega)|$ characteristic have been used in practice. For example, Vassiliades[5] has achieved the matching network solution for a Taylor-Butterworth and for a Tchebycheff characteristic by digital computer solution of the algebraic equations resulting when the load is expressible as a Darlington ladder network. His results yield the element for a lossless matching network in ladder form.

Other work where the lumped-coupling-element values are found for a Tchebycheff transfer characteristic, usually involving digital computer solution of the algebraic equations in continued fraction (Cauer) form, includes the work of Dan Varon,[6] Matthaei[7] and Kinariwalla.[8]

It is not necessary that the lossless coupling network for a Tchebycheff transfer characteristic be realized in the form of lumped elements. In fact, Dawirs and Tuloss[9] obtain the desired transfer with a matching network composed of a uniform series of quarter-wave segments of transmission line, with their junctions shunted by adjustable "stubs," i.e., segments of shorted transmission line.

Young[10] achieves a Tchebycheff characteristic by using a single quarter-wave segment of inhomogeneous (different width) waveguide to couple between two other waveguides. Cohn[11] obtains this transfer by a series of quarter-wave segments of transmission lines with different characteristic impedances. When the source R_o and load R_L are resistive with $R_o < R_L$, the characteristic impedances of the successive segments form a monotonic sequence with

$$R_o < Z_1 < Z_2 \ldots < Z_n < R_L$$

where Z_k is the impedance of the k^{th} segment of transmission line, counting from the source. If $R_o > R_L$, the sequence is monotonic in the other direction.

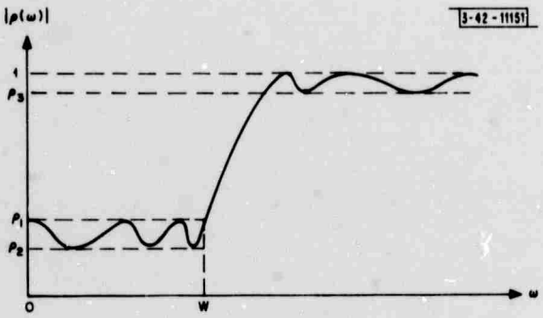

Fig. I-5. Jacobian elliptic function approximation to optimal $|\rho(\omega)|$ characteristic.

Some work has been done using elliptic functions to approximate the are $|\rho(\omega)|$ characteristic. The Jacobian elliptic function of modulus k, $Sn(\omega, k)$ yields a transfer which is equiripple both in and outside of the passband, as shown in Fig. I-5. Fano[12] discusses this approximation with respect to lumped-element lossless matching networks, and Matthaei[13,14] demonstrates that this same transfer may be realized by a nonuniform sequence of quarter-wave transmission line segments.

3. Approximations to Optimal Reflectionless Matching

The previous matching networks have been approximations to the $|\rho(\omega)|$ transfer which is uniform in the passband and unity (total reflection) outside the passband. If we now relax the specification that the matching network be lossless, we can obtain the (generally desirable) feature of no reflection from the matching network at any frequency. This situation is shown in Fig. I-6, with the Darlington realization of the lossy matching network. (A lossless network terminated in a 1-ohm resistor.) The impedance seen looking into Z is now 1 ohm at all frequencies, so the source is perfectly matched and no power is reflected back into the source.

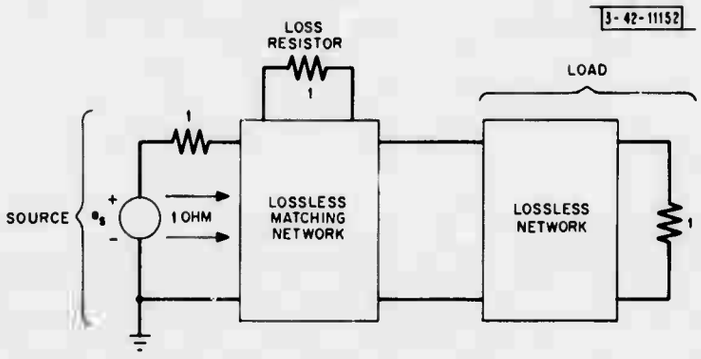

Fig. I-6. Lossy reflectionless matching circuit.

The power transfer into the load still approximates the square $|\rho(\omega)|$ characteristic, so, by conservation of power the power outside the passband and the power reflected from the load in the passband are dissipated in the "loss resistor" of the lossy coupling network. The matching network may thus be viewed as a crossover network delivering most of the input power into the load resistor or the "loss" resistor, depending on the input frequency.

Carlin and Larosa[15,16] have dealt with the necessary synthesis procedures in detail, achieving a procedure which is an extension of those used to design the lossless matching networks described previously; their procedure draws heavily on duality to obtain conjugate impedances. Their results include the fact that the overall power transfer into the load using a lossy reflectionless matching network is at worst 3 db less than that which can be obtained using a lossless matching network. In other words, we pay a price of up to 3 db in power delivered into the load to obtain the nice feature of a perfect 1-ohm input impedance. Ligomenides[17] also dealt with this reflectionless matching technique, giving applications in amplifiers and antenna systems.

Walter Ku[18] compared the theoretical limitations of lossless matching and lossy reflectionless matching, and showed that the power transfer of the lossy network is exactly 3 db less than that of its lossless equivalent. In other words, to obtain reflectionless matching, half the power which could have been delivered into the load must be dissipated in the "loss" resistor. This may be too high a price to pay, depending on the application.

4. Generalization to an Empirically Measured Load

All the synthesis techniques we have examined depend on having the load impedance expressed in terms of its complex poles and zeros at the outset. However, particularly in the case of antennas, this information is not known, and, in fact, there is no reason to suspect that the antenna impedance is a rational function of complex frequency s. In practice, the antenna impedance can be measured at a finite number of frequencies

$$s = j\omega_1, j\omega_2, \ldots j\omega_n \quad .$$

To utilize any of the previous methods, a ratio of polynomials in s must be found which agrees with the n data points, and this function used as a model for the antenna.

Sulzer,[19] however, eliminates this modeling procedure by developing an algorithm which yields the two- or three-lumped-element lossless matching network, based on

$$Z_L(j\omega_1, j\omega_2, \ldots j\omega_n)$$

which minimizes

$$\sum_{i=1}^{n} |Z(\omega_i) - 1 \text{ ohm}|^2 \quad .$$

This cost functional, magnitude-squared impedance deviation from match, is not equal to reflected power, but is a first-order approximation to reflected power when $Z \sim 1$ ohm. This generalization to an empirically-measured load is significant, but unfortunately the matching network is restricted to be either two or three lumped elements.

5. Generalization to Mixed Distributed-Lumped Systems

The matching networks described previously are composed either of lumped elements or of quarter-wave segments of distributed structures (transmission line, waveguide). A number of other coupling techniques are discussed in a handbook by Matthaei, Young and Jones,[14] including Tchebycheff and Butterworth transfers obtained with a sequence of half-wave transmission line segments.

Another interesting technique described uses both distributed structures and lumped elements in the coupling network to obtain the desired transfer: the structure consists of a series of segments of uniform transmission line, with either series-lumped capacitors or parallel-lumped inductances at each junction. The capacitors (inductances) have different values and the transmission line segments are of varying lengths, usually somewhat shorter than a half-wavelength for the examples given in the text. The appropriate lumped-element values and lengths of the segments are found algebraically from the coefficients of the Tchebycheff (Butterworth, etc.) polynomial. Of course, a dual realization could be used instead, with parallel lumped capacitors or series lumped inductances.

This technique is extremely appealing for matching into antennas in the 20 to 200 Mc frequency range: the match can be achieved merely by connecting series or parallel capacitors to the lead-in coaxial cable at appropriate points: the overall structure is simple and reliable.

6. Graphical-Geometric-Algebraic Techniques

A great number of references appear in the literature describing impedance matching techniques that use graphical aids or methods of analytic geometry (Refs. 20 – 24, for example).

These approaches provide very simple means of synthesizing an impedance-matching network which provides a perfect match at a single frequency, or (when the load is purely resistive) a perfect match at a number of discrete frequencies. However, we have seen that for maximum power transfer we generally do not want to obtain a perfect match at any frequency. Further, we are concerned about the match obtained over a continuous band of frequencies while the graphical and geometric techniques are appropriate for analyzing response for only a single frequency at one time, or at best, a number of discrete frequencies simultaneously.

7. Techniques Using a State Variable Approach

Several groups have used state variables in the design of transmission lines. For example, Rohrer, Resh and Hoyt[25, 26] investigate the problem of designing a lossy transmission line for

waveform generation or pulse shaping; an input (resistive) signal source is specified at $z = -\ell$ and the waveform delivered into a resistive load at $z = 0$ is to best match (in an integrated quadratic sense) the desired output waveform. The R(z), L(z), C(z) and G(z) are each constrained to lie in an interval; sometimes bang-bang solutions are found, but usually singular trajectories occur, where the parameters take on values inside their allowable interval.

This procedure was coded as a steepest descent iterative procedure in parameter space. Both because of the singular solutions and the necessity for numerical integration of the state and co-state partial differential equations, convergence was reported to be quite slow, typically requiring 5-1/2 hours per problem on the Control Data 1604 computer.

Moyer, Wohlers and Kopp[27, 28] use a state variable approach to design transmission line structures useful for impedance matching or filtering, selecting the real and imaginary parts of the line impedance as state variables. Unfortunately, this choice of state variables leads to a nonlinear set of partial differential equations for the state vector, requiring numerical integration. The parameters L, C, and G (the design functions) are each constrained to lie in some interval. As in the study described above, solutions sometimes have a bang-bang character, but usually correspond to singular extremals. This procedure also utilizes an iterative gradient or steepest descent in the parameter function space.

Considerable difficulty is reported with convergence to the singular extremal; typical run times are 5 to 15 minutes on an IBM 7094, with the convergence to the final solutions still somewhat in doubt at the end of that time. Efficient numerical computation of singular extremals is still considered to be a problem for further research.

C. RELATION OF PRESENT WORK TO PREVIOUS WORK

Most of the work in the literature surveyed in Sec. I-B suffers from several shortcomings: first, only the techniques in Refs. 19 and 25 to 28 permit direct use of experimentally obtained source and load impedance values in tabular form. All other techniques require finding some model for the load that would fit the measured data points. Unfortunately, the technique of Ref. 19 constrains the matching network to be only three lumped elements, which is severely restrictive.

Secondly, only the technique of Refs. 27 and 28 actually minimizes the reflected power of a given signal: Fano's square $|\rho(\omega)|$ characteristic is optimal when the signal to be transmitted has a uniform power density for $\omega \epsilon W$ and zero power for $\omega \notin W$, but this is a rather restrictive class of signals to be transmitted. Even in that case, the synthesis procedures only approximate the square $|\rho(\omega)|$ transfer by Tchebycheff Taylor-Butterworth, or $S_n(\omega, K)$ characteristics: these choices seem rather arbitrary, and there is no reason to believe that any of them actually minimizes the reflected power subject to the appropriate constraints.

However, even the technique of Refs. 27 and 28 has its drawbacks: the transmission line parameters L(z) and C(z) are only constrained to lie in some interval, so the resulting solution generally has a continuously varying L(z) and C(z). Such a structure is quite difficult to construct. A second difficulty with this procedure is computational complexity, as one is required to numerically integrate nonlinear partial differential equations.

The present work eliminates these drawbacks by placing constraints on L(z) and C(z) so that the solutions are piecewise constant; the structure can then be synthesized easily by placing intervals of various commonly available dielectric materials between the transmission line

conductors. In addition, a clever choice of state variables (in combination with the constraints mentioned above) results in constant-coefficient linear differential equations which may be solved using transition matrices, eliminating all necessity for numerical integration.

Third, the problem is generalized to include TE (waveguide structures) in addition to the TEM (transmission line structures) considered previously.

However, the procedure is merely a numerical procedure, so, in general, the burden is on the user to decide when the cost and the solution (parameter function) have converged sufficiently for his requirements. In addition, the user is required to modify his starting parameters in cases where the procedure fails to converge.

D. OUTLINE OF PRESENT WORK

The approach taken to this problem is the following: since the systems being considered are distributed through both a spatial domain and a frequency domain, we must use some version of a distributed parameter maximum principle.

In Sec. II, such a distributed parameter maximum problem is developed (following Wang[29]) which provides sufficient conditions for optimality. In the second part of Sec. II, a simple variational argument yields a set of necessary conditions for optimality. These two sets of conditions are the basis of all later work.

It is possible to make a "transmission line equivalent" for the significant aspects of the waveguide behavior, so mathematical descriptions of the two that have precisely the same form can be provided. In fact, with a proper choice of state variables in the two cases, each may be described by a linear partial differential equation and linear boundary conditions on the state. Further, the matrix multiplying the state in the partial differential equation is linear in the control variable in each case. For this reason, Sec. III develops the implications of the necessary conditions of Sec. II to such a general system as described above; these results can then be particularized to the TEM or TE case by an appropriate substitution of parameters.

In Sec. IV, the lossless TEM structure is considered and a set of state variables selected which meets the conditions of linearity described in Sec. III. The specific line parameters are substituted into the results from Sec. III, and a set of necessary conditions for optimality are given for the transmission line.

A parallel treatment is provided in Sec. V, yielding necessary conditions for optimality in the waveguide problem.

Section VI provides a description of the digital computer program written to mechanize an iterative numerical solution to the necessary conditions given in Secs. IV and V. Section VII contains a discussion of the limitations of this iterative procedure, in particular, suboptimality of solutions and possible failure of convergence, and provides suggestions for minimizing the effects of these limitations.

Section VIII provides the results obtained by actual computer runs on an SDS-940 and an IBM-360 computer for designing both transmission line and waveguide coupling structures. Included are interpretations of the results, conclusions, and suggestions for improving the numerical procedure. Suggestions for future research are given in Sec. IX.

II. OPTIMAL CONTROL OF DISTRIBUTED PARAMETER SYSTEMS

A. INTRODUCTION

The systems considered are transmission line (TEM) and waveguide (TE) structures. The behavior of such systems is characterized over an interval in two independent variables: space and frequency. The space interval is the physical length of the structure $z\epsilon[-\ell, 0]$, and the frequency interval is that band of complex frequencies $\omega\epsilon\Omega$, in which we are attempting to propagate real power through the coupling structure.

Since there are two independent variables, the behavior of the system will be characterized by a partial differential equation describing the evolution of the state of the system. Such a system is called a distributed parameter system, and optimization of the distributed parameters must be approached through a distributed parameter maximum principle.

The two structures, TEM and TE, can be described by partial differential equations of the same form; in effect, we are able to find a "transmission line equivalent" describing the essential features of the waveguide behavior. For this reason, we first consider in general the problem of optimization of distributed parameter systems, obtaining a form of a distributed parameter maximum principle. In later sections this principle is applied to the specific systems of interest, the TEM and TE structures.

Results on optimization of distributed parameter systems are available in the literature.[29] However, the systems considered are defined over an interval of time and space: the system is viewed as distributed through space ($s\epsilon S$) and evolving through time $t\epsilon[t_o, T]$ so the system is defined over $Sx[t_o, T]$. This same notation will be used in the following developments for notational convenience; however, we will be able to reinterpret the final results by substituting the independent variables of interest, $\omega\epsilon\Omega$ and $z\epsilon[-\ell, 0]$ for s and t, respectively, obtaining a system defined over $\Omega x[-\ell, 0]$. In effect, ω is the "spatial distribution" variable and z is the independent "time" variable.

B. PROBLEM STATEMENT

We consider the following system:

(1) A distributed parameter system whose state at time t is given by $x(t, s)$, a vector-valued function defined over $t\epsilon[t_o, T]$ and $s\epsilon S$, a compact subset of Euclidean N-space.

(2) The state of the system† evolves through time according to the partial differential equation:

---

† One example illustrating this type of system is the heat-equation relation for a uniform piece of material with internal (volume) heat sources:

$$\frac{\partial x(t,s)}{\partial t} = \frac{K}{pC}\frac{\partial^2 x(t,s)}{\partial s^2} + \frac{1}{pC}u(t,s)$$

where $x(t,s)$ is the temperature in °K, $u(t,s)$ is the rate of internal heat generation in cal/cm^3/sec, p is material density in gm/cm^3, C is specific heat in cal/cm-°K, and K is the thermal conductivity in cal/sec-cm-°K. Clearly, f is here a linear scalar operator involving a second space partial derivative on the state x plus a constant times the control u.

$$\frac{\partial x(t, s)}{\partial t} = f\,[x(t, s), u(t, s), t, s] \tag{2-1}$$

where u is the control strategy, a vector-valued function also defined over $[t_o, T] \times S$ and constrained to be in the set of admissible controls $U([t_o, T] \times S)$, and f is a given operator involving algebraic operations on the control u and spatial partial derivatives on the state x.

(3) There is a scalar cost functional or performance index on the control strategy $u([t_o \times T], S)$ which may be represented as

$$J\,\{x_o(s), t_o, u([t_o, T] \times S)\} = \int_S K\,[T, s, x(T, s)]\,dS + \int_{t_o}^{T} \int_S L\,[t, s, x(t, s), u(t, s)]\,dS\,dt \quad . \tag{2-2}$$

The first term represents a spatially integrated terminal time cost (a functional on the terminal state) and the second term represents the time integral of a cost rate which is itself a spatial integral.

Given the system specified by (1), (2) and (3), an initial state $x_o(s) = x(t_o, s)$ and a terminal time T, we want to find the optimal control u(t, s) for $t \in [t_o, T]$ and $s \in S$ which results in the minimum value of the cost functional:

$$J^*\,[x_o(s), t_o] = \min_{u \in U([t_o, T] \times S)} J\,\{x_o(s), t_o, u([t_o, T] \times S)\} \quad . \tag{2-3}$$

C. HAMILTON-JACOBI EQUATION IN FUNCTION SPACE†

Bellman's Principle of Optimality states that any portion of an optimal trajectory in state space (the trajectory described by the given system when the optimal control is applied) is itself an optimal trajectory between the initial and terminal states of that portion. If this were not true, a less costly control would exist for that portion of the trajectory and thus for the entire trajectory; this violates the hypothesis that the original trajectory is optimal.

Applying this principle of optimality to the problem stated above, with the portion of trajectory under consideration being x(t, s) for $s \in S$, $t \in [\tau, \tau + \epsilon]$, we have:

$$J^*\,[x(\tau, s), \tau] = \min_{u \in U\,[\tau, \tau+\epsilon] \times S} \left\{ J^*\,[x(\tau + \epsilon, s), \tau + \epsilon] + \int_{\tau}^{\tau+\epsilon} \int_S L\,[t, s, x(t, s), u(t, s)]\,dS\,dt \right\} \tag{2-4}$$

where, of course, $x(\tau + \epsilon, s)$ depends on u(t, s) for $t \in [\tau, \tau + \epsilon]$, $s \in S$. Thus,

$$J^*\,[x(\tau, s), \tau] - J^*\,[x(\tau + \epsilon, s), \tau + \epsilon] \leqslant \int_{\tau}^{\tau+\epsilon} \int_S L\,[t, s, x(t, s), u(t, s)]\,dS\,dt \quad . \tag{2-5}$$

† Adapted from Wang.[29]

We now make use of the following assumptions:

(1) $\int_S L\,[t, s, x(t, s), u(t, s)]\,dS$ is bounded from below.

(2) $f\,[t, s, x(t, s), u(t, s)]$ is a sufficiently smooth operator so that for a given initial state and control, the system partial differential Eq. (2-1) has a unique solution.

(3) $J^*\,[x(\tau, s), \tau]$ is smooth in τ, i.e., obeys the Lipschitz condition $|\partial J/\partial \tau| < \infty$.

(4) $J^*\,[x(\tau, s), \tau]$ is a smooth functional on $x(\tau, s)$.

Under these assumptions, the equation above may be expanded

$$-\frac{\partial J^*}{\partial \tau}\,[x(\tau, s), \tau] \leq \left\langle \left[\frac{\delta J^*\,[x(\tau, s), \tau]}{\delta x(\tau, s)}\right]' ,\ f\,[x(\tau, s), u(\tau, s), \tau, s]\right\rangle_S + \int_S L\,[\tau, s, x(\tau, s), u(\tau, s)]\,dS + \frac{o(\epsilon)}{\epsilon} \qquad (2\text{-}6)$$

where the inner product bracket denotes integration over S of the vector inner product, i.e.,

$$\langle g(\tau, s), h(\tau, s)\rangle = \int_{s\epsilon S} g'(\tau, s)\, h(\tau, s)\, dS$$

and

$$\lim_{\epsilon \to o} \frac{o(\epsilon)}{\epsilon} = 0 \quad .$$

Also

$$\left[\frac{\delta J\,\{x(\tau, s), \tau\}}{\delta x(\tau, s)}\right]'$$

is a Frechet derivative defined formally by

$$\frac{\delta J\,[x(\tau, s), \tau]}{\delta x_i(\tau, s)} = \lim_{\int_S |h_i(s)|\,dS \to o} \left[\frac{J(x + h_i) - J(x)}{\int_S h_i(s)\,dS}\right] \quad \text{(row vector)} \qquad (2\text{-}7)$$

where $h_i(s)$ is any continuous vector function (of the same dimension as x) whose only nonzero component is the i^{th} component, and which has compact support in a region ΔS in S, (i.e., $h(s) = 0$ for $s \notin \Delta S$, $h(s) \neq 0$ for $s \epsilon \Delta S$). The requirement that $J\,[x(s, \tau), \tau]$ be smooth in $x(s, \tau)$ is necessary for the existence of the limit corresponding to the above expression.

The Hamilton-Jacobi equation we have derived may be written more compactly if we define the costate column vector:

$$p(t, s) = \left[\frac{J^*\,\{t, x(t, s)\}}{\delta x(t, s)}\right]' \quad \text{(column vector)} \qquad (2\text{-}8)$$

and the Hamiltonian

$$H(t, p, x, u) = \langle p(t, s), f\,[t, s, x(t, s), u(t, s)]\rangle_S + \int_S L\,[t, s, x(t, s), u(t, s)]\,dS \qquad (2\text{-}9)$$

wherein the inner product brackets again denote the integral over S of the vector inner product of p and f.

Then the Hamilton-Jacobi equation is:

$$-\frac{\partial J^*[x(t,s),t]}{\partial t} = \min_{u \in U(t \times S)} H(t,p,x,u) \tag{2-10}$$

with boundary condition

$$J^*[x(T,s),T] = \int_S K[x(T,s),T]\,dS \quad . \tag{2-11}$$

It is simple to verify that

$$\frac{\partial x^*(t,s)}{\partial t} = \left[\frac{\delta H^*(t,p^*,x^*)}{\delta p^*}\right]' \tag{2-12}$$

and

$$\frac{\partial p^*(t,s)}{\partial t} = -\left[\frac{\delta H^*(t,p^*,x^*)}{\delta x^*}\right]' \tag{2-13}$$

where H^* is the u-minimal H, i.e.,

$$H^*(t,p^*,x^*) = \min_{u \in U(t \times S)} H(t,p^*,x^*,u) \tag{2-14}$$

and x^* and p^* are the corresponding optimal state and costate functions. Since

$$p^* = \left[\frac{\delta J^*}{\delta x^*}\right]' \tag{2-15}$$

then

$$p^*(T,s) = \left[\frac{\delta}{\delta x^*}\left\{\int_S K[T,s,x^*(T,s)]\right\} dS\right]' \tag{2-16}$$

(assuming that the indicated Frechet derivative exists) and we are also given the initial state

$$x(t_o,s) = x_o(s) \quad . \tag{2-17}$$

Thus we have a pair of partial differential equations with boundary conditions, and the optimal control problem reduces to that of solving a two-point boundary value problem in function space.

These conditions are sufficient for optimality, i.e., if the "optimal return function" $J^*[x(s),t]$ is found which provides the functions u^*, x^* and p^* satisfying all the conditions above, any other choice of $u \neq u^*$ will result in a cost at least as great.

D. SUMMARY

Sufficient conditions for optimality have been derived based on the following assumptions:

(1) $\int_S L[t,s,x(t,s),u(t,s)]$ is bounded from below. Any positive definite cost rate will trivially meet this requirement.

(2) $f[t,s,x(t,x),u(t,s)]$ is a sufficiently smooth operator such that, for a given initial state and control, the system partial differential Eq. (2-1) has a unique solution. This requirement is satisfied in most systems of physical interest, for example, the heat equation and the wave equation.

(3) $J^*[x(\tau, s), \tau]$ is smooth in τ, i.e., obeys the Lipschitz condition $|\partial J/\partial\tau| < \infty$. This condition is equivalent to requiring that the Hamiltonian remain finite for all $t \epsilon [t_o, T]$.

(4) $J^*[x(\tau, s), \tau]$ is a smooth functional on $x(\tau, s)$, i.e., the Frechet derivative

$$p(\tau, s) = \left[\frac{\delta J^*\{x(\tau, s), \tau\}}{\delta x(\tau, s)}\right]' \quad \text{exists for all } t \epsilon [t_o, T] \quad .$$

In particular, for $\tau = T$,

$$p(T, s) = \left[\frac{\delta}{\delta x(T, s)} \int_S K\{x(T, s), T\}\, dS\right]' \text{ exists.}$$

Under these four assumptions, sufficient conditions for a globally optimal $u^*(t, s)$ for $t [t_o, T]$ and $s \epsilon S$ are the following. If we define

$$H(t, p, x, u) = \langle p(t, s), f[t, s, x(t, s), u(t, s)]\rangle_S + \int_S L[t, s, x(t, s), u(t, s)]\, dS \qquad (2\text{-}18)$$

$$-\frac{\partial J^*[x(t, s), t]}{\partial t} = \min_{u \epsilon U(t x S)} H(t, p, x, u) \qquad (2\text{-}19)$$

and

$$J^*[x(T, s), T] = \int_S K[x(T, s), T]\, dS \qquad (2\text{-}20)$$

or equivalently, under all the assumptions made,

$$\frac{\partial x^*(t, s)}{\partial t} = \left[\frac{\delta H^*(t, p, x)}{\delta p^*}\right]' \qquad (2\text{-}21)$$

$$\frac{\partial p^*(t, s)}{\partial t} = -\left[\frac{\delta H^*(t, p, x)}{\delta x}\right]' \qquad (2\text{-}22)$$

then

$$H(x^*, p^*, u^*, t) \leqslant H(x^*, p^*, u, t) \;\forall\; u \epsilon U(t x S) \quad , \quad \forall\; t \epsilon [t_o, T] \qquad (2\text{-}23)$$

with the equality holding only for $u = u^*$.

$$x(t_o, s) = x_o(s) \qquad (2\text{-}24)$$

and

$$p(T, s) = \left[\frac{\delta}{\delta x(T, s)} \int_S K[x(t, s), T]\, dS\right]' \quad . \qquad (2\text{-}25)$$

E. NECESSARY CONDITIONS VIA VARIATIONAL METHODS

Given the system described in Sec. I, we can quite easily state a necessary condition which an optimal control strategy must satisfy: the cost must not decrease when any small allowable perturbation of the cost strategy is performed.

The candidate for optimality is $\hat{u}(t, s) \epsilon U([t_o, T] x S)$; the perturbed control is $\bar{u}(t, s) = \hat{u}(t, s)$ for $t \epsilon [\tau, \tau + \epsilon]$ and $\bar{u}(t, s) = w(t, s)$ for $t \epsilon [\tau, \tau + \epsilon]$, $(w \epsilon U)$. The initial conditions on the state $[x(t_o, s) = x_o(s)]$ remain unchanged; since the target set for $t = T$ is the entire function space,

this perturbed control satisfies the boundary conditions and is thus a candidate for optimality.

The cost

$$J\{x_o(s), t_o, \bar{u}([t_o, T] \times S)\} = \int_S K[x(T, s)]\, dS + \int_{t_o}^{T} H(t, p, x, \bar{u})\, dt$$

$$- \int_{t_o}^{T} \int_S p'(t, s) \frac{\partial x}{\partial t}(t, s)\, dS\, dt \quad . \tag{2-26}$$

We now make use of the following assumptions:

(1) $\int_S L(t, s, x, u)\, dS$ is bounded from below.

(2) $f(t, s, x, u)$ is sufficiently smooth that for a given initial state and control, there is a unique solution to the system Eq. (2-1).

(3) The Hamiltonian $H(t, x, p, u)$ is finite for finite norm u.

(4) $\int_S K[x(T, s), T]\, dS$ and $\int_S L[t, s, x(t, s), u(t, s)]\, dS$ are continuously differentiable in x, i.e., the Frechet derivative $\delta/\delta x$ of each exists.

(5) $p(t, s)$ is continuous in t.

Then by forming the difference in costs

$$J[x_o(s), t_o, \bar{u}] - J[x_o(s), t_o, \hat{u}] = \left\langle \left[\frac{\delta}{\delta x} \int_S K\{\hat{x}(T, s), T\}\, dS - p'(T) \right]', x(T, s) \right\rangle_S$$

$$+ \int_{t_o}^{T} \left\langle \left[\frac{\delta H}{\delta x}(\hat{x}, p, \hat{u}, t) + \frac{\partial p'}{\partial t} \right]', \delta x(t, s)\, dt \right\rangle_S$$

$$+ \int_{\tau}^{\tau+\epsilon} H(\hat{x}, p, \bar{u}, t) - H(\hat{x}, p, \hat{u}, t)\, dt \quad . \tag{2-27}$$

To insure that the cost difference above is ≥ 0, we select the continuous (Lagrange multiplier) function $p(t, s)$ to have the following properties:

$$\frac{\partial p'(t, s)}{\partial t} = - \frac{\delta H(\hat{x}, p, \hat{u}, t)}{\delta \hat{x}} \quad ; \tag{2-28}$$

$$p'(T, s) = \frac{\delta}{\delta \hat{x}} \int_S K[x(T, s), T]\, dS \quad . \tag{2-29}$$

The first two terms are thus zero for all permissible $\bar{u}(t, s)$; the remaining term must then be ≥ 0; letting $\epsilon \to 0$ we have:

$$H(x^*, p^*, u^*, t) \leq H(x^*, p^*, \bar{u}, t) \quad \text{for all } \bar{u} \in U(t \times S) \tag{2-30}$$

where the *'s now denote optimal quantities.

The necessary conditions are thus:

$$\frac{\partial x^*}{\partial t} = \left[\frac{\delta H^*(x, p, u, t)}{\delta p^*} \right]' \tag{2-31}$$

$$x^*(t_o, s) = x_o(s) \tag{2-32}$$

$$\frac{\partial p^*}{\partial t} = -\left[\frac{\delta H^*(x, p, u, t)}{\delta x^*}\right]' \tag{2-33}$$

$$p^*(T, s) = \frac{\delta}{\delta x^*} \int_S K[x^*(T, s), T]\, dS \tag{2-34}$$

$$H(x^*, p^*, u^*, t) \leqslant H(x^*, p^*, u, t) \tag{2-35}$$

for all $\bar{u} \epsilon U(txS)$.

F. DISCUSSION

The difference between these necessary conditions and the sufficient conditions derived previously is that in the sufficient conditions u^* uniquely minimizes the Hamiltonian, while in the necessary conditions, the minimizing u may not be unique. However, the sufficient conditions were derived under one additional assumption: that $J^*[x(s, t), t]$ is smooth {Frechet differentiable in x(s, t) for all $t \epsilon [t_o, T]$}.

If a system of interest satisfies all the assumptions of the sufficient conditions, then the solution of Eqs. (2-21) to (2-25) yields the globally optimal control function; this candidate must then be compared with all other candidates for optimality to determine which one is globally optimal.

There are two ways in which a solution could meet the requirements of the necessary conditions, but not those of the sufficient conditions. First, the optimal return function $J^*[x(t, s), t]$ may not be a smooth functional in x(t, s). In the finite-state optimal control problems, this occurs when the state-space trajectory strikes the target set tangentially, i.e., the trajectory barely clips the target; an infinitesimal change in the trajectory near the target would necessitate drastic changes in the system behavior, as, for example, having to overshoot the target, then turn around, and return. Such a condition is referred to as "abnormality," and means that the target is exactly on the border of the set of reachable states, and that an infinitesimal perturbation in the initial state cannot be corrected by an infinitesimal perturbation of the control strategy.

An essential feature of the abnormality condition is the restricted target set. In the distributed parameter problem at hand, we selected the entire function-space as the target set. It thus seems plausible that abnormality conditions and thus "corners" in $J^*[t, s, x(t, s)]$ with respect to x(t, s) will not appear: every state lies within the target set so there is no danger of the trajectory merely "clipping" the target tangentially.

If this is indeed the case, we need only worry about cases that satisfy the necessary conditions, but not the sufficient conditions because of the second reason: the function $u^*(t, s)$ which minimizes $H(x^*, p^*, u, t)$ is not unique. If the function $u^*(t, s)$ is only nonunique over a set of $t \epsilon [t_o, T]$ with measure zero, we need not be concerned, because any of the minimizing functions u will result in the same cost.

If $H(x^*, p^*, u, t)$ has some small number of minimizing solutions over a nonzero time interval, then a direct comparison of the costs resulting from these several strategies is possible, and will yield a globally optimal strategy. However, if there is an infinite number of minimizing functions u over some finite time interval, we are faced with the "singular" condition, and a different approach is needed to find the optimal control.

One method is to compute the time derivative of the Hamiltonian

$$\frac{d}{dt} H^*(x^*, p^*, t) = \frac{\partial H^*}{\partial t}(x^*, p^*, t) + \left\langle \frac{\delta H^*}{\delta x^*}, \frac{\partial x^*}{\partial t} \right\rangle_S + \left\langle \frac{\delta H^*}{\delta p^*}, \frac{\partial p^*}{\partial t} \right\rangle_S = \frac{\partial H}{\partial t} \quad .$$

Successive time derivatives of this relation will yield relations between u^*, x^*, p^*, and their derivatives. In any particular case, it may be possible [by substituting into the conditions of Eqs. (2-31) through (2-35)] to find a unique u^* which satisfies these new conditions and also satisfies the boundary conditions.

If a solution to the original problem does exist, this is then the solution.

III. LINEAR DISTRIBUTED PARAMETER SYSTEMS WITH LINEAR TERMINAL COST

A. INTRODUCTION

In the previous section we derived optimality conditions for systems distributed over space ($s \epsilon S$) and evolving through time, $t \epsilon [t_o, T]$, so the domain of system definition is $S \times [t_o, T]$. Now we wish to analyze electromagnetic structures which propagate real power in the +z direction (by standard convention), and thus have physical extent $z \epsilon [-\ell, 0]$. Power flow will be considered for complex frequencies ω in some frequency interval Ω, so we make a substitution of variables in our previous results. ω replaces the spatial variable s and z replaces the time variable t.

There is one additional point to be considered, however; since real power flow is in the +z direction, we connect the source to the matching structure at $z = -\ell$ and to the load at $z = 0$. The cost functional to be considered will be the power reflected into the source at $z = -\ell$. (Since the matching structures under consideration will be lossless, minimizing this reflected power will maximize the power delivered to the load.) In the original derivation the cost involves a terminal cost term which is a functional on the state at $t = T$. In the present system, the cost is a functional on the "terminal" state at $z = -\ell$. We must then consider $z = 0$ as the initial "time" and $z = -\ell$ as the terminal "time." The system is thus propagating backward through "time."

This makes an essential change in the necessary conditions. To minimize the total cost, the Hamiltonian must be maximized rather than minimized, as in Eq. (2-35); this may be seen by writing the cost as a "time" integral, then changing the sign of the integrand to interchange the limits of integration.

As we noted previously, the state equations describing the TEM structure and those describing the TE structure have the same form. In fact, both can be expressed as linear partial differential equations. In both cases, the cost due to reflected power loss can be expressed as a linear functional on the "terminal" state at $z = -\ell$.

Since the two problems are so similar, we will investigate our reinterpreted necessary conditions in the general case of a system with a linear first-order partial differential equation on the state and a linear terminal cost. The results obtained will then be applied to the specific examples of the TEM structure and the TE structure in later sections.

B. PROBLEM STATEMENT

We consider the following problem:

(1) A distributed parameter system whose state at location z is given by $x(z, \omega)$, a vector-valued function defined over $z \epsilon [-\ell, 0]$ and $\omega \epsilon \Omega$ (an interval of complex frequencies).

(2) The state of the system evolves through z according to the partial differential equation

$$\frac{\partial x(z, \omega)}{\partial z} = A[\omega, u(z)] \cdot x(z, \omega) \tag{3-1}$$

where u is the control strategy, a vector-valued function defined over $[-\ell, 0]$ and constrained to lie in the set

$$U = \{u_1, u_2, \ldots u_n\} \quad .$$

Further, $A[\omega, u(z)]$ is a matrix linear in u for all $z \epsilon [-\ell, 0]$ and $\omega \epsilon \Omega$:

$$A\,[\omega, u(z)] = A_o(\omega) + \sum_{i=1}^{m} A_i(\omega)\, u_i(z) \quad . \tag{3-2}$$

All $A_i(\omega)$ are continuous in ω. The initial condition on the state is $x(0, \omega) = x_o(\omega)$ with $x_o(\omega)$ continuous in ω.

(3) There is a scalar cost functional or performance index on the control strategy which may be represented as:

$$J\,\{x_o(\omega),\ u\,[-\ell, 0]\} = \int_{\omega \epsilon \Omega} K'(\omega)\, x(-\ell, \omega)\, d\omega \tag{3-3}$$

This is a frequency integrated "terminal location" cost, or a linear functional on the terminal state, with $K(\omega)$ an n-vector continuous in ω.

Given the system specified by (1), (2), and (3), an initial state $x_o(\omega) = x(0, \omega)$ and a terminal location $-\ell$, we want to find the (optimal) control $u(z)$ for $z \epsilon [-\ell, 0]$ which results in the minimum value of the cost functional:

$$J\,[x_o(\omega)] = \min_{u \epsilon U([-\ell, 0])} J\,\{x_o(\omega),\ u([-\ell, 0])\} \quad . \tag{3-4}$$

C. NECESSARY CONDITIONS FOR OPTIMALITY – THE HAMILTONIAN

For the problem outlined above, we define the Hamiltonian

$$H(x, p, u, z) = \int_{\omega \epsilon \Omega} p'(z, \omega)\, \frac{\partial}{\partial z}\, x(z, \omega)\, d\omega \quad . \tag{3-5}$$

The necessary conditions state that a costate vector $p^*(z, \omega)$ must exist (where the * indicates an optimal quantity) such that:

(1) $$\frac{\partial x^*(z, \omega)}{\partial z} = \left[\frac{\delta H^*(x, p, u, z)}{\delta p^*}\right]' = A\,[\omega, u^*(z)] \cdot x^*(z, \omega) \tag{3-6}$$

with $x^*(0, \omega) = x_o(\omega)$. This condition merely restates the partial differential equation of the system and its initial state:

(2) $$\frac{\partial p^*(z, \omega)}{\partial z} = -\left[\frac{\delta H^*(x, p, u, z)}{\delta x^*}\right]' = -A'\,[\omega, u^*(z)] \cdot p^*(z, \omega) \tag{3-7}$$

with boundary condition

$$p(-\ell, \omega) = \left[\frac{\partial}{\partial x} \int_{\omega \epsilon \Omega} K'(\omega)\, x(-\ell, \omega)\, d\omega\right]' \equiv K(\omega) \tag{3-8}$$

(3) $$H(x^*, p^*, u^*, z) \geqslant H(x^*, p^*, \bar{u}, z) \quad \text{for all } \bar{u} \epsilon U, \text{ i.e., } u^* \tag{3-9}$$

maximizes

$$\int_{\omega \epsilon \Omega} p'^*(z, \omega) \cdot A\,[(\omega, u(z)] \cdot x(z, \omega)\, d\omega = \int_{\omega \epsilon \Omega} p'^*(z, \omega)$$

$$\cdot A_o(\omega) \cdot x^*(z, \omega)\, d\omega + \sum_{i=1}^{M} u_i(z) \int_{\omega \epsilon \Omega} p'^*(z, \omega)\, A_i(\omega)\, x^*(z, \omega)\, d\omega \quad . \tag{3-10}$$

The first term is independent of u. Writing the Hamiltonian as

$$H(x^*, p^*, u, z) = m_o + \sum_{i=1}^{M} u_i m_i \tag{3-11}$$

this maximization requires:

$$u_i^*(z) = \begin{cases} u_{i_{MAX}} & \text{if } m_i(z) > 0 \\ u_{i_{MIN}} & \text{if } m_i(z) < 0 \\ \text{determined only to lie in } U & \text{if } m_i(z) = 0 \end{cases} \tag{3-12}$$

where the MAX and MIN subscripts denote the maximum and minimum available control values in U. The third possibility of Eq. (3-12), $m_i(z) = 0$, must be considered in more detail. First, suppose that $m_i(z) = 0$ only over a set of z having measure zero: then the selection of any $u \epsilon U$ at those locations will result in the same system trajectory and total cost. If, however, $m_i(z) = 0$ over some interval of z, the choice of u becomes significant. Different selections of u will generally result in different system trajectories and different costs because Eq. (3-12) merely gives a necessary condition for optimality, not a sufficient condition.

This condition, $m_i(z) = 0$ over a nonzero interval of z, is known as the singular condition. The appearance of this singular condition greatly complicates any attempt at numerical solution of the necessary conditions, as we shall discuss later on.

To avoid the complexities of this singular condition (which is usually present in the problems to be considered below) we employ a mathematical artifice: a slight modification of our original cost functional. Further, we consider u(z) to be a scalar for simplicity in the following arguments. Generalization to a vector is straightforward, but unnecessary for the problems at hand.

D. MODIFIED COST FUNCTIONAL

1. Necessary Conditions

It will be shown that it is desirable to make a small modification to the cost functional of Eq. (3-3). In particular we add a term such that

$$J(x_o, 0) = \int_{\omega \epsilon \Omega} K'(\omega)\, x(-\ell, \omega)\, d\omega + \frac{\Delta}{2} \int_{-\ell}^{o} |u - u_a|^2\, dz \quad . \tag{3-13}$$

The u_a term is some value of control intermediate between the extremes of $u \epsilon U = \{u_1, u_2, \ldots u_m\}$. Since we are in reality interested in the cost $\int_{\omega \epsilon \Omega} K'x\, d\omega$, but not about $(u - u_a)^2$, Δ is chosen sufficiently small that the contribution of the $\int |u - u_a|^2$ term is negligible (for engineering purposes) with respect to the $\int K'x d\omega$ term.

Even though this term is negligible for engineering purposes, it is quite significant mathematically. The term is a mathematical artifice that greatly simplifies consideration of the solutions of the necessary conditions that correspond to singular extremals; we would like to solve the problem in the limit as $\Delta \to 0$, but it is necessary to keep Δ sufficiently large in the numerical procedures that it does not disappear in round-off and truncation errors.

If we rewrite the Hamiltonian of Eq. (3-4) to include this term, we have

$$H(x, p, u, z) = \int_{\omega \epsilon \Omega} p'(z, \omega) \cdot A[\omega, u(z)] \cdot x(z, \omega)\, d\omega - \Delta |u - u_a|^2/2 \tag{3-14}$$

and Eq. (3-11) becomes

$$H(x, p, u, z) = m_o + M \cdot u - \Delta |u - u_a|^2/2 \quad . \tag{3-15}$$

The partial differential equations for the state and costate Eqs. (3-6) and (3-7), and also the boundary conditions on the state and costate are not changed by the addition of the Δ term. It only influences the total cost (by a very small amount) and the Hamiltonian.

The change in the Hamiltonian is quite helpful, however: we note that the Hamiltonian is now a quadratic function of the control instead of a linear function. The singular condition $m_1 = 0$ no longer prevents the Hamiltonian from having a well-defined maximum with respect to u.

In fact, since u is a scalar, it is evident that

$$u^* = u \in \{u_1, u_2, \ldots u_m\} \quad \text{closest to } (u_a + M/\Delta) \tag{3-16}$$

where M is the factor multiplying u in the Hamiltonian. This choice of u^* maximizes the Hamiltonian over all available $u \in U$, and this maximization usually provides a unique value for u^*.

However, for some values of M (this set has measure zero) two admissible values of u are equally close to $u_a - M/\Delta$. This condition will now be called the singular condition since Eq. (3-16) does not yield a unique u^*, but only specifies that the optimal value is one of the two.

Note that if we had not used the artifice of the $\Delta |u - u_a|^2/2$ term, whenever $M = 0$, we would be faced with <u>all</u> possible controls $u_1, u_2, \ldots u_n$ as equally good candidates for optimality.

2. Singular Condition

When

$$u_a + M/\Delta = \frac{u_k + u_{k+1}}{2}$$

we are faced with ambiguity in Eq. (3-16): both u_k and u_{k+1} maximize the Hamiltonian. If M takes on this value only over an interval of z having measure zero, then either control is equally good. However, if M remains at this critical value over some nonzero interval of z, its first and second derivatives must be zero in that interval:

$$\frac{dM}{dz} = 0 \tag{3-17}$$

$$\frac{d^2M}{dz^2} = 0 \tag{3-18}$$

Because $A[\omega, u(z)]$ is linear in u, Eq. (3-18) gives an explicit solution for u, i.e., Eq. (3-18) holds if and only if u takes on a particular value, say u_s.

Several possibilities arise: first, suppose Eq. (3-17) holds and u_s equals either u_k or u_{k+1}; then a singular extremal exists, and the value of u along this singular extremal is u_k or u_{k+1}, as specified by Eq. (3-18). This resolves the ambiguity of Eq. (3-16).

If either of the two above suppositions fails, then this is not a singular extremal, M maintains its critical value only over a distance of measure zero, and it makes no difference whether u_k or u_{k+1} is selected at this point.

Thus, because of the added $\Delta |u - u_a|^2$ term, the singular condition causes no new difficulties in specifying $u^*(z)$ in the numerical solution of the necessary conditions Eqs. (3-6) to (3-9).

However, as we will see, this singular condition can cause difficulty in obtaining convergence when an iterative method is used to obtain simultaneous solution of Eqs. (3-6) to (3-9).

E. PROPERTIES OF SOLUTIONS – THE HAMILTONIAN

Due to the imposed constraint on the control $u \in \{u_1, u_2, \ldots u_m\}$, any control function u(z) which satisfies the necessary conditions Eqs. (3-6) to (3-9) must be a piecewise constant function of z over $[-\ell, 0]$; it will switch between available values in $\{u_1, u_2, \ldots u_m\}$ over successive intervals of z. Over each of these intervals, the matrix $A[\omega, u(z)]$ will be constant in z.

This means that the state partial differential Eq. (3-6) and the costate partial-differential Eq. (3-7) may be solved over each of these z intervals, for each ω, as a constant coefficient linear differential equation. It is this simplification that makes computational solution of the necessary conditions practical: the state and costate may be propagated from the beginning to the end of a constant-u interval of z merely by multiplying the appropriate transition matrix (e^{Az} or $e^{-A'z}$). No numerical integration of the differential equations is necessary.

We now examine the behavior of the Hamiltonian over a constant-u interval of z:

$$H(x, p, u, z) = \int_{\omega \in \Omega} p'(z, \omega)\, A[\omega, u(z)]\, x(z, \omega)\, d\omega - \Delta |u - u_a|^2/2 \qquad (3\text{-}19)$$

for constant u(z), and

$$\frac{\partial H}{\partial z} = \int_{\omega \in \Omega} [-p'(z, \omega)\, A^2(\omega, u)\, x(z, \omega) + p'(z, \omega)\, A^2(\omega, u)\, x(z, \omega)]\, d\omega = 0 \quad . \qquad (3\text{-}20)$$

The Hamiltonian is therefore constant over each interval where u is constant. Further, the condition for switching between u_k and u_{k+1} is

$$H(x^*, p^*, u_k, z) = H(x^*, p^*, u_{k+1}, z) \quad .$$

The Hamiltonian is thus continuous across a time when the control switches.

These two conditions are sufficient to guarantee that the Hamiltonian is constant for all $z \in [-\ell, 0]$.

We may similarly differentiate the inner product of state and costate in a constant-u interval of z:

$$\frac{\partial}{\partial z} \int_{\omega \in \Omega} p'(z, \omega)\, x(z, \omega)\, d\omega = \int_{\omega \in \Omega} (-p'Ax + p'Ax)\, d\omega = 0 \quad . \qquad (3\text{-}21)$$

Since $p(z, \omega)$ and $x(z, \omega)$ are continuous in z, the inner product shown above is continuous across a location where the control u switches.

These two conditions are sufficient to guarantee that the inner product

$$\int_{\omega \in \Omega} p'(z, \omega)\, x(z, \omega)\, d\omega \qquad (3\text{-}22)$$

is constant for all $z \in [-\ell, 0]$.

At $z = -\ell$, this equals

$$\int_{\omega \in \Omega} K'(\omega)\, x(-\ell, \omega)\, d\omega \qquad (3\text{-}23)$$

but

$$J(x_o, 0) = \int_{\omega \in \Omega} K'(\omega)\, x\,(-\ell, \omega)\, d\omega + \frac{\Delta}{2} \int_{-\ell}^{o} |u - u_a|^2\, dz \quad . \tag{3-24}$$

Thus

$$J(x_o, 0) = \int_{\omega \in \Omega} p'(z, \omega)\, x(z, \omega)\, d\omega + \frac{\Delta}{2} \int_{-\ell}^{o} |u - u_a|^2\, dz \tag{3-25}$$

for all $z \in [-\ell, 0]$, in particular for $z = -0$. This yields

$$J(x_o, 0) = \int_{\omega \in \Omega} p'(0, \omega)\, x_o(\omega)\, d\omega + \frac{\Delta}{2} \int_{-\ell}^{o} |u - u_a|^2\, dz \quad . \tag{3-26}$$

We may consider the initial location and state as a pair of independent variables and suppress the subscripts in the equation above. Then

$$\frac{\delta J(x, z)}{\delta x} = p'(z, \omega) \tag{3-27}$$

and

$$\frac{\partial J(x, z)}{\partial z} = \int_{\omega \in \Omega} -p'(z, \omega)\, A(\omega)\, x(\omega)\, d\omega + \frac{\Delta}{2} |u - u_a|^2 \quad . \tag{3-28}$$

This equation is the function-space equivalent of the Hamilton-Jacobi equation:

$$-\frac{\partial J}{\partial z} = H(x^*, p^*, u^*, z) = \max_{u \in U} H(x^*, p^*, u, z) \quad . \tag{3-29}$$

F. SUMMARY

In the systems considered, the linear partial differential equation of the state plus the constraint that the control lies in a discrete set permits us to solve a linear constant-coefficient differential equation for each ω over each interval of z where u takes on a constant value. A similar set of equations holds for the costate, so we may propagate the state and costate through any constant-u interval of z by a simple matrix multiplication with the transition matrices.

This fact makes it possible to eliminate all numerical integration of the state and costate during iterative solution of the necessary conditions of Eqs. (3-6) to (3-9), and makes this numerical solution computationally feasible.

To apply these results to the specific examples of the transmission line and the waveguide, we need only specify the A matrix, the K vector, and the physical parameter corresponding to $u^*(z)$.

IV. TRANSMISSION LINE (TEM) PROBLEM

A. INTRODUCTION

The problem of interest is wide-band impedance matching. We are given a wide-band source of radio frequency energy and a load impedance, as shown in Fig. I-1.

The load impedance is

$$Z_L(\omega) = R_L(\omega) + jX_L(\omega) \tag{4-1}$$

which is a complex function of frequency defined over the frequency band of interest, $\omega \epsilon \Omega$.

The source impedance is

$$Z_S(\omega) = R_S(\omega) + jX_S(\omega) \tag{4-2}$$

(another complex function of frequency for $\omega \epsilon \Omega$) and this source has an available power density $S(\omega)$, a real function of frequency also defined for $\omega \epsilon \Omega$.

Practical examples of such elements might be a vacuum tube RF amplifier as the source and an antenna as the load; we would then like to design a lossless coupling structure or impedance matching structure which maximizes the real power delivered from the source to the load.

The first example of such an impedance matching structure is the transmission line or TEM structure shown in Fig. IV-1. Here the structure length is fixed as ℓ. The transmission line is considered lossless so it is completely characterized by its inductance per unit length L(z) and its capacity per unit length C(z). Note that both these are dependent on position z, but not on the frequency ω.

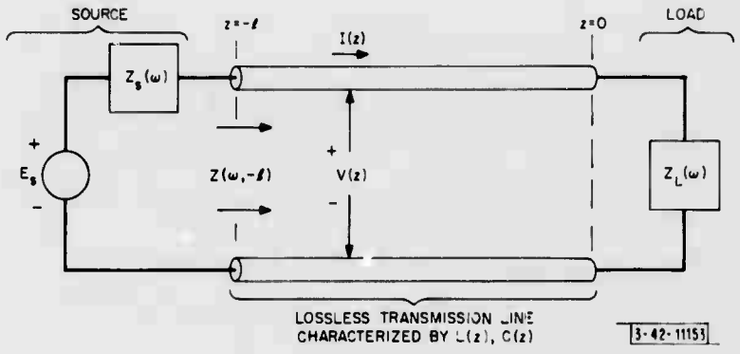

Fig. IV-1. Impedance match using a TEM structure.

By standard convention, real power flow is in the +z direction, so we connect the source at $z = -\ell$ and the load at $z = 0$. Since the source has available power density $S(\omega)$, we consider that a forward wave with power density $S(\omega)$ flows from $-\ell$ to 0, where partial reflection occurs and a reflected wave having power density $T(\omega)$ returns from 0 to $-\ell$. The net power delivered to the load is then

$$V = \int_\Omega [S(\omega) - T(\omega)]\, d\omega \quad . \tag{4-3}$$

The line is lossless, so $S(\omega)$ and $T(\omega)$ are naturally independent of z. The power "lost" through reflection is

$$J = \int_{\Omega} T(\omega)\, d\omega \quad . \tag{4-4}$$

In the design procedure, we may either maximize V or minimize J; both are exactly equivalent because the line is lossless. The problem we consider is thus to select L(z) and C(z), $z\ [-\ell, 0]$, subject to appropriate constraints in such a way as to minimize J.

The particular constraints selected for this design are the following:

(1) $L(z) \equiv L$ is constant for all z (4-5)

(2) $C(z) \in \{C_1, C_2, \ldots, C_m\}$ where $0 < C_i < \infty$ for all i (4-6)

These constraints were selected to make the physical implementation of the resulting structure practical. Consider a stripline formed by parallel conducting strips; to synthesize a transmission line having constant inductance per unit length and piecewise constant capacity per unit length, one need only fill the space between the conductors with successive intervals of various dielectric materials (see Fig. IV-2). The available capacities $\{C_1, C_2, \ldots, C_m\}$ should be chosen to correspond to the capacities realized by standard or readily available dielectric materials.

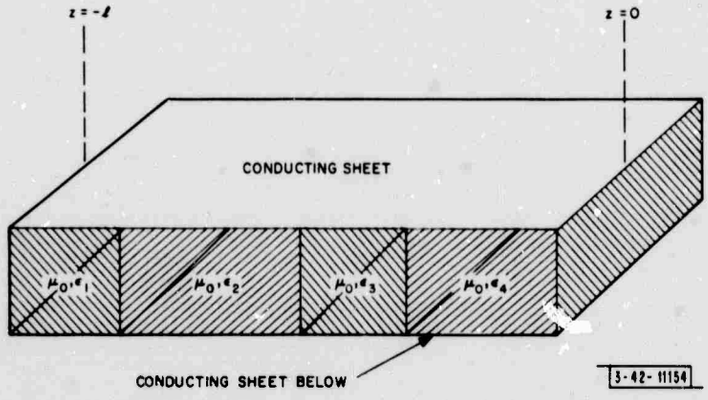

Fig. IV-2. Stripline realization of TEM structure.

The construction utilizes dielectric materials rather than magnetic materials because magnetic materials having constant magnetic susceptance over a wide range of frequencies are not readily available.

B. THE STATE PARTIAL DIFFERENTIAL EQUATION

A TEM (transverse electro-magnetic) structure or transmission line is characterized by an inductance per unit length L(z) and a capacity per unit length C(z) if we assume a lossless line. Line losses are accounted for by R(z), the resistance per unit length of the conductors, and G(z), the conductance for unit length of the material between the conductors.

Voltages (V') and currents (I') on the line satisfy the following differential equations:[30]

$$\frac{\partial V'}{\partial z} = -L\,\frac{\partial I'}{\partial t} - RI' \quad ; \quad \frac{\partial I'}{\partial t} = -C\,\frac{\partial V'}{\partial t} - GV' \tag{4-7}$$

where z is the spatial distance down the line and t is the time variable.

Assuming sinusoidal steady-state with

$$I'(z,t) = \mathrm{Re}\,[I(z)\,e^{j\omega t}] \quad \text{and} \quad V'(z,t) = \mathrm{Re}\,[V(z)\,e^{j\omega t}] \quad .$$

$$\frac{dV(z)}{dz} = -j\omega L(z)\,I(z) - R(z)\,I(z) \quad ;$$

$$\frac{dI(z)}{dz} = -j\omega C(z)\,V(z) - G(z)\,V(z) \quad . \tag{4-8}$$

The complex voltage and complex current are continuous functions of z and could be used as state variables for the system. However, it is more convenient to select a different set of state variables, because a particular choice can make the state partial differential equation far easier to solve. First, define the real power flow in the $+z$ direction as

$$S_R(z,\omega) = \mathrm{Re}\,\{VI^*/2\}$$

and the imaginary power flow in the $+z$ direction as

$$S_I(z,\omega) = \mathrm{Im}\,\{VI^*/2\}$$

where the superscript asterisk denotes a complex conjugate quantity.

We then select as the state vector

$$\underline{x}(z,\omega) = \begin{bmatrix} |V(z,\omega)|^2 \\ |I(z,\omega)|^2 \\ \sqrt{8}S_I(z,\omega) \\ \sqrt{8}S_R(z,\omega) \end{bmatrix} \quad . \tag{4-9}$$

The state $\underline{x}(z,\omega)$ then obeys the partial differential equation

$$\frac{\partial x(z,\omega)}{\partial z} = \sqrt{2}\begin{bmatrix} 0 & 0 & -\omega L(z) & -R(z) \\ 0 & 0 & \omega C(z) & -G(z) \\ \omega C(z) & -\omega L(z) & 0 & 0 \\ -R(z) & -G(z) & 0 & 0 \end{bmatrix} \cdot x(z,\omega)$$

$$= A(\omega, L, C, R, G) \cdot x(z,\omega) \quad . \tag{4-10}$$

This equation is obtained by evaluating the partial derivative of the state with respect to z and substituting the line differential equation, Eq. (4-8).

The $R(z)$ entry in the A matrix is the resistance per unit length of the conductors, and $G(z)$ denotes leakage conductance between the conductors. In the problem at hand, the line is considered lossless so $R(z) = G(z) \equiv 0$. Due to the constraints imposed, $L(z) = L$ is a constant, and $C(z)$ is a piecewise constant. This means that over each constant-C interval, Eq. (4-10) is a constant coefficient linear differential equation for each ω. The state may then be propagated

from one end of the interval to the other using a single matrix multiplication by the transition matrix for each ω:

$$x(z+d,\omega) = \begin{bmatrix} \left(\frac{1+\cos\Theta}{2}\right) & \frac{L}{C}\left(\frac{1-\cos\Theta}{2}\right) & -\sqrt{\frac{L}{2C}}\sin\Theta & 0 \\ \frac{C}{L}\left(\frac{1-\cos\Theta}{2}\right) & \left(\frac{1+\cos\Theta}{2}\right) & \sqrt{\frac{C}{2L}}\sin\Theta & 0 \\ \sqrt{\frac{C}{2L}}\sin\Theta & -\sqrt{\frac{L}{2C}}\sin\Theta & \cos\Theta & 0 \\ 0 & 0 & 0 & 1 \end{bmatrix} \cdot x(z,\omega) \qquad (4\text{-}11)$$

where $\Theta = 2\omega\sqrt{LC}\,d$, and d is the length of the constant-capacity interval. This eliminates any numerical integration of the partial differential equation and makes the computation practical.

The boundary conditions on the state are as follows: at z = 0 a load $Z_L = R_L + jX_L$ is connected. Remembering the definition of impedance in terms of voltage and current,

$$x(0,\omega) = \begin{bmatrix} |V(0,\omega)|^2 \\ |I(0,\omega)|^2 \\ \sqrt{8}S_I(0,\omega) \\ \sqrt{8}S_R(0,\omega) \end{bmatrix} = \begin{bmatrix} |Z_L(\omega)|^2 \\ 1 \\ \sqrt{2}X_L(\omega) \\ \sqrt{2}R_L(\omega) \end{bmatrix} \cdot \frac{\sqrt{8}S_R(0,\omega)}{\sqrt{2}R_L(\omega)} \qquad (4\text{-}12)$$

This provides three conditions on the state. The fourth condition appears at $z = -\ell$:

$$S(\omega) = \frac{1}{8R_S(\omega)}\left[1,\ |Z_S(\omega)|^2,\ \sqrt{2}X_S(\omega),\ \sqrt{2}R_S(\omega)\right] \begin{bmatrix} |V(-\ell,\omega)|^2 \\ |I(-\ell,\omega)|^2 \\ \sqrt{8}S_I(-\ell,\omega) \\ \sqrt{8}S_R(-\ell,\omega) \end{bmatrix} \qquad (4\text{-}13)$$

The reflected power is also evaluated at this point:

$$T(\omega) = \frac{1}{8R_S(\omega)}\left[1,\ |Z_S(\omega)|^2,\ \sqrt{2}S_X(\omega),\ -\sqrt{2}R_S(\omega)\right] \begin{bmatrix} |V(-\ell,\omega)|^2 \\ |I(-\ell,\omega)|^2 \\ \sqrt{8}S_I(-\ell,\omega) \\ \sqrt{8}S_R(-\ell,\omega) \end{bmatrix}$$

$$= K'(\omega)\,x(-\ell,\omega) \qquad (4\text{-}14)$$

C. APPLICATION OF MAXIMUM PRINCIPLE

1. Necessary Conditions

The transmission line problem above satisfies the restrictions of the development described in Sec. III, namely, a linear system with linear terminal cost, so we may restate the necessary conditions developed in Sec. III:

$$\frac{\partial x^*(z,\omega)}{\partial z} = \frac{\delta H^*(x,p,C,z)}{\delta p^*(z,\omega)} = A(\omega, C)\, x^*(z,\omega) \tag{4-15}$$

$$\frac{\partial p^*(z,\omega)}{\partial z} = -\frac{\delta H^*(x,p,C,z)}{\delta x^*(z,\omega)} = -A'(\omega, C)\, p^*(z,\omega) \tag{4-16}$$

$$H(x^*, p^*, C^*, z) \geq H(x^*, p^*, \bar{C}, z) \quad \text{for all } \bar{C} \in \{C_1, C_2, \ldots, C_m\} \tag{4-17}$$

where

$$J = \int_{\omega\in\Omega} T(\omega)\, d\omega + \int_{-\ell}^{0} \frac{\Delta}{2} (C - C_a)^2\, dz$$

$$= \int_{\omega\in\Omega} K'(\omega)\, x(-\ell,\omega)\, d\omega + \frac{\Delta}{2} \int_{-\ell}^{0} (C - C_a)^2\, dz \tag{4-18}$$

and the Hamiltonian is

$$H(x,p,C,z) = \int_{\omega\in\Omega} p'(z,\omega)\, A(\omega, C)\, x(z,\omega)\, d\omega - \frac{\Delta}{2} (C - C_a)^2 \quad . \tag{4-19}$$

Note the addition (as in Sec. III) of the small term quadratic in capacity (control). Here C_a denotes some intermediate capacity, such as $(C_{MAX} + C_{MIN})/2$, where the MAX and MIN subscripts denote the extremes in $\{C_1, C_2, \ldots, C_m\}$.

The boundary conditions on the state and costate are:

$$x(0,\omega) = x_o(\omega) \tag{4-20}$$

$$p(-\ell,\omega) = \frac{\delta J}{\delta x}\,[x(-\ell,\omega), -\ell] = \frac{\delta}{\delta x} \int_{\omega\in\Omega} K'(\omega)\, x(-\ell,\omega)\, d\omega = K(\omega) \quad . \tag{4-21}$$

2. Properties of Solutions

The necessary condition of Eq. (4-15) is merely a restatement of the system equation Eq. (4-10). Equation (4-16) yields

$$\frac{\partial}{\partial z}\, p(z,\omega) = -\sqrt{2}\omega \begin{bmatrix} 0 & 0 & -L & 0 \\ 0 & 0 & C(z) & 0 \\ C(z) & -L & 0 & 0 \\ 0 & 0 & 0 & 0 \end{bmatrix} \cdot p(z,\omega) = -A'(\omega, C)\, p(z,\omega) \quad . \tag{4-22}$$

Over any constant-C interval this is a linear constant coefficient differential equation and may be solved using the transition matrix:

$$p(z+d,\omega) = \begin{bmatrix} \left(\frac{1+\cos\Theta}{2}\right) & \frac{C}{L}\left(\frac{1-\cos\Theta}{2}\right) & -\sqrt{\frac{C}{2L}}\sin\Theta & 0 \\ \frac{L}{C}\left(\frac{1-\cos\Theta}{2}\right) & \left(\frac{1+\cos\Theta}{2}\right) & \sqrt{\frac{L}{2C}}\sin\Theta & 0 \\ \sqrt{\frac{L}{2C}}\sin\Theta & -\sqrt{\frac{C}{2L}}\sin\Theta & \cos\Theta & 0 \\ 0 & 0 & 0 & 1 \end{bmatrix} \cdot p(z,\omega) \qquad (4\text{-}23)$$

where $\Theta = 2\omega\sqrt{LC}\,d$, and d is the length of the constant-capacity interval. This eliminates any numerical integration of the costate.

The boundary condition on the costate is:

$$p(-\ell,\omega) = K(\omega) = \frac{1}{8R_S(\omega)} \begin{bmatrix} t \\ |Z_S(\omega)|^2 \\ \sqrt{2}X_S(\omega) \\ \sqrt{2}R_S(\omega) \end{bmatrix} . \qquad (4\text{-}24)$$

Note the duality between this condition and the state boundary condition, Eq. (4-12). In fact, this duality goes much further: imagine opening the transmission line at any point $z \in [-\ell, 0]$. Some impedance will be measured at that point looking to the right (+z direction); call this impedance $Z_+(z,\omega) = R_+(z,\omega) + jX_+(z,\omega)$. Similarly, one sees an impedance $Z_-(z,\omega)$ looking to the left, toward the source (see Fig. IV-3). In general

$$x(z,\omega) = \begin{bmatrix} |Z_+(z,\omega)|^2 \\ 1 \\ \sqrt{2}X_+(z,\omega) \\ \sqrt{2}R_+(z,\omega) \end{bmatrix} \cdot \frac{2S_R(z,\omega)}{R_+(z,\omega)} \qquad (4\text{-}25)$$

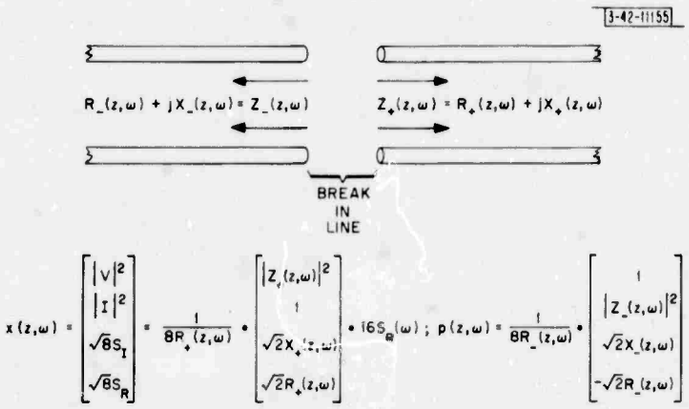

Fig. IV-3. Impedance interpretation of state and costate.

by definition of the impedance in terms of voltage and current. Similarly,

$$p(z,\omega) = \frac{1}{8R_-(z,\omega)} \begin{bmatrix} 1 \\ |Z_-(z,\omega)| \\ \sqrt{2}X_-(z,\omega) \\ -\sqrt{2}R_-(z,\omega) \end{bmatrix} . \tag{4-26}$$

Thus, the state is a characterization of the impedance seen looking to the right at any point and the costate characterizes the impedance looking to the left. If we evaluate Eqs. (4-25) and (4-26) in the special cases $z = 0$ and $z = -\ell$, respectively, we obviously obtain the previously stated boundary conditions on the state and costate.

It is interesting to interpret the maximization of the Hamiltonian in this light. If we eliminate the added cost term which was quadratic in capacity, the question, "Is there some allowable capacity change one can make to increase the Hamiltonian?" is exactly equivalent to the question, "Is there some allowable capacity change one can make (over some dz interval) so that the parallel combination of $Z(z,\omega)$ and this capacity is closer to $Z_+^*(z,\omega)$?" (Here the superscript asterisk means complex conjugate.) Either of these two problems results in the same equation and the same capacity change.

The Hamiltonian evaluates to:

$$H(x, p, C, z) = -\frac{\Delta}{2}(C - C_a)^2 + \int_{\omega\in\Omega} \sqrt{2}\omega C \left[x_3(z,\omega)\, p_2(z,\omega) + x_1(z,\omega)\, p_3(z,\omega)\right] d\omega$$

$$- \int_{\omega\in\Omega} \sqrt{2}\omega L \left[x_3(z,\omega)\, p_1(z,\omega) + x_2(z,\omega)\, p_3(z,\omega)\right] d\omega \tag{4-27a}$$

where the numerical subscripts denote the different components of state or costate vector.

More simply,

$$H(x, p, C, z) = -\frac{\Delta}{2}(C - C_a)^2 + M_c \cdot C + \text{constant}^{\dagger} \quad . \tag{4-27b}$$

The capacity multiplier is then

$$M_c = \sqrt{2} \int_{\omega \epsilon \Omega} \omega (x_3 p_2 + x_1 p_3)\, d\omega \quad . \tag{4-28}$$

As shown in Sec. III, this specifies the capacity which maximizes the Hamiltonian as

$$C^* = C \epsilon \{C_1, C_2, \ldots, C_m\} \quad \text{closest to } C_a + M_c/\Delta \quad . \tag{4-29}$$

It is possible for $C_a + M_c/\Delta$ to lie precisely half way between two available capacities. If this condition holds over an interval of z, we have the singular condition, where

$$\frac{dM_c}{dz} = \frac{d^2 M_c}{dz^2} = 0 \tag{4-30}$$

These relations yield

$$\frac{dM}{dz} = 2L \int_{\omega \epsilon \Omega} \omega^2 (x_t p_1 - x_2 p_2)\, d\omega = 0 \tag{4-31a}$$

and

$$\frac{d^2 M}{dz^2} = -2\sqrt{2} L \left[L \int_{\omega \epsilon \Omega} \omega^3 (x_2 p_3 + x_3 p_t)\, d\omega + C \int_{\omega \epsilon \Omega} \omega^3 (x_t p_3 + x_3 p_2)\, d\omega \right] = 0 \tag{4-31b}$$

or

$$C = \frac{-L \int_{\omega \epsilon \Omega} \omega^3 (x_3 p_t + x_2 p_3)\, d\omega}{\int_{\omega \epsilon \Omega} \omega^3 (x_3 p_2 + x_1 p_3)\, d\omega} \quad . \tag{4-31c}$$

If either Eq. (4-31a) fails to be true, or the C of Eq. (4-31c) equals neither of the two candidate C_k values, we are not on a singular extremal and the ambiguous condition only lasts over an interval of z having measure zero. If both equations can be satisfied for one of the candidates, we are on a singular extremal and the capacity indicated in Eq. (4-31c) is optimal.

3. Summary

We have now specified a differential equation for the state and costate for each frequency ω, a practical method of solution (the transition matrices), a complete set of boundary conditions, and a procedure for uniquely specifying $C(z)$ as a function of $x(z, \omega)$ and $p(z, \omega)$ even in the case of the singular extremal. This coupled set of equations may be solved iteratively on a digital computer, and when convergence is obtained, the functions obtained will satisfy all our necessary conditions for optimality.

---

† This constant is independent of C.

If we had not included the modification to the cost by a term quadratic in C, we would have been forced to follow a completely different approach; namely, to obtain the solution of the problem when C is constrained to an interval by using Eq. (4-31c) to determine C over all intervals of z where $M_c(z) = 0$. This solution will provide a smoothly varying function $C(z)$, as a function of z, requiring numerical integration of the state and costate differential equations. Such a procedure is computationally very slow. Moreover, after convergence is obtained we are still faced with the problem of finding some piecewise constant approximation to $C(z)$ to permit construction of the structure.

The procedure selected, on the other hand, has the benefits of computational efficiency and a naturally piecewise constant solution $C(z)$.

BLANK PAGE

V. WAVEGUIDE (TE) PROBLEM

A. INTRODUCTION

In the development discussed in this section, we are again concerned with the problem of designing a lossless impedance matching structure. However, the frequencies of interest in this case are generally in the microwave region, far higher than the radio frequencies dealt with in the transmission line coupler.

At these very high frequencies, waveguides are used rather than transmission lines for power transmission, because the waveguides provide considerably lower power loss (dissipation). The source of microwave power might be a klystron, magnetron, or even a receiving antenna. The load in this case might then be a transmitting antenna or the input circuit of a UHF receiver.

In any case, the design goal is a lossless impedance matching waveguide structure which maximizes the power delivered to the load, or equivalently, minimizes the reflected power.

The structure to be considered is a uniform rectangular waveguide whose axis extends in the +z direction from $z = -\ell$ to $z = 0$. In accordance with the convention of real power flow in the +z direction, the source will be at $z = -\ell$ and the load at $z = 0$.

This waveguide will be filled (uniformly across every cross section) with lossless material having dielectric constant $\epsilon(z)$ and magnetic permeability $\mu(z)$ (Fig. V-1). The design job is to select these functions under appropriate constraints so as to maximize the power delivered to the load.

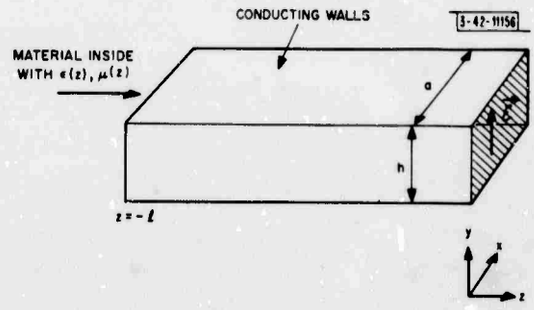

Fig. V-1. Waveguide structure.

The constraints selected are the following:

(1) $\mu(z) \equiv \mu_o$ for all $z \in [-\ell, 0]$.

(2) $\epsilon(z)$ is in $\{\epsilon_1, \epsilon_2, \ldots \epsilon_m\}$.

(3) The waveguide is operated solely in the $TE_{1,0}$ mode and every frequency $\omega \in \Omega$ (the frequency band of interest) is above the low frequency cut-off corresponding to μ_o, ϵ_{MIN}.

The first two constraints guarantee that a solution for the dielectric constant must be a piecewise constant function of z. The structure may then be physically realized by filling the waveguide with successive intervals of various dielectric materials. Of course, $\epsilon_1, \epsilon_2, \ldots \epsilon_m$ should be selected to correspond to readily available materials.

The third constraint is merely a guarantee that it is possible to propagate real power down the waveguide at all frequencies of interest. If a frequency ω is above cut-off in the μ_o, ϵ_{MIN} material, it will, of course, be safely above cut-off for all the other materials considered.

B. WAVEGUIDE EQUATIONS[24]

The waveguide structure under consideration is shown in Fig. V-1. The cavity is filled with material whose susceptance ϵ and permeability μ varies with position z down the waveguide, but at a given z is constant over the cross section

$$\{x\epsilon\,[0,a]\} \times \{y\epsilon\,[0,h]\} \quad .$$

There are no free charges or currents in the material, so Maxwell's equations yield:

$$\nabla x\vec{E} = -\mu \frac{\partial \vec{H}}{\partial t} \quad ; \quad \nabla x\vec{H} = \epsilon \frac{\partial \vec{E}}{\partial t} \quad . \tag{5-1}$$

If we consider the transverse electric field (TE) solution,

$$\vec{E} = E_y \quad ; \quad E_x = E_z = 0 \quad . \tag{5-2}$$

Then

$$\nabla x\vec{E} = -\frac{\partial E_y}{\partial z}\vec{i}_x + \frac{\partial E_y}{\partial x}\vec{i}_z = -\mu \frac{\partial \vec{H}}{\partial t} \quad . \tag{5-3}$$

Thus, $H_y = 0$, since the left-hand side of Eq. (5-3) has no y components.

$$\nabla x\vec{H} = \frac{\partial H_z}{\partial y}\vec{i}_x + \left(\frac{\partial H_x}{\partial z} - \frac{\partial H_z}{\partial z}\right)\vec{i}_y - \left(\frac{\partial H_x}{\partial y}\right)\vec{i}_z = \frac{\partial E_y}{\partial t}\vec{i}_y \quad . \tag{5-4}$$

Since the right-hand side of Eq. (5-4) has no $\vec{i}_x$ or $\vec{i}_z$ components

$$\frac{\partial H_z}{\partial y} = \frac{\partial H_x}{\partial y} = 0 \quad . \tag{5-5}$$

Also,

$$\text{div}\ \vec{D} = \epsilon \frac{\partial E_y}{\partial y} = 0 \quad . \tag{5-6}$$

Therefore, there is no y-variation of $\vec{E}$ or $\vec{H}$.

Thus we have the following equations:

$$E_x = E_z = H_y = 0 \quad . \tag{5-7}$$

$$\frac{\partial E_y}{\partial z} = \mu \frac{\partial H_x}{\partial t} \quad ; \quad \frac{\partial E_y}{\partial x} = -\mu \frac{\partial H_z}{\partial t} \quad ; \quad \frac{\partial H_x}{\partial z} - \frac{\partial H_z}{\partial x} = \frac{\partial E_y}{\partial t} \quad . \tag{5-8}$$

To meet the boundary conditions at the sides of the waveguide, we must have

$$E_y \equiv 0 \quad \text{at } x = 0 \quad \text{and} \quad \text{at } x = a.$$

This solution is constructed as the superposition of two equal amplitude uniform plane waves in phase propagating in different directions, as shown in Fig. V-2.

If both waves are equal in amplitude, are in phase, and propagate at an angle Θ with respect to the X-axis, where $\cos\Theta = \lambda/2a$, then the two waves interact destructively and cancel to zero along the entire lines $x = 0$ and $x = a$. We merely set the solution to zero for $x < 0$ and $x > a$ to obtain the solution for waves in the waveguide. (Interpret the waves inside as multiple internal reflections.) Superposition of the two waves gives:

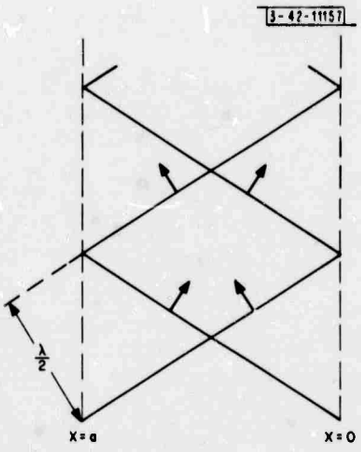

Fig. V-2. Superposition of plone woves in woveguide.

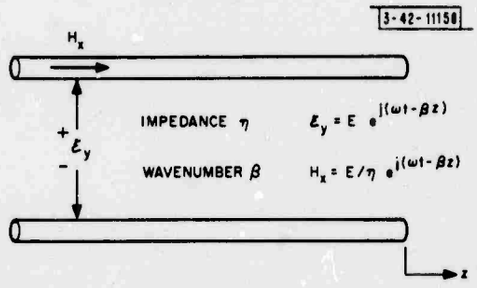

Fig. V-3. Equivolent transmission line model for waveguide.

$$\vec{E} = -\vec{i}_y\,[2jE\,\sin(\beta_o X \cdot \cos\Theta)]\,e^{j\beta_o z\sin\Theta} \tag{5-9}$$

$$\vec{H} = \frac{2E}{\eta_o}\,[\vec{i}_z\cos\Theta\,\cos(\beta_o X - \cos\Theta) - \vec{i}_x j\sin\Theta\,\sin(\beta_o X \cdot \cos\Theta)]\,e^{j\beta_o z\sin\Theta} \tag{5-10}$$

where

$$\eta_o = \sqrt{\frac{\mu}{\epsilon}} \quad , \quad \beta_o = \sqrt{\epsilon\mu} \quad .$$

$\vec{E}_y \times \vec{H}_z$ gives the Poynting (power flow) vector component in the x-direction. It is purely imaginary, indicating that power merely "rattles back and forth" in the x-direction. However, $\vec{E}_y \times \vec{H}_x$ gives us real power flow in the z-direction (along the waveguide) so we will focus attention on these two components.

Define η = "radiation resistance" = E_y/H_x:

$$\eta = \frac{\eta_o}{\sin\Theta} = \sqrt{\frac{\mu}{\epsilon}} \cdot \frac{1}{\sin\Theta} = \frac{\mu}{\sqrt{\mu\epsilon - \pi^2/a^2\omega^2}} \quad . \tag{5-11}$$

Define β = 2π/wavelength in z-direction:

$$\beta = \beta_o \sin\Theta = \sqrt{\epsilon\mu}\,\sin\Theta = \sqrt{\mu\epsilon - \pi^2/a^2\omega^2} \quad . \tag{5-12}$$

This gives rise to the equivalent transmission line model of Fig. V-3, where E_y is the analog of line voltage and H_x is the analog of line current. We have the two "transmission line" equations,

$$\frac{dE_y}{dz} = -j\omega\mu H_x \quad ; \quad \frac{dH_x}{dz} = -\frac{j\omega}{\mu}\left(\mu\epsilon - \frac{\pi}{a^2\omega^2}\right)E_y \quad . \tag{5-13}$$

The electric and magnetic fields above are continuous in z and could be used as the system state. However, it is far more convenient to select the following state vector $x(z,\omega)$:

$$x(z,\omega) = \begin{bmatrix} |E_y(z,\omega)|^2 \\ |H_x(z,\omega)|^2 \\ \sqrt{8}\, S_I(z,\omega) \\ \sqrt{8}\, S_R(z,\omega) \end{bmatrix} \tag{5-14}$$

where $S_I(z,\omega)$ is the imaginary part of the Poynting vector $S_I(z,\omega) = \text{Im}\{E_y H_x^*/2\}$ and S_R is the real part $S_R(z,\omega) = \text{Re}\{E_y H_x^*/2\}$.

This choice of a state vector yields the following state partial differential equation for lossless waveguide.

$$\frac{\partial}{\partial z} x(z,\omega) = \sqrt{2}\omega \begin{bmatrix} 0 & 0 & -\mu_o & 0 \\ 0 & 0 & e(z,\omega) & 0 \\ e(z,\omega) & -\mu_o & 0 & 0 \\ 0 & 0 & 0 & 0 \end{bmatrix} \cdot x(z,\omega) = A(\omega,e) \cdot x(z,\omega) \tag{5-15}$$

where

$$e(z,\omega) = \epsilon(z) - \frac{\pi^2}{\mu_o a^2 \omega^2} \quad . \tag{5-16}$$

Since $\epsilon(z)$ is a piecewise constant function of z, Eq. (5-15) is a constant coefficient linear differential equation for each ω, which may be solved over a constant-ϵ interval by using the transition matrix:

$$x(z+d,\omega) = \begin{bmatrix} \left(\frac{1+\cos\Theta}{2}\right) & \frac{\mu_o}{e}\left(\frac{1-\cos\Theta}{2}\right) & -\sqrt{\frac{\mu_o}{2e}}\sin\Theta & 0 \\ \frac{e}{\mu_o}\left(\frac{1-\cos\Theta}{2}\right) & \frac{1+\cos\Theta}{2} & \sqrt{\frac{e}{2\mu_o}}\sin\Theta & 0 \\ \sqrt{\frac{e}{2\mu_o}}\sin\Theta & -\sqrt{\frac{\mu_o}{2e}}\sin\Theta & \cos\Theta & 0 \\ 0 & 0 & 0 & 0 \end{bmatrix} \cdot x(z,\omega) \tag{5-17}$$

where ϵ is defined by Eq. (5-16),

$$\Theta = 2\omega\sqrt{\epsilon\mu_o}\, d$$

and d is the length of the constant-ϵ interval. This eliminates any numerical integration of the partial differential equation.

The boundary condition at z = 0 is determined from the "wave impedance"

$$\eta_L(\omega) = \frac{E_y(z=0,\omega)}{H_x(z=0,\omega)} = R_L(\omega) + jX_L(\omega) \tag{5-18}$$

which is a measured characteristic of the load.

A similar wave impedance is available for the source:

$$\eta_S(\omega) = R_S(\omega) + jX_S(\omega) \tag{5-19}$$

and this source has available power density $S(\omega)$.

The boundary conditions on the state are

$$x(0,\omega) = \begin{bmatrix} |E_y(0,\omega)|^2 \\ |H_x(0,\omega)|^2 \\ \sqrt{8}\, S_I(0,\omega) \\ \sqrt{8}\, S_R(0,\omega) \end{bmatrix} = \begin{bmatrix} |\eta_L(\omega)|^2 \\ 1 \\ \sqrt{2}\, X_L(\omega) \\ \sqrt{2}\, R_L(\omega) \end{bmatrix} \cdot \frac{\sqrt{8}\, S_R(0,\omega)}{\sqrt{2}\, R_L(\omega)} \tag{5-20}$$

This provides three conditions on the state. The fourth condition appears at $z = -\ell$.

$$S(\omega) = \frac{1}{8R_S(\omega)} \left[1, |\eta_S(\omega)|^2, \sqrt{2}X_S(\omega), \sqrt{2}R_S(\omega)\right] \begin{bmatrix} |E_y(-\ell,\omega)|^2 \\ |H_x(-\ell,\omega)|^2 \\ \sqrt{8}\, S_I(-\ell,\omega) \\ \sqrt{8}\, S_R(-\ell,\omega) \end{bmatrix} . \tag{5-21}$$

$T(\omega)$, the reflected power, is also evaluated at this point:

$$T(\omega) = \frac{1}{8R_S(\omega)} \left[1, |\eta_S(\omega)|^2, \sqrt{2}X_S(\omega), -\sqrt{2}R_S(\omega)\right] \begin{bmatrix} |E_y(-\ell,\omega)|^2 \\ |H_x(-\ell,\omega)|^2 \\ \sqrt{8}\, S_I(-\ell,\omega) \\ \sqrt{8}\, S_R(-\ell,\omega) \end{bmatrix}$$

$$= K'(\omega)\, x(-\ell,\omega) \quad . \tag{5-22}$$

C. APPLICATION OF THE MAXIMUM PRINCIPLE

1. Necessary Conditions

The neeessar; conditions for optimality are those developed in See. III, namely: Given the cost

$$J = \int_{\omega \in \Omega} T(\omega)\, d\omega + \int_{-\ell}^{0} \frac{\Delta}{2} (\epsilon - \epsilon_a)^2\, dz$$

$$= \int_{\omega \in \Omega} K'(\omega)\, x(-\ell,\omega)\, d\omega + \frac{\Delta}{2} \int_{-\ell}^{0} (\epsilon - \epsilon_a)^2\, dz \qquad (5\text{-}23)$$

(here ϵ_a denotes some intermediate dieleetric constant), we define the Hamiltonian as

$$H(x,p,\epsilon,z) = \int_{\omega \in \Omega} p'(z,\omega)\, A(\omega,\epsilon)\, x(z,\omega)\, d\omega - \frac{\Delta}{2} (\epsilon - \epsilon_a)^2 \qquad (5\text{-}24)$$

Note the addition (as in See. III) of the small quadratie term in ϵ.

Then there must exist a costate $p^*(z,\omega)$ sueh that:

$$\frac{\partial x^*(z,\omega)}{\partial z} = \left[\frac{\delta H^*(x,p,\epsilon,z)}{\delta p^*(z,\omega)}\right]' = A(\omega,e^*)\, x^*(z,\omega) \qquad (5\text{-}25)$$

$$\frac{\partial p^*(z,\omega)}{\partial z} = -\left[\frac{\delta H^*(x,p,\epsilon,z)}{\delta p^*(z,\omega)}\right]' = -A'(\omega,e^*)\, p^*(z,\omega) \qquad (5\text{-}26)$$

and

$$H(x^*, p^*, \epsilon^*, z) \geqslant H(x^*, p^*, \bar{\epsilon}, z) \quad \text{for all } \bar{\epsilon} \text{ in } \{\epsilon_1, \epsilon_2, \ldots \epsilon_m\} \quad . \qquad (5\text{-}27)$$

The boundary conditions on the state and costate are:

$$x(0,\omega) = x_o(\omega)$$

$$p(-\ell,\omega) = \frac{\delta J\,[x(-\ell,\omega),-\ell]}{\delta x} = \frac{\delta}{\delta x} \int_{\omega \in \Omega} K'(\omega)\, x(-\ell,\omega)\, d\omega = K'(\omega) \quad . \qquad (5\text{-}28)$$

2. Properties of Solutions

Equations (5-23) are merely a restatement of the system equation, Eq. (5-15). Equation (5-24) yields:

$$\frac{\partial}{\partial z}\, p(z,\omega) = -\sqrt{2}\omega \begin{bmatrix} 0 & 0 & e(z,\omega) & 0 \\ 0 & 0 & -\mu_o & 0 \\ -\mu_o & e(z,\omega) & 0 & 0 \\ 0 & 0 & 0 & 0 \end{bmatrix} \cdot p(z,\omega) = -A'(\omega,\epsilon) \cdot p(z,\omega) \qquad (5\text{-}29)$$

where $e(z,\omega)$ is given by Eq. (5-16).

This may be solved over any constant-ϵ interval by the transition matrix:

$$p(z+d,\omega) = \begin{bmatrix} \left(\frac{1+\cos\Theta}{2}\right) & \frac{e}{\mu_o}\left(\frac{1-\cos\Theta}{2}\right) & -\sqrt{\frac{e}{2\mu_o}}\sin\Theta & 0 \\ \frac{\mu_o}{e}\left(\frac{1-\cos\Theta}{2}\right) & \frac{1+\cos\Theta}{2} & \sqrt{\frac{\mu_o}{2e}}\sin\Theta & 0 \\ \sqrt{\frac{\mu_o}{2e}}\sin\Theta & -\sqrt{\frac{e}{2\mu_o}}\sin\Theta & \cos\Theta & 0 \\ 0 & 0 & 0 & 1 \end{bmatrix} \cdot p(z,\omega) \qquad (5\text{-}30)$$

where

$$\Theta = 2\omega\sqrt{e\mu_o}\,d$$

and d is the length of the constant-ϵ interval. This eliminates numerical integration of the costate.

The boundary condition on the costate is

$$p(-\ell,\omega) = K(\omega) = \frac{1}{8R_S(\omega)} \begin{bmatrix} 1 \\ |\eta_S(\omega)|^2 \\ \sqrt{2}\,X_S(\omega) \\ -\sqrt{2}\,R_X(\omega) \end{bmatrix} . \qquad (5\text{-}31)$$

An interpretation of the state and costate analogous to that of Sec. IV is possible here. The state is a characterization of the wave impedance looking to the right (toward the load) at any point in the waveguide, and the costate is a characterization of the wave impedance looking to the left at that point. Equation (5-31) is an obvious special case of this for $z = -\ell$.

The Hamiltonian evaluates to:

$$H(x,p,\epsilon,z) = -\frac{\Delta}{2}(\epsilon-\epsilon_a)^2 + \epsilon\int_{\omega\in\Omega}\sqrt{2}\omega\,(x_3p_2 + x_1p_3)\,d\omega$$

$$-\mu_o\int_{\omega\in\Omega}\sqrt{2}\omega(x_3p_1 + x_2p_3)\,d\omega - \frac{\pi^2\sqrt{2}}{\mu_o a^2}\int_{\omega\in\Omega}\frac{(x_3p_2 + x_1p_3)}{\omega}\,d\omega \quad . \qquad (5\text{-}32)$$

The dielectric multiplier in the Hamiltonian is then

$$M_\epsilon = \sqrt{2}\int_{\omega\in\Omega}\omega(x_3p_2 + x_1p_3)\,d\omega \quad . \qquad (5\text{-}33)$$

As shown in Sec. III, this specifies the capacity which maximizes the Hamiltonian as:

$$\epsilon^* = \epsilon \text{ in } \{\epsilon_1, \epsilon_2, \ldots \epsilon_m\} \quad \text{closest to } \epsilon_a - M_\epsilon/\Delta \quad . \tag{5-34}$$

It is possible for $\epsilon_a - M_\epsilon/\Delta$ to lie precisely half way between two available dielectric constants. If this condition holds over an interval of z, we have the singular condition, where

$$\frac{dM_\epsilon}{dz} = \frac{d^2M_\epsilon}{dz^2} = 0 \quad .$$

These relations yield:

$$\int_{\omega \epsilon \Omega} \omega^2 (x_1 p_1 - x_2 p_2)\, d\omega = 0 \quad . \tag{5-35}$$

$$\epsilon = \frac{\frac{\pi^2}{\mu_o a^2} \int_{\omega \epsilon \Omega} \omega (x_3 p_2 + x_1 p_3)\, d\omega - \mu_o \int_{\omega \epsilon \Omega} \omega^3 (x_3 p_1 + x_2 p_3)\, d\omega}{\int_{\omega \epsilon \Omega} \omega^3 (x_3 p_2 + x_1 p_3)\, d\omega} \quad . \tag{5-36}$$

If Eq. (5-35) fails to be true, or the ϵ of Eq. (5-36) equals neither of the two candidate values for ϵ, we are not on a singular extremal and the ambiguous condition only lasts over an interval of z having measure zero. If both equations can be satisfied by one of the candidates, we are on a singular extremal and the dielectric constant indicated by Eq. (5-36) is optimal.

D. SUMMARY

A differential equation has been specified for the state and costate for each ω, as well as an efficient method of solution (the transition matrices), a complete set of boundary conditions, and a procedure for uniquely specifying $\epsilon(z)$ as a function of $x(z,\omega)$ and $p(z,\omega)$ even in the case of the singular extremal. The resulting set of equations is almost identical to that obtained for the transmission line problem with the obvious exception of variable names. This waveguide problem may thus conveniently be solved by the same iterative digital computer scheme (program) which solves the transmission line problem.

When convergence is obtained, the functions obtained will satisfy all our necessary conditions for optimality.

As in the transmission line problem, if we had not modified the cost functional by the term quadratic in ϵ, we would have been forced to use Eq. (5-36) over all intervals of z where $M_\epsilon(z) = 0$ to determine $\epsilon^*(z)$. This would require the (computationally inefficient) numerical integration of the state and costate equations, then the approximation of this continuous $\epsilon(z)$ by some piecewise constant function to permit construction of the structure.

On the other hand, the present method is computationally efficient and provides a solution $\epsilon(z)$ which is naturally a piecewise constant.

VI. NUMERICAL PROCEDURE

A. INTRODUCTION

The necessary conditions, Eqs. (3-6) to (3-8) and (3-16) were programmed for iterative solution on a digital computer. Equation (3-16) is used to find the control u(z) (C(z) for the transmission line, and $\epsilon(z)$ for the waveguide) in terms of the state and costate vectors $x(z, \omega)$ and $p(z, \omega)$. Since the same procedures are carried out in the transmission line case and the waveguide case, both problems are solved by the same program.

Flow charts for this solution procedure are given in Appendix B, and a complete Fortran-IV source listing is provided in Appendix C. Once Eq. (3-16) is used to eliminate the control from the state and costate equations, we have two coupled four-vector systems to solve subject to split boundary value conditions. This solution proceeds iteratively by guessing the function $x(-\ell, \omega)$ [$p(-\ell, \omega)$ is given in Eq. (4-24) or Eq. (5-31)] and integrating the equations in the $+z$ direction to $z = 0$. There $x(0, \omega)$ will not meet the boundary condition imposed by the load, so the initial guess for $x(-\ell, \omega)$ must be changed and this process iterated until $x(0, \omega)$ does meet the load boundary conditions. At this time, the solution $x(z, \omega)$ $p(z, \omega)$ and u(z) will satisfy all our necessary conditions.

It is interesting to note that at each iteration we have obtained a solution to <u>some</u> optimal control problem, namely that of matching to the load which corresponds to our intermediate result for $x(0, \omega)$.

B. SIMULTANEOUS SOLUTION OF NECESSARY CONDITIONS

As noted above, we start at $z = -\ell$ with $p(-\ell, \omega)$ given by Eq. (4-20) or Eq. (5-31) and an initial guess for $x(-\ell, \omega)$. We then use Eq. (4-28) to determine $M(-\ell)$ (the multiplier in the Hamiltonian). This will specify a starting value for $u(-\ell)$ (Eq. 3-16), depending on which threshold values M lies between. By differentiating the expression for M(z) with respect to z, we obtain two frequency integrals of products of state and costate components which specify

$$\frac{dM}{dz} \quad \text{and} \quad \frac{d^2M}{dz^2} \quad . \qquad \text{[Eqs. (4-31a) and (4-31b) or (5-35) and (5-36)]}$$

Evaluate these terms at $z = -\ell$, fit an osculating parabola to the M(z) function at this point and predict at what z location M(z) will first cross one of its threshold values (see Fig. VI-1).

Now that we have a guess at the location of the first switch point, use the transition matrices to propagate $x(-\ell, \omega)$ and $p(-\ell, \omega)$ down to this predicted switch point. This is accomplished by the subroutine "STEP" flow charted in Fig. B-5. Here we re-evaluate

$$M(z) \quad , \quad \frac{dM}{dz} \quad \text{and} \quad \frac{d^2M}{dz^2} \quad .$$

If M(z) has not yet reached the threshold value, fit another parabola and repeat the process. If M(z) has passed its threshold, we have overshot the switch point and a parabola is fitted to take us back to the switch point. This process repeats itself, as indicated in flow charts B-2 and B-3, converging quadratically fast on the switch point. (Three iterations are almost always sufficient to converge on the switchpoint with 10^{-6} accuracy.)

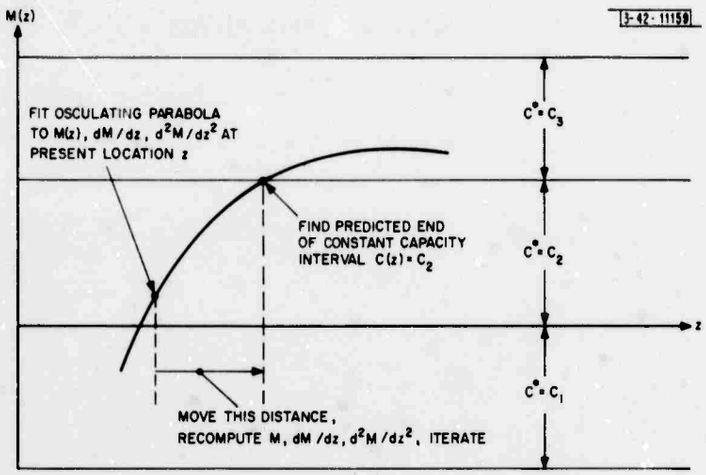

Fig. VI-1. Extropolotion by fitting osculoting parabola to M(z).

Once this switch point is determined, the subroutine "SWITCH" is called (Fig. B-4) to change to a new constant-capacity interval. In this routine, the new value of u is computed, d^2M/dz^2 is recomputed (since it is a function of u), and a parabola is fitted to carry us forward to the next switch point. This process continues to the end of the line, (Fig. B-2), generally taking 40 or 50 steps in a line one wavelength long and having five admissible control values.

A number of other considerations are taken into account in the actual program, of course; sometimes it is impossible to fit a parabola which intersects a threshold value in the correct direction. If this happens, a linear fit is tried and if that fails a step equal to about $1/20^{th}$ of the line length is taken in the appropriate direction. Since the parabolic and linear fits sometimes give ridiculously large distance estimates, in no case is a step larger than $1/20^{th}$ of the line length taken. Also, one is not permitted to step off either end of the line.

This process now provides a fast and efficient mapping from the initial guess $x(-\ell, \omega)$ to the state $x(0, \omega)$. This mapping will serve as a single step in the larger iteration process described below.

C. TCHEBYCHEFF APPROXIMATIONS FOR BOUNDARY FUNCTIONS

In the problems considered, the state and costate have been expressed as the continuous functions of ω and the Hamiltonian was expressed as an integral over ω. In actual practice, however, a digital computer cannot handle an entire function numerically. At best, one can establish a grid on ω and approximate the integral over ω as a sum over the grid. This was done in the program, selecting 11 discrete values for ω. The state and costate transition matrices were used only with these 11 values of ω, and all ω-integrals became sums over these 11 points.

Still, representation of the source impedance, load impedance, or impedance looking into the line [which determines our $x(-\ell, \omega)$ guess] each required 22 numbers: the real part and the imaginary part of the impedance over 11 frequencies. The load impedance, the guess on the initial impedance, or the resulting impedance at the other end of the line can thus be considered 22-vectors. Iteration to convergence in this 22-space seemed numerically unattractive, so it was decided to use a more compact (lower dimensional) representation of these impedance functions – the Tchebycheff approximation.

Each impedance function (defined over 11 points) may be considered as a sampled version of a linear combination of the first 11 Tchebycheff polynomials. These polynomials were selected because an approximation of this type tends to minimize the maximum approximation error over an interval ($\omega \epsilon \Omega$). Further, a series expansion of a function in Tchebycheff polynomials tends to converge far faster (in that interval) than some other polynomial expansion; it can be truncated sooner for the same error.

In the problem at hand, the Tchebycheff expansion was truncated after 4 terms, resulting in a cubic approximation for the real part and another for the imaginary part of each impedance function. Such a function is now described by 8 numbers instead of 22, and iteration proceeds in an 8-dimensional space. The Tchebycheff functions used for this approximation are shown in Fig. VI-2.

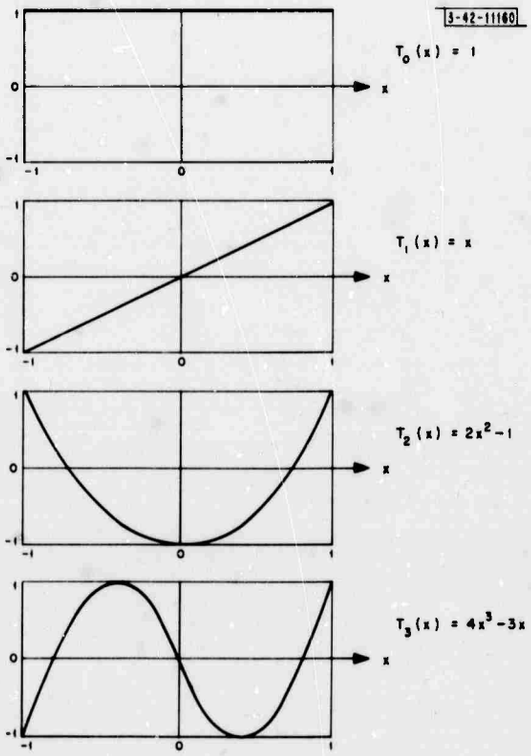

Fig. VI-2. First four Tchebycheff polynomials.

The real part of a load impedance is represented by 11 numbers (its value at 11 frequencies). To convert to four numbers (the first 4 coefficients of its Tchebycheff series expansion) it is necessary to multiply the original 11-vector by the 4×11 matrix, QUAD, described below.

First, form the 11×11 matrix A such that

$$A_{ij} = T_{j-1}\,[(i - 6)/5]$$

where T_{j-1} represents the $(j - 1)^{st}$ Tchebycheff polynomial.

Now

$$\text{TCHEB} = A \cdot \begin{bmatrix} 1 & & & \\ & 1 & & \\ & & 1 & \\ & & & 1 \\ \hline & & -0- & \end{bmatrix}$$ (an 11×4 matrix, actually a truncated version of A)

and

$$\text{QUAD} = \left[\begin{array}{cccc:c} 1 & & & & \\ & 1 & & & \\ & & 1 & & -0- \\ & & & 1 & \end{array}\right] \cdot A^{-1}$$ (a 4×11 matrix which is a truncated version of A^{-1}) .

A Tchebycheff quadrature is performed by premultiplying an 11-vector by QUAD, obtaining the 4-vector Tchebycheff representation. The opposite conversion is obtained by premultiplying the 4-vector Tchebycheff representation by TCHEB to obtain the equivalent 11-vector (function of frequency).

It is simple to verify that

$$\text{QUAD} \times \text{TCHEB} = \begin{bmatrix} 1 & & & -0- \\ & 1 & & \\ & & 1 & \\ -0- & & & 1 \end{bmatrix}$$, the 4×4 identity matrix ,

so the desired Tchebycheff quadrature (with truncation to four terms) has indeed been accomplished.

The program in Appendix C accepts these two matrices as input data before the beginning of computation. If for some reason one desired to expand the load impedances (functions of frequency) in a different polynomial series representation, say $p_n(x)$, it is only necessary to set

$$A_{ij} = P_{j-1}\,[(i-6)/5] \quad .$$

in the above procedure and input the two resulting matrices to the program in place of QUAD and TCHEB.

D. ITERATION ON BOUNDARY CONDITIONS

Now we have a compact 8-vector representation for impedance functions and a programmed procedure to map between such functions. Starting with an initial guess on the impedance presented by the coupler, map this into an impedance at the other end and express as an 8-vector. Repeat the process for eight small Tchebycheff variations on the initial guess (the first four Tchebycheff polynomials as variations to the real part, then the last four as variations to the imaginary part of our guess impedance). Form the 8×8 sensitivity matrix describing the

variation in the terminal 8-vector with respect to our 8 variations:

$$\text{SNSMAT}(i, j) = \frac{\partial \text{TBUFF}_i}{\partial \text{TGUESS}_j}$$

where TGUESS is the 8-vector Tchebycheff representation of our starting impedance guess, and TBUFF the representation of the resulting load impedance obtained by the mapping procedure of Fig. B-2.

To obtain a gradient vector in this 8-space describing the changes in TGUESS necessary to drive TBUFF to TLOAD, the representation for the actual load impedance we are attempting to match, a linear mapping is assumed between TGUESS and TBUFF; then

$$\text{GRAD} = \text{SNSMAT}^{-1} (\text{TLOAD} - \text{TBUFF}) \quad ,$$

the desired gradient vector.

If the mapping of Fig. B-2 were exactly linear, changing TGUESS by GRAD to obtain the new guess would drive TBUFF to TLOAD exactly in one step, thus providing immediate convergence of our boundary-function iteration scheme. In reality the mapping is not linear, so the process described above must repeat at this point, iterating until convergence is obtained. This procedure is flow charted in Fig. B-1. This Newton-Raphson procedure will converge quadratically fast when the mapping from guess impedance to resulting load impedance is approximately linear over a region containing both the starting guess and the final (solution) guess.

E. SUMMARY

We have described an iterative procedure that iterates on boundary conditions of the problem and, when it converges, provides quadratically fast convergence. Of course, this is only a general description which skips over the myriad of tiny details and special cases with which the programmer must concern himself.

For the sake of completeness, the entire program, written in Fortran-IV, is provided as Appendix C. This, plus the above general description, should permit mechanization of the same procedure on another system or in another language, such as ALGOL or PL-I.

BLANK PAGE

VII. LIMITATIONS OF THE PROCEDURE

A. SOLUTION FOR AN INTERVAL CONSTRAINT ON THE CONTROL

1. Introduction

In all of the problems considered to this point, the control u(z) [either C(z) or $\epsilon(z)$] has been constrained to lie in some discrete set:

$$u \epsilon \{u_1, u_2, \ldots u_m\} \quad .$$

This constraint was imposed for two reasons: first, the control function is then piecewise constant in z, permitting the use of transition matrices to propagate the state and costate down the line; this eliminates the necessity for numerical integration of the state and costate partial differential equations, yielding far better accuracy in considerably less computer time. If the control were merely constrained to lie in an interval U, the piecewise constant property of the control function would be lost and numerical integration would become a necessity.

The second reason for the discrete set constraint is convenience of physical realization. An interval constraint would yield a smoothly varying $\epsilon(z)$; however, a material having this same $\epsilon(z)$ is not readily obtainable and would be extremely difficult to synthesize. One would wind up making a piecewise constant approximation to this $\epsilon(z)$ by sandwiching very thin sheets of the various dielectrics; it would be far simpler in the first place to solve for the best piecewise constant $\epsilon(z)$ by using the discrete set constraint.

However, the solution to the problem when an interval constraint is imposed is quite important as a basis of comparison for the performance obtained when the control is constrained to a (more restrictive) discrete set having the same maximum and minimum value. For this reason, we will examine the interval constraint problem.

2. Sufficient Conditions

We consider the following system:

(a) A distributed parameter system whose state obeys the partial differential equation.

$$\frac{\partial x(z, \omega)}{\partial z} = A(\omega, u) \cdot x(z, \omega) \quad ; \quad \omega \epsilon \Omega \tag{7-1}$$

$$x(0, \omega) = x_o(\omega) \tag{7-2}$$

where $A(\omega, u)$ is linear in u.

(b) There is a cost functional on the control u(z) of the following form:

$$J\{x_o(\omega), u[-\ell, 0]\} = \int_{\omega \epsilon \Omega} K'(\omega)\, x(-\ell, \omega)\, d\omega + \Delta \int_{-\ell}^{o} \frac{(u - u_a)^2}{2}\, dz \tag{7-3}$$

We want now to find the optimal control u(z), $z \epsilon [-\ell, 0]$, which minimizes the value of the cost functional J. This minimization is subject to the constraint that u(z) is in the interval U for all $z \epsilon [-\ell, 0]$.

Define the Hamiltonian

$$H(x, p, u, z) = \int_{\omega \epsilon \Omega} p'(z, \omega)\, A(\omega, u)\, x(z, \omega)\, d\omega - \frac{\Delta}{2} (u - u_a)^2 \quad . \tag{7-4}$$

The sufficient conditions for optimality derived in Sec. II yield:

$$\frac{\partial x^*(z,\omega)}{\partial z} = \left[\frac{\delta H^*(x,p,u,z)}{\delta p^*}\right]' = A(z,u)\,x(z,\omega) \tag{7-5}$$

$$x(0,\omega) = x_o(\omega) \tag{7-6}$$

$$\frac{\partial p^*(z,\omega)}{\partial z} = -\left[\frac{\delta H(x,p,u,z)}{\delta x}\right]' = -A'(z,u)\,p(z,\omega) \tag{7-7}$$

$$p(-\ell,\omega) = K(\omega) \tag{7-8}$$

$$H(x^*, p^*, u^*, z) \geqslant H(x^*, p^*, \bar{u}, z) \quad \text{for all } \bar{u}\epsilon U \tag{7-9}$$

with equality holding only for $\bar{u} = u^*$.

The Frechet derivative of the optimal cost function $J(x, z)$ must exist:

$$\frac{\delta J(x,z)}{\delta x}$$

is a valid Frechet derivative, i.e.,

$$\lim_{\int_{\omega\epsilon\Omega}|h(\omega)|\,d\omega\to 0} \frac{J[x(\omega)+h(\omega),z] - J[x(\omega),z]}{\int_{\omega\epsilon\Omega} h(\omega)\,d\omega} \tag{7-10}$$

exists for all $h(\omega)$ having compact support in Ω.

First, examine the validity of Eq. (7-10) in the present system; this required Frechet derivative certainly exists for $z = -\ell$, because we can differentiate Eq. (7-3) with respect to $x(-\ell, \omega)$ to obtain:

$$\frac{\delta J\,[x(-\ell,\omega),-\ell]}{\delta x(-\ell,\omega)} = K(\omega) = p(-\ell,\omega) \quad . \tag{7-11}$$

$\delta J/\delta x$ obeys the same partial differential equation as $p(-\ell, \omega)$ if it exists:

$$\frac{\partial}{\partial z}\left\{\frac{\delta J}{\delta x}[x(\omega),z]\right\} = -A'(\omega,u)\left\{\frac{\delta J}{\delta x}[x(\omega),z]\right\} \tag{7-12}$$

so $\delta J/\delta x$ merely obeys a linear partial differential equation.

Since $\delta J/\delta x$ is well defined at the boundary $z = -\ell$ [and is there equal to $K(\omega)$], it will be well defined for all $z\epsilon\,[-\ell, 0]$. The system does satisfy the sufficient condition Eq. (7-10).

Now check the validity of sufficient condition, Eq. (7-9): we know that $u(z)$ is independent of ω and $A(\omega, u)$ is linear in u. The u may then be taken outside the frequency integral in Eq. (7-4), demonstrating that the Hamiltonian is a function of u of the form

$$H(x,p,u,z) = -\frac{\Delta}{2}(u-u_a)^2 + M\cdot u + \text{constant} \quad . \tag{7-13}$$

Since $\Delta > 0$, there is a uniquely maximizing value of $u\epsilon U$:

$$u^* = \begin{cases} u_a + M/\Delta & \text{if } u_a + M/\Delta \text{ is in interval } U \\ u_{MIN} & \text{if } u_a + M/\Delta < \text{every } u\epsilon U \\ u_{MAX} & \text{if } u_a + M/\Delta > \text{every } u\epsilon U \end{cases} \quad . \tag{7-14}$$

Thus, the system under consideration satisfies sufficiency condition Eq. (7-9). The remaining conditions are exactly the same as the necessary conditions for the same system; if any solution u(z) is found which satisfies the (necessary) conditions Eq. (7-5) to (7-9), then this solution is the unique globally optimal solution under the constraint $u \in$ interval U.

Merely solving the necessary conditions for $u \in U$ yields the unique optimal control which will be the basis for our performance comparisons. Since the set $\{u_1, u_2, \ldots u_m\}$ is a subset of U, the value of the cost functional for the discrete set constraint must be $\geq$ the cost functional for the less restrictive $u \in U$ constraint.

In the limit, as the set $\{u_1, u_2, \ldots u_m\}$ is allowed enough members to become dense on the interval U, the optimal cost functional for this constraint approaches the cost for the interval constraint. In addition, the control function $u^*(z)$ converges in the L_1 norm to the control function for the interval constraint because of the uniqueness property of this solution and the smoothness (Lipschitz condition) of the system partial differential equations.

B. SOLUTIONS OBTAINED FOR CONTROL CONSTRAINED TO A DISCRETE SET

1. A First Variation Test

Let us suppose that by numerical means we have found a solution u(z), $x(z, \omega)$, $p(z, \omega)$ for $z \in [-\ell, 0]$ and $\omega \in \Omega$ which satisfies all the necessary conditions Eqs. (3-6), (3-7), (3-8), (3-16) under the constraint $u \in \{u_1, u_2, \ldots u_m\}$.

This control u(z) is necessarily a piecewise constant, and is a candidate for the optimal control. It is, of course, not guaranteed to be the optimal control because it satisfies only necessary, not sufficient, conditions. In this case, the sufficient condition of Eq. (7-10) (cost smooth in x) is satisfied, but the requirement for a u which uniquely maximizes the Hamiltonian is not satisfied whenever two u values are equally close to $u_a + M/\Delta$.

First, let us suppose that this candidate solution does not correspond to a singular extremal, i.e., the

$$\frac{dM}{dz} = \frac{d^2M}{dz^2} = 0$$

relations were not explicitly used during the solution of necessary conditions of Eqs. (3-6) to (3-8) and (3-16). Now we can interpret the results of the maximum principle. Note that the control variation analyzed to derive the necessary conditions of Sec. II is a first variation, in particular, a narrow pulse added to the candidate control function. The result is: if the necessary conditions of Eqs. (3-6) to (3-9) are satisfied, such a variation of the control can only increase the cost J. Two examples of this type of perturbation on the control are shown in Fig. VII-1 applied to a candidate control which is a switching solution.

As shown in Fig. VII-1, the specified first variations may merely correspond to a first order (ϵ-sized) change in switching time τ. The analysis yielded the result that $\delta J \geq 0$ for each variation, $\delta J = 0$ for $\epsilon = 0$, and J is continuous in ϵ. These combine to yield:

$$\left.\frac{\delta J}{\delta \tau}\right|_{\tau^*} = 0 \quad \text{and} \quad J(\tau^*) \leq J(\tau) \quad \text{for } \tau \approx \tau^*$$

where we are considering the switching time τ to be the independent variable we are perturbing.

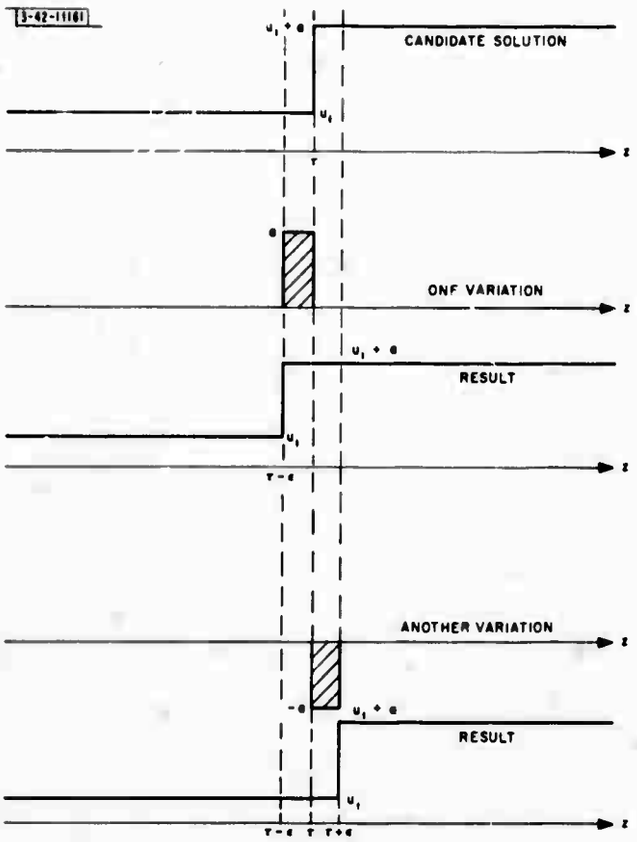

Fig. VII-1. Two possible first variations.

In short, if a candidate switching solution u(t) satisfies the necessary conditions of Eqs. (3-6) to (3-9) then the cost J is at a local minimum with respect to each of the switching times τ_i; any perturbation of these times can only increase the cost J.

2. A Second Variation Test

Now we consider a second variation of the control u(t), in particular:

$$u(t) = \begin{cases} 0 & \text{for } t \notin [\tau - \epsilon, \tau + \epsilon] \\ a & \text{for } t \in [\tau - \epsilon, \tau] \\ -a & \text{for } t \in [\tau, \tau + \epsilon] \end{cases} .$$

Such a perturbation may be called a "doublet" pulse.

To utilize the results of previous work dealing with second variation tests, we must first define a modified Hamiltonian:

$$\hat{H}(x, p, u, t) = \text{convex cover of } H(x, p, u, t) \quad .$$

The function $\hat{H}(x, p, u, t)$ is a linear function of u and

$$\left(\frac{\partial^2 \hat{H}}{\partial u^2}\right) = 0$$

over intervals of u where H is undefined ($u \notin \{u_1, u_2, \ldots u_m\}$), performing a linear interpolation between points $u_1, u_2, \ldots u_m$ where H is defined.

Assuming that the candidate switching solution is not a singular extremal, then it is easily seen that minimizing $\hat{H}(x, p, u, t)$ with respect to u yields precisely the same switching solution as in Eq. (3-16) which minimizes H(x, p, u, t). This requirement may be substituted for Eq. (3-16) yielding the relation

$$\frac{\partial^2 \hat{H}}{\partial u^2} = 0$$

over every interval of u where switching occurs between the endpoints.

Now we may use the results of H. J. Kelley[31] in determining the second variation of the cost under the "doublet" control variation described above. The result is

$$\delta^2 J = -\frac{2}{3} a^2 \epsilon^3 \frac{\partial}{\partial u}\left(\frac{d^2}{dz^2}\frac{\partial H}{\partial u}\right) + \text{higher order terms in } \epsilon \qquad (7\text{-}15)$$

as long as the perturbed control remains in an interval of u where

$$\frac{\partial^2 H}{\partial u^2} = 0 \quad .$$

Thus, if

$$\frac{\partial}{\partial u}\left[\frac{d^2}{dz^2}\left(\frac{\partial H}{\partial u}\right)\right] \leq 0$$

no second variation on the control will reduce the cost. If, however, this term is positive, an allowable second variation will reduce the cost; the candidate solution is not optimal.

An allowable second variation is shown in Fig. VII-2: note that the effect of this variation is to cause a "chattering" transition rather than a single switch. The cost can be reduced still more (assuming that

$$\frac{\partial}{\partial u}\left[\frac{d^2}{dz^2}\left(\frac{\partial H}{\partial u}\right)\right] > 0$$

at each of the three switching times of Fig. VII-2) by making additional second variations, i.e., turning each of the three transitions into a 3-transition chatter (see Fig. VII-3). Similarly, we reduce the cost by going from 9 to 27 transitions, etc. The limit of this process is not well defined, as it corresponds to infinitely fast chattering over some interval of time, in particular, the interval of time where

$$\frac{\partial}{\partial u}\left[\frac{d^2}{dz^2}\left(\frac{\partial H}{\partial u}\right)\right] > 0 \quad .$$

However, an interpretation of this control behavior is still possible in terms of duty cycle: if u(t) is chattering infinitely fast between u_1 and u_2, taking on the value of u_1 a fraction K of the time and u_2 a fraction (1 − K) of the time (of course, these fractions must be defined as Lebesque integrals on the measure-space of a distance), then the trajectories of the state and costate are identical to those observed when the control takes on the value $Ku_1 + (1 - K)\, u_2$ (Ref. 32).

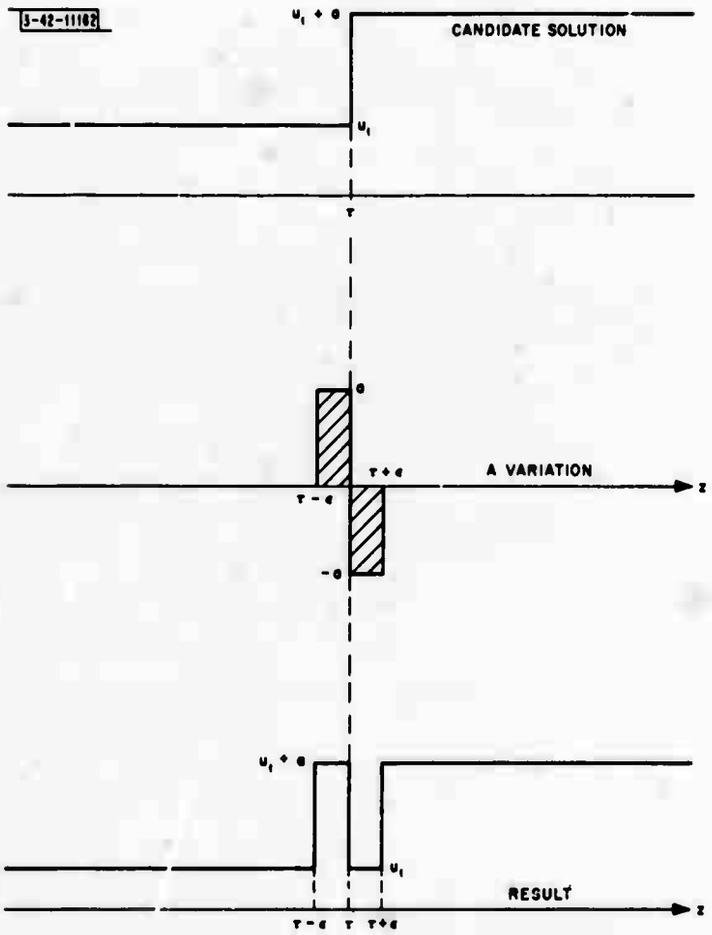

Fig. VII-2. A possible second variation.

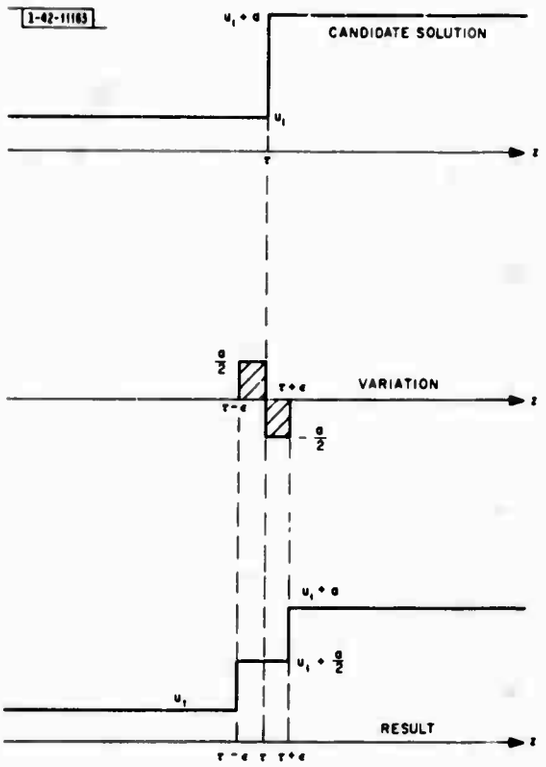

Fig. VII-3. Another possible second variation.

This behavior,

$$\frac{\partial}{\partial u}\left[\frac{d^2}{dz^2}\left(\frac{\partial H}{\partial u}\right)\right] > 0 \quad , \quad \text{i.e.,} \int_{\Omega} \omega^3 (x_3 p_2 + x_1 p_3)\, d\omega < 0 \tag{7-16}$$

at a switching point, implies that the candidate solution, which makes a single transition at the switch point, is inferior to a control which takes on intermediate values around the switch point – a continuous change from u_1 to u_2 will result in a lower cost. This smooth transition takes place over the interval where Eq. (7-16) holds.

This simple test [Eq. (7-16)] permits us to evaluate the performance of the candidate solution by comparison with the solution obtained in Sec. VIIA under an interval constraint. Let the optimal cost for this interval constraint be denoted by J_1, and the (sometimes continuously varying) control function by $u_1(z)$.

At each switching point of the candidate solution, if relation (7-16) fails to hold, then the "doublet" control perturbation at that point will merely increase the cost functional. This happens over those regions of z where "bang-bang" solutions u(z) appear, switching between u_{MIN} and u_{MAX}. This says that around the switch point in question, u(z) provides an optimal approximation to $u_1(z)$ under the constraints imposed. On the other hand, at switch points where Eq. (7-16) holds, there should be a continuous transition rather than a step discontinuity; a control perturbation that approaches this smooth $u_1(z)$ transition will decrease the cost because $\delta^2 J < 0$ (see Fig. VII-4).

Instead of approaching the $u_1(z)$ behavior by incorporating infinitely fast "chattering" (which is impractical for a digital computer numerical scheme), we need merely relax the control

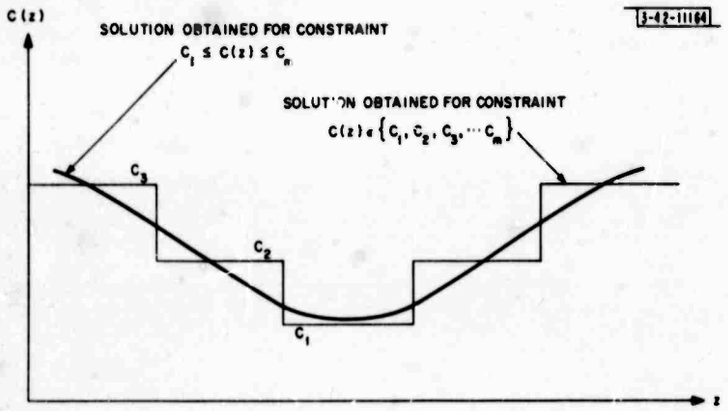

Fig. VII-4. Stairstep approximation to continuous C*(z) solution.

constraint $u \in \{u_1, u_2, \ldots u_m\}$; we add admissible control values $\{u_{m+1}, u_{m+2}, \ldots u_n\}$, which fall between the previous values. The cost for these new control values is such that

$$H(x, p, u_{K+1}) - 2H(x, p, u_{K+1/2}) + H(x, p, u_K) > 0 \qquad (7\text{-}17)$$

where

$$u_K < u_{K+1/2} < u_{K+1} \quad .$$

This is a type of convexity defined over discrete points of u. Again take $\hat{H}(x, p, u, t)$ as the convex cover of $H(x, p, u, t)$.

The algorithm previously used will now converge to a switching solution which takes on the newly defined intermediate values of control over intervals of time where before there was a single transition between u_K and u_{K+1}. This stairstep behavior is shown in Fig. VI-1, and this "interpolating" behavior is a consequence of the fact that M(z) is a continuous function of z.

The total cost of this solution will be less than the previous solution because a second variation decreases the cost as long as Eq. (7-16) holds. The convexity assured by Eq. (7-17) further decreases the cost, making it less expensive to take on the value

$$\frac{u_{K+1} + u_K}{2}$$

than chattering infinitely fast with 50 percent duty cycle between u_{K+1} and u_K. However, assuming that Eq. (7-16) still holds at each of the two switch points in Fig. VI-1, the cost could be reduced still more by providing a smooth transition rather than a switching for each.

The same argument again applies, so defining a still finer grid of permissible u values and repeating the solution of Eqs. (3-6) to (3-8) and (3-16) will result in a lower cost.

Making the partition on available values of u increasingly finer can only decrease the value of the cost functional J, because the new solution corresponds to a less restrictive set of constraints on the problem. The cost obtainable as the partition becomes finer is bounded from below by the cost J_I corresponding to the solution with an interval constraint on the control.

Since J is monotone nonincreasing and bounded from below as the fineness of partition is increased, it must approach a limit J*. In fact, $J^* = J_I$ and u(z) converges (in L_1 norm) to $u_I(z)$, the unique control solution for an interval constraint, as the points of available capacity

become more dense in the interval U. [This is a consequence of the smoothness (Lipschitz condition) of the system partial differential equations.]

This result provides a straightforward means of evaluating just how close to optimal (in terms of cost) a particular suboptimal solution is. Having obtained the solution and the cost J_n when we are constrained to n values of capacity, repeat the solution with finer partition to obtain J_{2n}, J_{4n}, etc. When one is satisfied that the cost has converged, i.e., a finer partitioning of available capacity values will not result in a cost which is measurably lower, then that cost equals $J^* = J_1$. The cost improvement that has been obtained through finer partitioning is precisely the amount by which the original candidate was suboptimal.

This process of obtaining solutions for successively finer partitions on u may be viewed as a method of numerical integration of the differential equations which correspond to solution of the necessary conditions with an interval constraint on the control. In this case, discretization occurs for the interval U, rather than the more common discretization of $[-\ell, 0]$. As with any scheme for numerical integration, the burden lies on the user to decide when partitioning is sufficiently fine, i.e., when making the partition still finer will not result in a significant change in cost.

3. Discussion

We have noted previously that a candidate switching solution which satisfies Eqs. (3-6) to (3-8) and (3-16), minimizes the cost with respect to each of the switching times τ_i: any perturbations of these times can only increase the cost. If Eq. (7-16) does not hold at these switch times, even a second variation cannot decrease the cost. However, at those switch points where Eq. (7-16) holds, the cost may be reduced by either the chattering behavior shown in Fig. VII-2, or the stair-step control behavior shown in Fig. VII-3.

Either of these changes increases the number of switchings in the control function. If there is some realistic cost associated with the total number of switchings (viz., the cost of cutting and assembling many different lengths of dielectric material) there will be a trade-off between the two costs; increasing the fineness of the grid on u (thus increasing the number of switchings) without limit can only reduce the cost J to J_1, that achieved by the control $u_1(z)$.

One thus enjoys the consolation that a candidate solution which satisfies Eqs. (3-6) to (3-8) and (3-16) is at least optimal when the number of switchings is constrained to the number appearing in the solution. To decrease the cost, the number of switchings must be increased; when there is some nonzero cost associated with the number of switchings, the point of diminishing returns is reached very rapidly.

4. Conclusion

The sign of

$$\frac{\partial}{\partial u}\left[\frac{d^2}{dz^2}\left(\frac{\partial H}{\partial u}\right)\right]$$

at switching times of a candidate switching solution tells whether the candidate is optimal or whether there is a singular extremal of lower cost. When the singular extremal is better, the cost of the solution may be decreased by increasing the fineness of the grid on admissible values of u: repeated solution of the necessary conditions [Eqs. (3-6) to (3-8) and (3-16)] will yield a

control function which has a cost closer to the lower bound J_I. In fact, solution for successively finer partitions will provide a measure of J_I and thus a measure of the suboptimality of our switching solution.

However, this lower cost is achieved only at the expense of an increased number of switchings. This process automatically yields a trade-off between complexity of the control function (number of switchings and dollar cost of constructing the indicated structure) and the cost achieved.

C. FAILURE OF CONVERGENCE – THE SINGULAR EXTREMAL

In the previous discussion (Sec. VIIB), we assumed that the numerically derived numerical solution did not correspond to a singular extremal. However, we found that in many cases [where Eq. (7-16) holds] there is a nearby singular extremal which provides a lower cost.

One interesting question to ask is, "What happens when the numerical solution tries to track the singular extremal exactly? Does the infinitely fast switching behavior (approximating $u_I(z)$ and yielding cost J_I) appear in the numerical results?" To answer these questions, we need only examine the implications of Eq. (7-16): (we assume in the following that relation (7-16) does hold, i.e., that our candidate solution is suboptimal).

$$\frac{\partial}{\partial u}\left[\frac{d^2}{dz^2}\left(\frac{\partial H}{\partial u}\right)\right] > 0 \quad .$$

On this singular extremal, the multiplier function $M = \partial H/\partial u$ is on a boundary such that both u_k and u_{k+1} maximize the Hamiltonian; if M were only slightly larger, the unique choice from Eq. (3-16) would be u_{k+1}. (Here $u_{k+1} > u_k$). If M were slightly smaller, the unique choice is u_k. We also have the relation $dM/dz = 0$ on this extremal, so M is precisely tracking (in z) the value which causes ambiguity in u (see Fig. VII-5).

First, suppose that we are "integrating" the state and costate equations forward in z, obtaining the function M(z) from $x(z, \omega)$ and $p(z, \omega)$ at each point, then finding u(z) from M(z). Now suppose that due to finite numerical resolution on M(z), the control value u_{k+1} is selected.

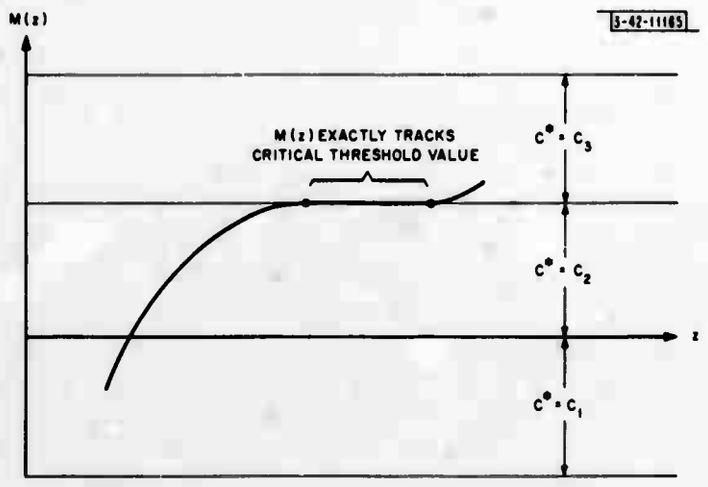

Fig. VII-5. M(z) versus z in the case of a singular extremum.

(This value is, of course, larger than the intermediate control which would be derived from Eq. (3-18) and realized by infinitely fast chattering between u_k and u_{k+1}.)

Since, by assumption,

$$\frac{\partial}{\partial u}\left(\frac{d^2M}{dz^2}\right) > 0 \quad ,$$

in the next distance dz, d^2M/dz^2 will be > 0, and dM/dz > 0, so M increases above its threshold value corresponding to the singular extremal. Since M is now larger, the u_{k+1} selected by accident is now the unique choice of Eq. (3-16); we have left the singular extremal. An identical argument shows that if u_k had been selected instead, M would decrease and we would leave the singular extremal with unique control choice u_k.

Thus, the singular extremal is unstable with respect to integration in the forward direction whenever Eq. (7-16) holds; the numerical solution will very soon "fall off" this trajectory. Further, an infinitesimal change in the initial conditions at the beginning of the singular trajectory can make a large difference in the distance Δz before the solution "falls off" (diverges) and even in the direction in which the solution diverges. For this reason, infinitesimal changes in the initial state and costate will map into large changes in the terminal state and costate whenever a portion of the trajectory is a singular extremal (or appears to be within the numerical accuracy of the machine).

Interestingly enough, the singular extremal is not only unstable with respect to integration in the forward direction, it is also unstable when the equations are integrated in the backward $(-z)$ direction. A simple repetition of the above argument with z replaced by $-z$ will verify this:

$$\frac{d^2M}{dz^2} = \frac{d^2M}{d(-z)^2} \quad .$$

This means that an infinitesimal change in the terminal state and costate will map into a large change in the initial state and costate if a portion of the trajectory is (within measurement accuracy) a singular extremal.

This answers questions about whether fast chattering should show up in numerical results (it should not, because independent of the direction of integration, the solution very quickly diverges from the singular extremal). Moreover, it points up an important limitation of the numerical technique described in Sec. VI.

The basic technique used there is an iteration on the boundary conditions until all are solved; the convergence properties of this iteration are based on a smooth mapping between initial state and costate and the terminal state and costate; a small change in these functions at one end of the line must map into a small change at the other, and when the changes are sufficiently small, this mapping is approximately linear. As a matter of fact, this linear mapping shows up as a sensitivity matrix in the Newton-Raphson procedure employed.

However, when part of the trajectory is a singular extremal, this smoothness of mapping (and linearity for small changes) is lost. The instability shows up whether we are integrating in the forward or reverse direction, so it makes no difference which boundary condition we are iterating upon. In such a case, the procedure of Sec. VI will, in general, not converge. Any scheme which iterates on boundary conditions is useless for solving singular extremal trajectories.

Whether the numerical procedure does "get onto" a singular extremal is critically dependent on two factors: the first is the choice of the set of available u values $\{u_1, u_2, \ldots u_m\}$, because this set determines the threshold values of M where ambiguities in u occur. A change in the constraint set U may be adequate to remove the singular extremal problem and its instabilities for a given source and load. The second factor is the exact values of the state and costate functions at the end of the line where iterations begin; a very slight change in the source impedance may cause a sufficient change in these functions so that the procedure no longer "gets onto" the singular trajectory for that choice of $\{u_1, u_2, \ldots u_m\}$. In Fig. VII-5, an infinitesimal change in either the function M(z) or the threshold value between different capacity regions will eliminate this singular extremal behavior.

Since we are generally interested in solving the design problem for a sequence of successively finer grids on the available controls u, the first suggestion above is the more natural way to escape convergence troubles when a singular extremal shows up. This suggests the following scheme:

During an iteration, the program checks for simultaneous occurrence of the three conditions:

(a) $M \approx$ a threshold value which gives an ambiguity in u (7-18)

(b) $\frac{dM}{dz} \approx 0$ (7-19)

(c) $\frac{\partial}{\partial u} \frac{d^2M}{dz^2} > 0$. (7-20)

When all three of the above conditions occur, the procedure is attempting to iterate along a singular extremal; all hope of convergence on future iterations is lost.

Abort the run on the present problem, define a new problem with a different (generally more finely partitioned) discrete constraint set $\{u_1, u_2, \ldots u_m\}$, and begin iterating with the same state and costate functions used in the last iteration. The new trajectory will generally miss the singular extremal [having provided a slight change in M(z)] and should eventually converge.

D. RECOMMENDATIONS

The first limitation of the procedure outlined in Sec. VI is that the solutions will appear which are merely suboptimal. These are piecewise continuous approximations to the optimal solution, which contains infinitely fast chattering.

The recommended procedure is then to solve the necessary conditions of Eqs. (3-6) to (3-8) and (3-16) for a number of successively finer grids on available U, in each case indicating the region of z where Eq. (7-16) holds. Over these regions there is a nearby singular extremal having lower cost, and we may expect to obtain improvement by a yet finer partitioning on the range of available controls. In the limit as this grid becomes dense, we approach the previously derived global optimal control $u_1(z)$ and the lower bound on cost, J_1. However, this cost improvement occurs only at the expense of increased control complexity; the person constructing the physical realization for u(z) will most likely pick a tradeoff point corresponding to a very gross grid on u(z). This will be especially true because the cost decrease due to finer partitioning reflects the amount of curvature in the Hamiltonian; this curvature is extremely small.

The second limitation is that convergence difficulties may appear because a singular extremal subarc appears in the numerical solution of the necessary conditions of Eqs. (3-6) to (3-8) and (3-16). During the iteration, such an occurrence will be signaled by the relations in Eqs. (7-18), (7-19) and (7-20) being simultaneously true. In such a case, the run has little chance of convergence and should be aborted. The problem can then be run for a different and finer partition on the available U, which will change the threshold values of M and generally cause the new trajectory to miss the singular extremal.

If, however, due to overriding physical considerations, one were forced to solve the design problem for the precise constraint set, source and load specified, then the only reasonable way to proceed (in the singular extremal case) is to convert to a numerical scheme which performs its iterations in the policy space of u(z) rather than iterating on the boundary conditions.

One such scheme could involve iterating on the switch point locations z where u changes value. However, this type of scheme also suffers from a number of difficulties, and it is not clear whether such a procedure would generally be an improvement on the boundary-function iteration method of Sec. VI.

BLANK PAGE

VIII. NUMERICAL RESULTS

A. RESULTS OBTAINED ON THE SDS-940 COMPUTER

1. Introduction

Computer time was made available by Bolt Beranek and Newman Inc., for implementation of the procedure described in Sec. VI. The computer used was the research computer of the Interactive Systems Division, an SDS-940 operating as a general purpose, time-sharing system. The programming language selected for this implementation was CAL, Conversational Algebraic Language, an interpreter/incremental compiler that features on-line interactive program running, debugging and editing.

Because of the interactive ability of the system, the size of step to be taken for each successive iteration in the boundary-function space (the size of the vector GRAD) was not determined automatically. Instead, the program would type out the results of each iteration and permit the user to select a step size based on his estimate of how well convergence was proceeding. Of course, in a later implementation of the program operated under a batch-processing system, such interaction was impossible and the above decision process was automated (accomplished by the program itself).

2. Examples of Transmission Line Problem

The problems run on the SDS-940 were all examples of the transmission line impedance matching problem described in Sec. IV. To make the problem realistic, the basic parameters were taken from the standard RG-8U coaxial cable:

$$L(z) \equiv 80.16 \times 10^{-6} \text{ henrys/ft} \quad , \quad CMIN = 29.5 \times 10^{-12} \text{ farads/ft} \quad .$$

The characteristic impedance of this cable is 52.2 ohms, and this was selected to be the source impedance at $z = -\ell$ for all frequencies (a resistive source perfectly matched to the unmodified RG-8/U cable).

CMAX was selected to be 2^* CMIN, a condition which could be realized by filling a section of the cable with dielectric having twice the dielectric constant of the standard filler material. The frequency band of interest was selected as 50 to 70 Mc, and the source was assumed to have a uniform available power density $S(\omega)$ over this frequency interval. (This would be considered a wide-band impedance matching problem because it involves a 33-1/3 percent bandwidth around the center frequency of 60 Mc.)

The line length was selected to correspond to one wavelength in the CMIN material at 60 Mc, or 10.82 ft.

This procedure was then solved (using the procedure of Sec. VI) for a number of different load impedances, ranging from resistances of $8 \times R_o = 8 \times 52.2$ ohms to $2.5 \times R_o$. Complex (reactive) load impedances were not considered.

Figure VIII-1 shows a typical result obtained using this procedure. The source was connected at $z = -\ell$ (the left side of the graph) and the load of a resistor equal to $2.5\ R_o$ connected at $z = 0$. The total available power was 52.2 watts, of which 2.1 watts was reflected due to impedance mismatch. The VSWR (voltage standing-wave ratio) between the source and load in the absence of an impedance matching device would be 2.5 to 1; this one-wavelength coupler has reduced it to 1.5 to 1. The cost from the added term which is quadratic in capacity was

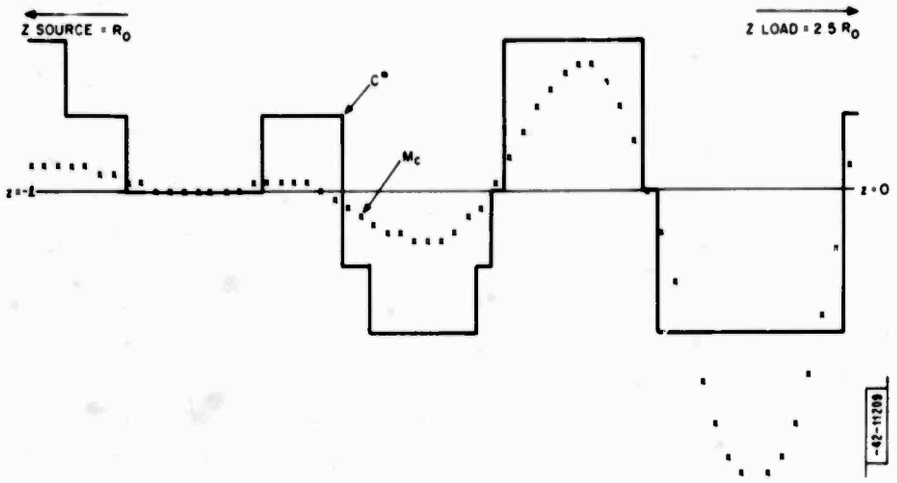

Fig. VIII-1. Plot of C(z) and M(z) for typical transmission line solution.

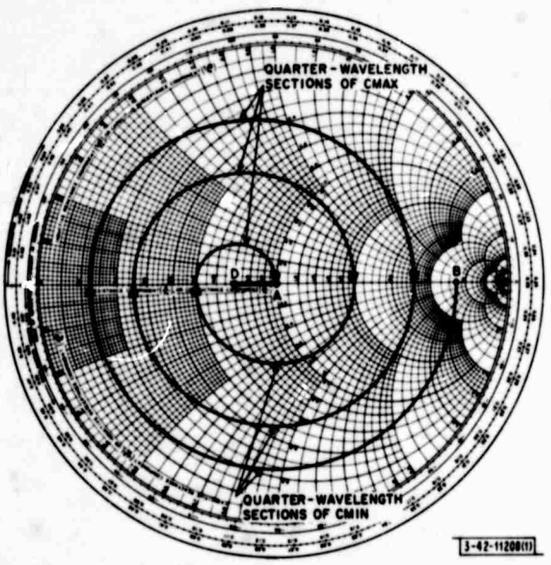

Fig. VIII-2. Impedonce matching using successive quarter-wove sections.

unrealistically large in this particular example, amounting to 0.5 watt, or 25 percent of the cost due to reflected power. This solution should be run again with the quadratic cost term (QCOST) about ten times smaller to obtain a solution which does a better job of minimizing reflected power per se.

The two functions plotted in Fig. VIII-1 are the capacity multiplier function $M_c(z)$ (represented by x's) and the capacity $C^*(z)$ obtained (the solid black line). The center line represents the zero for $M_c(z)$, but the zero for C(z) is located at the bottom of the page ($29.5\,pf/ft \leq C(z) \leq 59\,pf/ft$). The two functions are overlaid to show the close correlation in their variations. As indicated, there were five available values for capacity per unit length, ranging in equal steps between CMIN and CMAX.

We note that over intervals of z when $M_c(z)$ is sufficiently negative, $C^*(z)$ takes on the value CMIN; when $M_c(z)$ is sufficiently positive, $C^*(z)$ takes on value CMAX. However, for intermediate values of $M_c(z)$ (≈ 0), $C^*(z)$ takes on the three values available to it which are intermediate between CMIN and CMAX, as indicated by Eq. (3-16).

There is one particularly important aspect of this solution; at the right-hand end of the line where the load $2.5\,R_o$ is connected, $M_c(z)$ goes through large sinusoid-like variations having successive zero-crossings about 1/4 electrical wavelength apart. (An electrical wavelength is $\sqrt{2}$ times shorter in the CMAX material than in the CMIN material.) These large excursions in $M_c(z)$ cause rapid switching of $C^*(z)$ between CMIN and CMAX over successive intervals of 1/4 electrical wavelength. If the quadratic cost term were made considerably smaller (as it in fact should be) then the region of M_c values giving rise to intermediate $C^*(z)$ values would shrink to a very narrow band around zero. This would cause the previously mentioned switchings between CMIN and CMAX to become sharper (occur over a smaller distance) so the C(z) waveform at the right end of the line would approach a "bang-bang" solution, switching between CMIN and CMAX over successive intervals about 1/4 electrical wavelength apart. This same behavior was noted not only in the 2.5:1 match above, but also in the other problems ranging up to an 8:1 match, and even in the waveguide problems described in the next section.

To understand what is happening in terms of impedance matching, we look at an 8:1 impedance matching method on the Smith Chart of Fig. VIII-2. For clarity, we consider matching at only a single frequency, rather than over an interval of frequencies. The source will be a resistor R_o, represented by the center (A) of the Smith Chart; the load will be a resistor $8\,R_o$, represented by the point (B). The available capacities CMIN and CMAX = 2 CMIN correspond to impedances R_o (Point A) and $R_o/\sqrt{2}$ (Point D). Moving down the line from load B toward source A is represented on this chart by a circular motion around a center specified by the capacity in use: center A for C = CMIN, center D for C = CMAX. To achieve a perfect impedance match, we wish to describe a trajectory from B to A using the smallest possible electrical length (rotation on chart).

This optimal match is obtained as follows: starting at the load end (Point B) use 1/4 electrical wavelength of CMIN: this results in 180° rotation about center A on the chart. Now use 1/4 electrical wavelength of CMAX, for 180° rotation about Point D. Repeating this sequence twice more results in spiraling inward from B to A, achieving perfect match with 3/4 electrical wavelength of CMIN and the same for CMAX.

It is easy to convince oneself that the use at any time of a capacity intermediate between CMIN and CMAX (corresponding to rotation about a center between A and D) will result in a slower inward spiraling and hence will require a longer electrical length to achieve the same match.

This is then the reason for the appearance of "bang-bang" solutions switching between CMIN and CMAX over successive 1/4-electrical wavelength intervals near the high-resistance load: this resistance is being "pumped" in toward the origin by the same mechanism indicated in Fig. VIII-2.

This "bang-bang" behavior is only apparent at the right end of the line, however; at the left side is a region where $M_c(z) \approx 0$, causing $C^*(z)$ to take on intermediate values. If $M_c(z)$ is equal to zero over an interval, then making the quadratic cost QCOST arbitrarily small will not change this behavior: $C^*(z)$ will still take on intermediate values. Such behavior appears to be the case in all examples studied, so it is expected that, in general, as QCOST is made arbitrarily small, the solution $C^*(z)$ will converge to a function that is "bang-bang" over part of the line (like the successive 1/4 electrical wavelengths near the high resistance load) and takes on intermediate values over the remainder of the line.

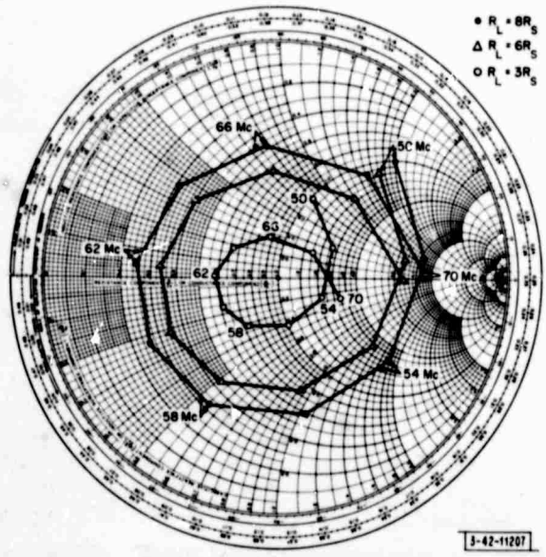

Fig. VIII-3. Performance of some transmission line solutions.

The performance obtained in the 8:1, 6:1 and 3:1 resistive matching problems studied is shown in Fig. VIII-3. Here we plot on the Smith Chart the normalized impedance (as a function of frequency) seen by the 52.2-ohm source looking to the right into the coupler; the magnitude of the reflection coefficient $\rho(\omega)$ is represented by the radial distance from the origin to the impedance curve.

The striking result is that the resulting impedance functions wrap uniformly around the origin, maintaining almost constant $|\rho(\omega)|$ over the entire frequency band. This behavior, a uniformly good match at all frequencies rather than a perfect match at some frequencies and poor match at others, was predicted in Sec. I and by the results of Appendix I.

3. Conclusions

The transmission line problems studied all show a bang-bang behavior in C(z) near the high resistance load, switching between CMAX and CMIN over successive 1/4 electrical wavelengths. Such behavior is expected to be common in the case of severe mismatches, as this behavior pumps the impedance level down toward the origin of the Smith Chart (indicating perfect match) as fast as possible (in the minimum electrical length). Over other regions of the line, however (in particular, near the source which is matched to the CMIN characteristic impedance of the line), the function $C^*(z)$ takes on intermediate values of capacity and is expected to do so even when QCOST is made arbitrarily small. The resulting matching structure tends to provide an equally good impedance match at all frequencies of interest.

B. RESULTS USING THE IBM-360 COMPUTER

1. Introduction

Computer time was made available by the M.I.T. Lincoln Laboratory Group 42 for implementation of the program described in Sec. VI. The computer used was the IBM-360, Model 65, and the language selected for the implementation was Fortran-IV-G. The source program is maintained as a card deck and is submitted for runs under a batch-processing monitor.

Since no interaction is possible between the user and the program running in this mode, the programmed procedure was made fully automatic. This automation was accomplished by requiring as input, besides the cards specifying the parameters of the problem, a set of control cards which specify the maximum number of iterations to be performed, the maximum step size in the Newton-Raphson procedure, and flags indicating whether the initial guess for the impedance presented by the coupler to the source should be read in from additional cards, generated by the program itself, or be set equal to the impedance obtained during the final iteration of the previous problem solution.

A number of different problems can be run in one session by stacking as many control decks plus parameter specification decks as one desires in the input deck submitted. The procedure will terminate the run of one problem and read in the next control deck and parameter deck to start the next problem, under any of the four following conditions:

(a) The procedure has converged to the desired boundary function impedance.

(b) The procedure has performed the indicated maximum number of iterations on the problem.

(c) Input parameters are specified improperly; for example, the waveguide width is too narrow to permit propagation of real power at the frequencies of interest.

(d) The iteration is proceeding along a singular extremal trajectory and thus has no hope of convergence.

The parameter specification deck includes specification of the problem type (waveguide or transmission line), the waveguide width if the problem type is waveguide, the length of the structure, the inductance value (inductance per unit length for transmission line, μ_o for waveguide), the maximum available values of the control parameter (capacity per unit length in transmission line, ϵ in the waveguide), the center frequency and bandwidth of operation, the desired load impedances sampled at eleven equally-spaced frequencies across this band, the available power at each of the above frequencies. In addition, an upper bound on the cost due to quadratic control term, QCOST, and the number of available control values, NVALS, are specified. These available control values are then taken to be equally spaced between the max and min available values specified earlier.

This procedure was run for a number of variations on a particular problem to determine the change in cost and in the control parameter function when the parameters NVALS, QCOST, and length are changed in the problem specification. The results obtained are described below.

2. A Practical Waveguide Example

One problem of particular interest for practical application was studied extensively: the problem of obtaining a good impedance match between a narrow slot which forms one element

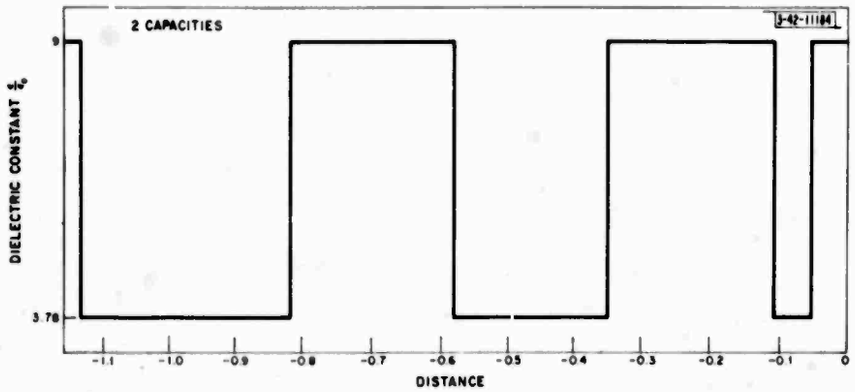

Fig. VIII-4. Waveguide solution for NVALS = 2.

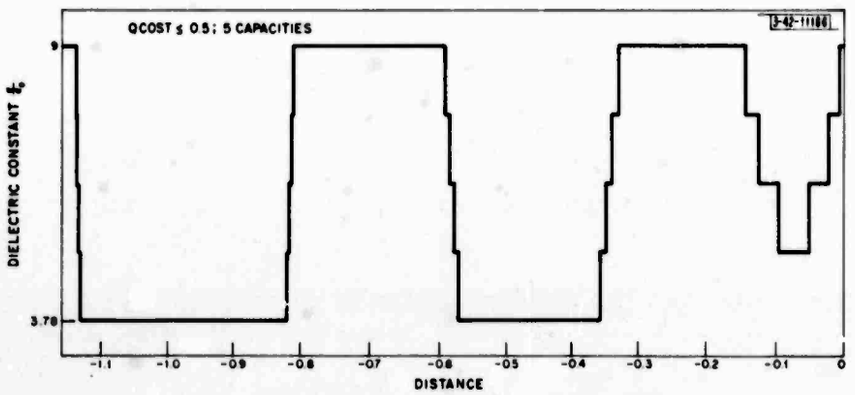

Fig. VIII-5. Solution for NVALS = 5, QCOST < 0.5.

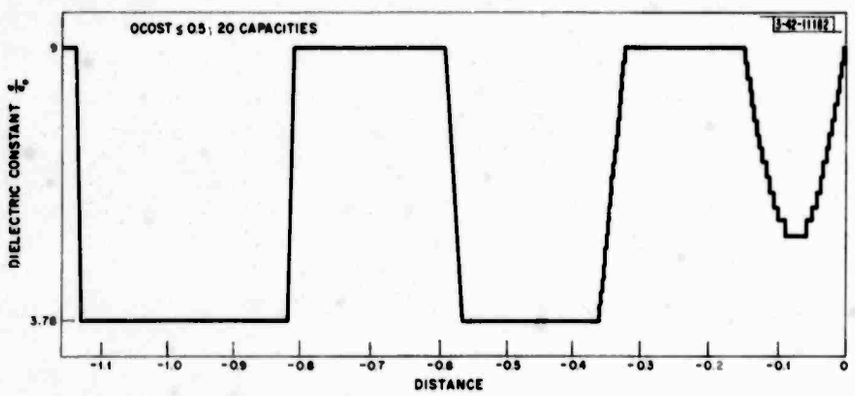

Fig. VIII-6. Solution for NVALS = 20, QCOST < 0.5.

of a phased array receiving antenna, and a quartz-loaded waveguide having the same cross section connected to the slot. The received power is then conducted to a strip-line receiver (also of the same cross section) by the quartz-loaded waveguide.

The receiving element was selected as a narrow slot 0.25 by 0.9 inch to match the dimensions of the stripline receiver and thus simplify mechanical construction (eliminate the need for tapered waveguides, etc.). However, this slot is so narrow that there is a severe mismatch in wave impedance between a wave in the waveguide section and the wave impedance of the free-space wave impinging on the slot. In fact, this mismatch is so severe that it typically results in greater than 20:1 VSWR and more than 7.5 db of reflection loss. The receiving slot end of the waveguide presents an impedance considerably more reactive than resistive, and the impedance match is desired over a fairly wide (10 percent) bandwidth from 5 to 5.5Ge. Such a difficult impedance matching problem does not lend itself to standard techniques, so there was excellent incentive to apply the technique outlined in Sec. VI.

The problem was run using the following constraints: $\epsilon_{MIN} = 3.78\ \epsilon_o$ (quartz dielectric); $\epsilon_{MAX} = 9.0\ \epsilon_o$ (alumina dielectric); length = 1.15 inches = one wavelength at center frequency 5.25Ge in quartz dielectric. The available power was assumed to be uniform at eleven equally spaced frequencies ranging from 5 to 5.5Ge, and normalized to 1 watt at each frequency. (This normalization has no effect on the resulting $\epsilon^*(z)$ solution because all system equations and boundary conditions are linear in power.)

An upper limit on the quadratic cost term [length $\times \Delta (\epsilon_{MAX} - \epsilon_a)^2/2$, where $\epsilon_a = (\epsilon_{MAX} + \epsilon_{MIN})/2$] was selected to be 0.5 watt, or about 4.5 percent of the total available power of 11 watts. The solution was then obtained for five equally spaced available $\epsilon(z)$ values ranging from ϵ_{MIN} to ϵ_{MAX} (NVALS = 5). The starting guess for the impedance presented to the source by the coupler was generated by the program: this impedance would result if the waveguide were filled everywhere with the ϵ_{MIN} dielectric.

The solution required about 10 minutes of run time on the IBM-360 because the starting guess was considerably different from the final impedance obtained. The solution was then repeated for NVALS = 2, 3, 10, 15 and 20, starting with the impedance obtained from the NVALS = 5 solution above. Each of these solutions required about 5 minutes of run time, demonstrating a considerable improvement because the initial guess was fairly close to the final solution in these problems.

The $\epsilon^*(z)$ solutions obtained for NVALS = 2, 5 and 20 are shown in Fig. VIII-4, -5, and -6, respectively. In each case we note the successive quarter-electrical-wavelength sections of essentially bang-bang nature (between ϵ_{MIN} and ϵ_{MAX}) beginning from the high impedance source at $z = -\ell$. This is the same behavior as that shown in the transmission line problems, and may be explained by the same reasoning (Fig. VIII-3).

At the right-hand end of the waveguide ($z = 0$), near the resistive load having the characteristic impedance of quartz-loaded waveguide, we see quite a different behavior. Here the appropriate $\epsilon^*(z)$ does not behave in bang-bang fashion, but appears as a quantized continuously-varying function taking on values of ϵ intermediate between ϵ_{MIN} and ϵ_{MAX}. As the quantization (partition on ϵ) becomes increasingly finer going from NVALS = 2 to 5 to 20, we see that this "quantized" solution appears to be approaching a continuous solution which is in fact $\epsilon^*_I(z)$, the solution obtained when $\epsilon(z)$ is only constrained to lie in the interval $[\epsilon_{MIN}, \epsilon_{MAX}]$. As in the case of any other numerical integration scheme, the burden of deciding when the partition is sufficiently fine, i.e., when $\epsilon(z)$ has converged to a function sufficiently close to $\epsilon^*_I(z)$, rests upon the user.

The performance obtained for NVALS = 5 is as follows: the VSWR has been reduced from 20:1 to 5.4:1, reducing reflection losses from 7.5 to 2.7 db, a significant improvement over the performance without an impedance-matching coupler. The total cost obtained is 5.5814 watts, of which 5.152 watts is true reflected power and 0.4294 watt is due to the quadratic cost term. In all these problems, the quadratic cost term took on about 85 percent of the value we specified as its upper limit, because about 3/4 of the line length demonstrated bang-bang or ϵ_{MIN}, ϵ_{MAX} behavior.

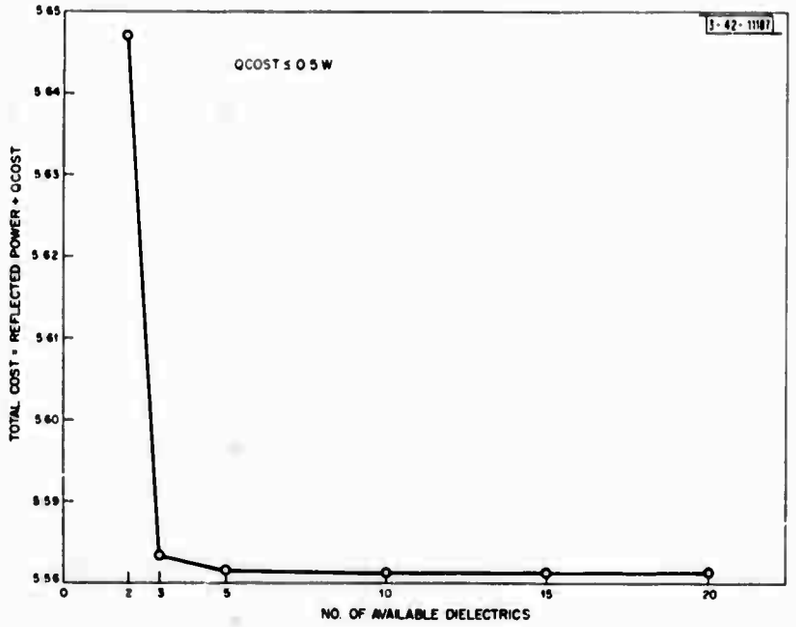

Fig. VIII-7. Behavior of total cost versus NVALS for QCOST < 0.5.

We stated above that the user must decide when the partition on ϵ is fine enough that $\epsilon(z)$ has converged sufficiently close to $\epsilon^*_I(z)$. Another parameter we may observe to make decisions about convergence is J_{NVALS}, the total cost corresponding to a partition having NVALS available values. J_{NVALS} is monotone decreasing with NVALS and converges to J_I, the total cost when $\epsilon(z)$ is constrained only to lie in the interval $[\epsilon_{MIN}, \epsilon_{MAX}]$. In Fig. VIII-7 we plot J_{NVALS} versus NVALS. First we note that J_{NVALS} is indeed a decreasing function, but only a 3 percent improvement is obtained in total cost as the partition is increased from two available values to 20. In fact, most of that improvement is obtained in going from NVALS = 2 to NVALS = 3, because the addition of the third (intermediate) value permits a significant reduction in the quadratic cost term over the right-hand quarter of the line. The total cost appears to have converged to J_I by the time NVALS = 20, so $J_I \approx 5.5812$ watts. Of this cost 5.154 watts is reflected power and 0.4272 watt is due to the quadratic cost term.

We note that even for NVALS = 2, we could have attained this cost of 5.5812 watts merely by permitting infinitely fast switching at a duty cycle indicated approximately by the $\epsilon(z)$ curve of Fig. VIII-6. Therefore, the NVALS = 2 solution that was obtained was suboptimal by about 3 percent. However, this 3 percent improvement which is possible by going from NVALS = 2 to an infinitely fine partition is certainly not worth the additional difficulty of constructing

such a complex device, so the practical implementation would be done with NVALS = 2 (two different dielectrics), or at most, NVALS = 3.

Since the quadratic cost term was quite noticeable compared to the true reflected power cost (about 8 percent in these solutions), it was decided to repeat the solutions for an upper bound of 0.1 watt on QCOST (five times smaller than before).

It was unnecessary to repeat the solution for NVALS = 2, because the quadratic cost term has no effect on this solution, and, in fact, QCOST is explicitly ignored by the program when NVALS = 2. The solution was repeated for NVALS = 5 and 20 starting from the impedance obtained in the original NVALS = 5, QCOST < 0.5 watt solution. Because of the change in the QCOST bound, Δ was five times smaller and so was each threshold value of the multiplier function M(z). (A threshold value is an M(z) value where $\epsilon^*(z)$ switches from one value to another.)

It happened that the function M(z) was then almost tangent to the most negative threshold value at $z \approx -0.1$ inch (a situation analogous to that of Fig. VII-5), so the computer was almost iterating along a singular extremal. Such a situation caused small changes in the impedance guess at $z = -\ell$ to map (in a quite nonlinear manner) into large changes in the impedance function obtained at z = 0. For this reason, the convergence properties of the iteration were considerably worse than before, requiring a very small maximum step size to guarantee convergence, and about 10 minutes of run time to obtain this convergence.

This difficulty could easily be avoided by further decreasing the upper bound on QCOST so that the critical threshold value of M is moved away from its tangency at $z = -0.1$ inch [a local minimum of M(z)]. In fact, as QCOST is made very small, the convergence properties of the iteration will be identical to those of the NVALS = 2 solution, which in this case were quite stable and fast to converge.

The $\epsilon(z)$ solution for NVALS = 5, QCOST < 0.1 is shown in Fig. VIII-8. Note that the bang-bang region of the line is unchanged from that of Fig. VIII-5, except that the transitions are five times sharper (a transition between ϵ_{MIN} and ϵ_{MAX} occurs in 1/5 as much distance). In fact, as QCOST is reduced to zero, the transitions in this bang-bang region occur in zero distance, just as in the NVALS = 2 solution of Fig. VIII-4.

The right-hand end of the line shows a significant change from Fig. VIII-5, in particular, $\epsilon(z)$ is farther away from its intermediate value ϵ_a for points z where $\epsilon(z) \neq \epsilon_a$. This change is reasonable, since the quadratic cost term, $\Delta(\epsilon - \epsilon_a)^2/2$, is a "centralizing" force which

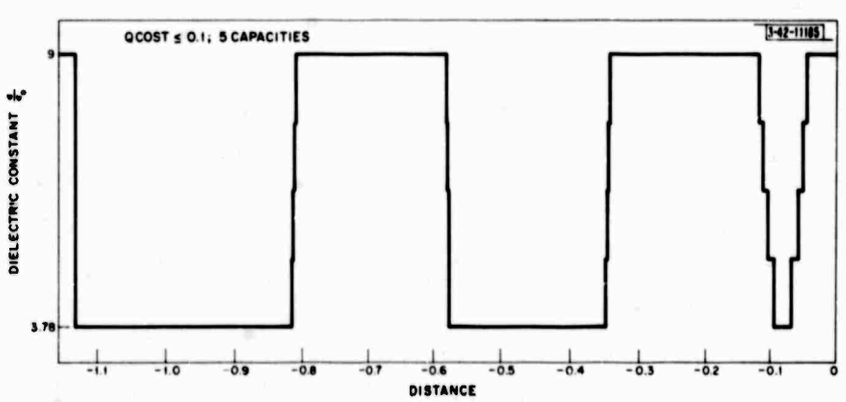

Fig. VIII-8. Solution for NVALS = 5, QCOST < 0.1.

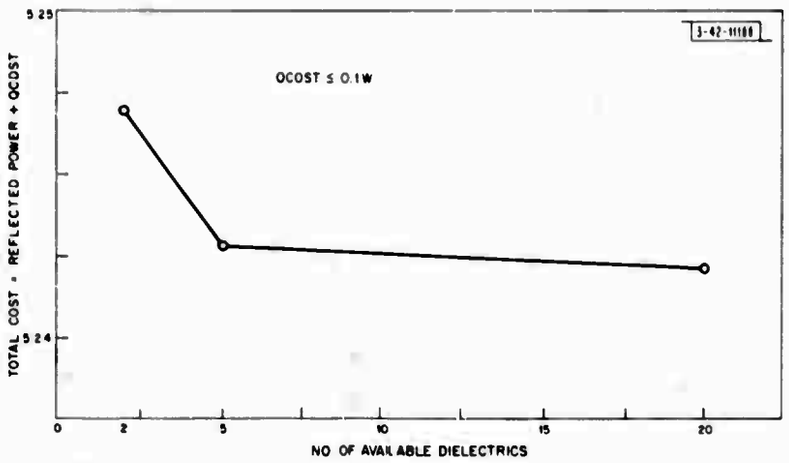

Fig. VIII-9. Behavior of totol cost versus NVALS for QCOST < 0.1.

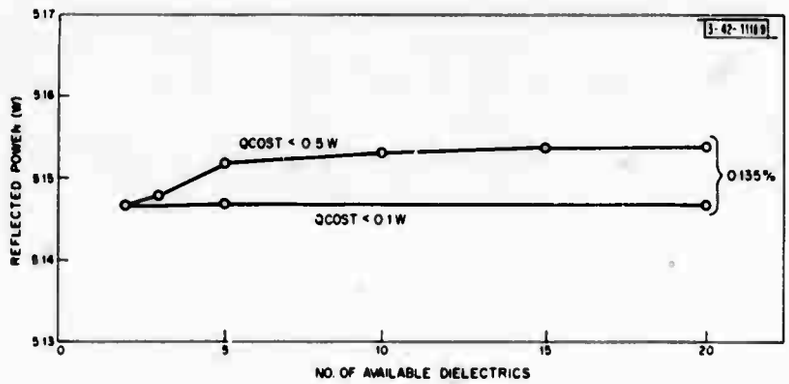

Fig. VIII-10. Variation of reflected power with NVALS and QCOST.

tends to keep $\epsilon(z)$ near ϵ_a. When QCOST, and thus Δ, is reduced, this centralizing effect is also reduced and the solution becomes nearer to the bang-bang or $\epsilon(z) = \epsilon_{MIN}$ or ϵ_{MAX} solution with the exception of points where $\epsilon = \epsilon_a$ (here the quadratic cost term is zero, so the scaling on this term has no effect).

In fact, for this particular example, a further decrease in Δ will only sharpen the switchings between ϵ_{MIN} and ϵ_{MAX} until the solution converges to that of Fig. VIII-4 (obtained for NVALS = 2). However, in a solution where $M(z) \approx 0$ over an interval of z, the solution would not necessarily converge to such a bang-bang solution as QCOST $\rightarrow$ 0.

For this example, we may view Figs. VIII-4, -5, -6 as a progression demonstrating that $\epsilon(z)$ converges to the continuous function $\epsilon_I(z)$ as NVALS $\rightarrow \infty$. Further, Figs. VIII-4, -8 and -5 are a progression demonstrating that increasing QCOST changes $\epsilon(z)$ from a bang-bang function to a smoother function approaching closer to the uniform function $\epsilon(z) \equiv \epsilon_a$ (this solution is obtained in the limit as $\Delta \rightarrow \infty$).

The variation of the total cost for QCOST < 0.1 is shown in Fig. VIII-9 for NVALS = 2, 5, and 20. Here the cost improvement is only 1/3 percent as NVALS is increased from 2 to 20, indicating that the physical structure should certainly be constructed for NVALS = 2. This also indicates that our solution obtained here for NVALS = 2 is only suboptimal by 1/3 percent.

So far, we have only examined

changes in total cost = reflected power + QCOST

as the number of available ϵ values, NVALS, and the upper bound on the quadratic cost term QCOST are varied. The engineer using the solution is only interested in the variations of the reflected power, so we examine this in Fig. VIII-10. First, we note that for every condition examined, the reflected power does not vary by more than 0.135 percent. The reflected power for NVALS = 2 is independent of QCOST, as is $\epsilon(z)$, so the curves for QCOST < 0.5 and QCOST < 0.1 meet at this point. For the QCOST < 0.1 curve, there is no measureable change in reflected power between NVALS = 2 and NVALS = 20, again making it obvious that only two dielectrics should be used in the construction of the coupler.

A feature that seems surprising at first is that for the QCOST < 0.5 curve, reflected power increases with NVALS, that is, with more available ϵ values we do a worse matching job. This behavior is possible because we are not really minimizing reflected power, but reflected power plus quadratic cost. This function is (and must be) a decreasing function of NVALS. The explanation for the increasing reflected power is that the intermediate values of ϵ permit a noticeable decrease in the quadratic term (which was fairly large in this problem), and taking on these intermediate values of ϵ reduces the quadratic cost (with increasing NVALS) faster than it increases the reflected power cost. Thus, the system trades some reflected power cost to attain lower cost from the quadratic term. When the quadratic term is made smaller, as on the QCOST < 0.1 curve, the tendency toward a trade-off is greatly reduced and we see no change in reflected power with increasing NVALS. As QCOST $\rightarrow$ 0, the plot of reflected power versus NVALS must become a monotone decreasing curve (or at least a monotone nonincreasing curve), so one could repeat the solution for NVALS = 5 with successively smaller upper bounds on QCOST to see if a reflected power cost less than 5.147 watts (that obtained for NVALS = 2) can be obtained, or until one is satisfied that the reflected power cost has converged.

3. Conclusions

The main conclusion possible from these examples is that performance is essentially independent of NVALS, so just two dielectrics should be used in construction. If better performance (less reflected power) is desired, one must relax the problem constraints by either permitting longer structure length or a greater range of ϵ in the dielectric materials.

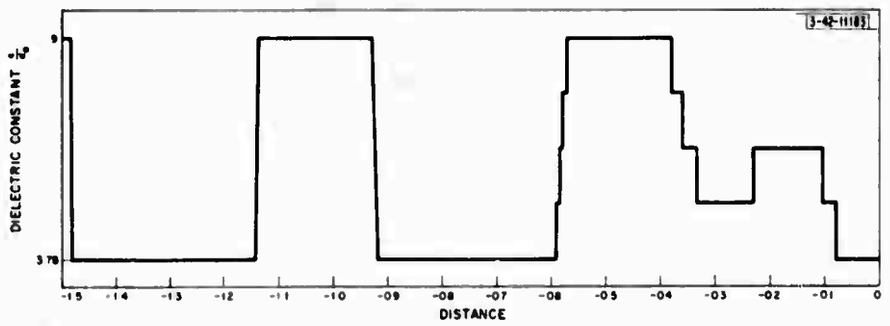

Fig. VIII-11. Solution for length = 1.5 inches, NVALS = 5, QCOST <0.5.

One such example was run, where the structure length was increased from 1.15 to 1.5 inches (again, NVALS = 5 and QCOST < 0.5). The resulting $\epsilon(z)$ function is shown in Fig. VIII-11. We note that the successive quarter-electrical-wavelength sections of ϵ_{MIN} and ϵ_{MAX} appear, just as in all previous solutions, beginning at the source ($z = -\ell$). The additional 0.35 inch has been taken up by the intermediate-value $\epsilon(z)$ behavior at the right-hand end of the line. The cost of this solution was 5.626 watts, of which 5.223 was reflected power and 0.4040 was due to the quadratic cost term. This performance was slightly worse than that afforded by the shorter line because the quadratic cost term was being integrated over a longer distance, thus resulting in a greater cost. In the limit as QCOST → 0, the reflected power for this longer line must be ≤ the reflected power for the shorter line.

Coupler performance considerably better (having a reflected power less than 1 watt) than that obtained so far is desired. A series of future runs is being planned which will attempt to reach this figure by loosening up the constraints, increasing the length to 3 inches and ϵ_{MAX} to $16 \cdot \epsilon_0$ (boron nitride). These runs will be tried for NVALS = 2 and NVALS = 5, but no significant improvement is expected for the increase in NVALS.

C. RECOMMENDATIONS

Several convergence difficulties were noted during the computer runs described above. First, quadratically fast convergence was only observed during the NVALS = 2 run. The other runs ended by exceeding the specified maximum number of iterations, usually in a state of oscillation about the solution; in such a situation, the step size would be limited by the specified maximum step size, and the gradient vector (having magnitude greater than this maximum step size) would be alternating between two completely different vectors on successive iterations. To shut down the extent of this behavior of "rattling back and forth" across the solution, it was necessary to reduce the step size. This generally terminated in the same oscillatory behavior, but in a much smaller range about the solution.

Such behavior is the result of a noticeable nonlinearity of the mapping between the initial guess function for the impedance and the resulting impedance function at z = 0, when the

impedance guess is varied by the indicated maximum amount. Of course, if the procedure is not attempting to iterate along a singular extremal, this mapping is linear for sufficiently small variations. Making the maximum variation of the impedance guess sufficiently small will then cause quadratically fast convergence from functions near the solution. However, experience indicates that this maximum step size must be made very small indeed to cause quadratically fast convergence, wasting a large number of iterations (and a great deal of time) to go from a distant initial guess to a function so close to the solution that oscillations would appear.

A suggested remedy for this problem is conversion from the saturating Newton-Raphson procedure used now (where the magnitude of the variation vector is truncated whenever it exceeds a specified limit) to the segmented Newton-Raphson procedure described below.

Each iteration begins in the same way as the present iteration: nine scans are made down the line to find the load corresponding to the initial guess impedance and the variation of this load with respect to eight independent variations of the guess impedance. The sensitivity matrix is formed, inverted, and postmultiplied by the error in load impedance to find the gradient vector. This gradient vector indicates the change in the guess function (assuming linear mapping between guess and result) which will cause the resulting load to match the actual load.

Instead of operating a saturation function on the magnitude of this gradient vector G, we imagine scaling it by a scalar r to produce a variation of our guess function indicated by rG. Now we ask what value of the scalar r minimizes in L_2 norm the distance between the resulting load impedance and the desired load impedance. First try r = 1, then if the load error is worse, try r = 1/2, then depending on the previous result, r = 1/4 or r = 3/4, etc. In short, one performs a binary search over the scalar variable r to find the value which minimizes the load impedance error. Each test requires one scan down the line, so if a half dozen points are tried, the overall time for one iteration is increased by 60 percent. Once a "good" choice of r is found, the next iteration begins from this point.

This procedure is expected to at least halve the number of iterations required to obtain convergence to the desired load impedance, as the oscillatory behavior on successive iterations would be eliminated. Instead of jumping back and forth across the solution, the procedure would move to the solution (to first order) in one iteration. Such a procedure would provide quadratically fast convergence from a much larger range of initial guess functions.

The second difficulty noted was that it was possible for M(z) to be almost tangent to one of its threshold values, thus causing the computer to almost track a singular extremal. This results in a very nonlinear mapping between guess function and resulting load impedance, so the convergence properties of the iteration are very poor. This problem is easily avoided by simply changing the upper bound on QCOST, and thus Δ, or by a slight change in ϵ_{MAX} or ϵ_{MIN}.

The third and most serious difficulty is that for some impedance guesses far from the solution, the procedure fails to converge at all. This is a property common to Newton-Raphson procedures, as they all have some region of convergence; the initial guess must be in this region or the procedure will not converge. The extent of this region is a direct measure of the linearity between guess and result; the more nonlinear this mapping, the smaller is the region of convergence.

When this failure of convergence occurs, the error in the load impedance is large, but is at a local minimum; to first order, no change in the guess function improves this error, and the sensitivity matrix used in the Newton-Raphson procedure becomes almost singular (develops very small eigenvalues).

One improvement would be to truncate all eigenvalues less than some threshold magnitude to zero during the inversion process and return the pseudo-inverse of this sensitivity matrix. The iteration procedure would then continue reducing some components of the error vector even if it could not reduce all of them. However, if the troublesome point is a local minimum with respect to all possible variations (and not just a saddle point) then all eigenvalues will become arbitrarily small and the pseudo-inverse will be the zero matrix, which will break down the procedure at that point.

In this case, a smoothing factor is needed which makes the mapping more linear between guess and result, and which thus makes the region of convergence large enough to include our initial guess function. The upper bound on QCOST is just such a factor: if we increase this bound, $\Delta \to \infty$, and the solution $\epsilon^*(z) \to \epsilon_a$ everywhere. In an example where an initial guess fails to converge, we need merely take Δ very large and guess the initial impedance corresponding to $\epsilon(z) \equiv \epsilon_a$. Once convergence has been obtained for this Δ, we take a smaller Δ and start from the result of the previous problem. For a small enough change in Δ, the old solution will be within the range of convergence of the new problem. This procedure can obviously be continued, and by the time we reach the value of Δ we were originally considering, we will have a guess function within the range of convergence of this problem.

In fact, this is precisely the procedure that was employed above, i.e., finding the solution for NVALS = 5, QCOST < 0.1 by starting from the solution for NVALS = 5, QCOST < 0.5.

In short, the indicated operating procedure is to start with a rather large value for the bound on QCOST, obtain convergence starting from some simple initial guess, then use the resulting impedance function for a starting guess for a new problem having a considerably smaller bound on QCOST. This procedure may be continued until the user is satisfied that the reflected power cost will not decrease any further. This procedure should be run for NVALS = 3, since the change in cost with increasing NVALS is extremely small, and the time per iteration is proportional to the number of switchings, which is proportional to NVALS. After final convergence is obtained, one may start from this solution to find the cost for NVALS = 10, 20, etc.

IX. CONCLUSIONS AND SUGGESTIONS FOR FURTHER RESEARCH

A. PRACTICAL APPLICATIONS

The solutions to the waveguide problem examined in Sec. VIII are a great improvement upon the performance of the receiving slot antenna in the absence of an impedance-matching coupler. Further, this particular problem involves such a severe mismatch over a wide bandwidth (10 percent) that standard rule-of-thumb impedance-matching techniques are of little help. The technique described in Sec. VI thus provides a method of proceeding to a practical solution where other methods fail. However, the solutions obtained for the particular constraints considered (a length of one wavelength and $\epsilon_{MAX} = 9\epsilon_o$) leave something to he desired in terms of power transmitted to the stripline receiver load (almost 50 percent of the availahle power is reflected through mismatch).

For this reason, future runs will be made relaxing the constraints on length and ϵ_{MAX}. If the reflected power loss can be reduced to 10 percent with reasonable values for length and ϵ_{MAX}, it is expected that the indicated structure will be constructed and tested experimentally for performance (by Lincoln Laboratory Group 44) in anticipation of actually using the design in a working phased array radar.

B. POSSIBLE IMPROVEMENTS

Convergence of the numerical procedure should be improved by converting from the saturating Newton-Raphson iteration technique used at present to the segmented Newton-Raphson technique, which was described in Sec. VIII, using a binary search along the gradient vector to find the minimum error point. This should provide a considerable improvement in speed of convergence.

In addition, the numerical procedure should recognize when it is almost iterating along a singular extremal [M(z) almost tangent to one of its threshold values] and reduce Δ or increase ϵ_{MAX} enough to avoid this problem (giving notice of the change to the user, of course).

Third, the inversion of the sensitivity matrix in the Newton-Raphson procedure should truncate to zero all eigenvalues having magnitudes less than 1 percent of the maximum eigenvalue and should return the pseudo-inverse of the matrix. However, if even the largest eigenvalue is less than some small number, say 0.01, then the procedure is caught in a local minimum of the error function and the quadratic cost term (Δ) should be increased by 10 to smooth out the mapping between guess and result. This increases the extent of the region of convergence; once convergence is obtained, Δ should be reduced to its original value and the iterations continued from this point.

In addition, once a solution has been obtained, the following functions should be plotted on the automatic plotter:

1. The multiplier function M(z).
2. The dielectric solution $\epsilon(z)$.
3. The reflection coefficient $\rho(\omega)$ presented by the coupler to the source.
4. The reflection coefficient $\rho_1(\omega)$ presented by the coupler to the load.
5. The reflected power loss versus angle of incoming plane wave, as ZSOURCE is varied over the functions corresponding to a number of different angles of incidence. (ZSOURCE is a tabulated function of ω and Θ, the angle of incidence.)

C. RELATED TOPICS FOR INVESTIGATION

Two very interesting related topics present themselves for investigation at this point: the first is the question of the behavior of the solution C(z) and corresponding cost J in the transmission line as the maximum available capacity, CMAX, is increased without limit.

Suppose now that NVALS = 2 so C* = CMAX when M(z) > 0. Note that d^2M/dz^2 is linear in C from Eq. (4-31b). If we now assume that there is some point z_o such that

$$M(z_o) = 0 \quad , \quad \frac{dM(z_o)}{dz} > 0 \quad , \tag{9-1}$$

and from Eq. (4-31b)

$$\frac{d^2M}{dz^2} \approx -\alpha C \quad \text{for large } C \quad ,$$

then

$$M(z_o + \sigma) = 0 \quad , \quad \frac{dM(z_o + \sigma)}{dz} = -\frac{dM(z_o)}{dz} \quad \text{for} \quad C\sigma \approx \frac{2}{\alpha}\frac{dM(z_o)}{dz} \tag{9-2}$$

when C is very large. This behavior

$$\lim_{C\to\infty} C\sigma = \text{constant}$$

indicates an impulse of capacity per unit length. Such an impulse of capacity per unit length (plotted as a function of distance z) has the units of capacity and may be interpreted as a fixed lumped capacity tapped across the transmission line at $z = z_o$. Of course, such a solution is quite attractive physically because it is so easy to construct

The above rationalization for impulsive C(z) solutions is, of course, not at all rigorous. To develop a more reasonable argument, we examine the limits of the transition matrices of Eq. (4-11) and (4-23) as $C \to \infty$ for $z \in [z_o, z_o + \sigma]$ in such a way that $C\sigma \to \infty$ constant K.

The result is:

$$\begin{bmatrix} |V|^2(z_o + \sigma) \\ |I|^2(z_o + \sigma) \\ \sqrt{8}S_I(z_o + \sigma) \\ \sqrt{8}S_R(z_o + \sigma) \end{bmatrix} = \begin{bmatrix} |V|^2(z_o) \\ |I|^2(z_o) + \omega^2K^2|V|^2(z_o) + \sqrt{2}\omega K\,[\sqrt{2}S_I(z_o)] \\ \sqrt{8}S_I(z_o) + \sqrt{2}\omega K|V|^2(z_o) \\ \sqrt{8}S_R(z_o) \end{bmatrix} . \tag{9-3}$$

Thus the magnitude of the voltage and the real power flow are continuous across the impulse of K farads, while the magnitude squared of the current and the imaginary power undergo finite step changes linear in $|V|^2$ and $\sqrt{8}S_I$ at $z = z_o$.

A similar result holds for the costate.

$$\begin{bmatrix} p_1(z_o + \sigma) \\ p_2(z_o + \sigma) \\ p_3(z_o + \sigma) \\ p_4(z_o + \sigma) \end{bmatrix} = \begin{bmatrix} p_1(z_o) + \omega^2 K^2 p_2 - \sqrt{2}\omega K p_3 \\ p_2(z_o) \\ p_3(z_o) - \sqrt{2}\omega K p_2 \\ p_4(z_o) \end{bmatrix} \tag{9-4}$$

Thus, p_2 and p_4 are continuous while p_1 and p_3 undergo step changes linear in p_2 and p_3. Since we are considering the case of NVALS = 2, there is no reason for a quadratic cost term; this means that, as shown in Sec. III, the cost J (which is now exclusively reflected power) may be evaluated as $p'(z)\, x(z)$. Evaluating the cost on both sides of the impulse using the above state equation and analogous costate equations (9-3) and (9-4),

$$J(z_o + \sigma) - J(z) = p'(z_o + \sigma)\, x(z_o + \sigma) - p'(z_o)\, x(z_o) = 0 \tag{9-5}$$

which was certainly to be expected if the solution is to be physically meaningful. A further evaluation establishes that the Hamiltonian is also continuous across the impulse of capacity, so the impulsive solution seems to be a perfectly proper and reasonable solution to the problem.

To really develop this idea, two phases of work would be necessary: first, one must formulate a distributed parameter maximum principle for impulsive controls, then apply this principle to the transmission line problem being considered as CMAX $\to \infty$ to demonstrate that impulses of capacity per unit length, i.e., lumped capacitors, are a valid solution to the problem. Then one must modify the procedure given in Sec. VI, in particular causing the scan down the line to find the points z_i where $M(z_i) = 0$, $dM(z_i)/dz > 0$, and there inserting lumped capacitors of value

$$k_i = \frac{-2(dM/dz)\,(z_i)}{\partial/\partial C\,(d^2M/dz^2)}$$

$$= \frac{\sqrt{2}\int_{\omega\in\Omega} \omega^2(x_1p_1 - x_2p_2)\, d\omega}{\int_{\omega\in\Omega} \omega^3(x_1p_3 + x_3p_2)\, d\omega} \tag{9-6}$$

with the x's and p's evaluated at $z_i - \sigma$. Then the appropriate step change must be made in the state and costate (Eqs. (9-3) and (9-4) and the scan down the line continued to find the next point where

$$M(z_i) = 0 \quad , \quad \frac{dM(z_i)}{dz} > 0 \quad .$$

Such a change is not a very drastic modification to the program, and seems well worthwhile in terms of transmission line couplers which are extremely easy to construct.

The other topic which seems well worth investigating at this point is the design of lossless ladder impedance matching networks using a "discrete-time" distributed parameter maximum principle. Consider the lumped L-C ladder network shown in Fig. IX-1, with complex voltages and currents defined over the rung index as V(n) and I(n). The ladder is assumed to have a fixed number of rungs, N.

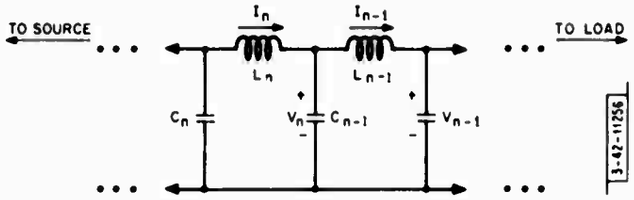

Fig. IX-1. Lumped L-C ladder impedance matching network.

These complex variables obey the difference equations,

$$V_n = V_{n-1} + j\omega L_{n-1} I_{n-1}$$

$$I_n = I_{n-1} + j\omega C_{n-1} V_n = (1 - \omega^2 L_{n-1} C_{n-1})\, I_{n-1} + j\omega C_{n-1} V_{n-1} \tag{9-7}$$

If, in analogy with the transmission line, we select as state variables $|V_n|^2$, $|I_n|^2$, $\sqrt{8}S_{I_n}$, $\sqrt{8}S_{R_n}$, we have the linear difference equation:

$$\begin{bmatrix} |V_n|^2 \\ |I_n|^2 \\ \sqrt{8}S_{I_n} \\ \sqrt{8}S_{R_n} \end{bmatrix} = \begin{bmatrix} 1 & \omega^2 L_{n-1}^2 & \sqrt{2}\omega L_{n-1} & 0 \\ \omega^2 C_{n-1}^2 & (1 - \omega^2 L_{n-1} C_{n-1}) & -\sqrt{2}\omega C_{n-1}(1 - \omega^2 L_{n-1} C_{n-1}) & 0 \\ \sqrt{2}\omega C_{n-1} & -\sqrt{2}\omega L_{n-1}(1 - \omega^2 L_{n-1} C_{n-1}) & (1 - 2\omega^2 L_{n-1} C_{n-1}) & 0 \\ 0 & 0 & 0 & 1 \end{bmatrix} \begin{bmatrix} |V_{n-1}|^2 \\ |I_{n-1}|^2 \\ \sqrt{8}S_{I_{(n-1)}} \\ \sqrt{8}S_{R_{(n-1)}} \end{bmatrix} \tag{9-8}$$

or

$$X_n(\omega) = [I - A_{n-1}(\omega, L_{n-1} C_{n-1})]\, X_{n-1}(\omega) \quad . \tag{9-9}$$

We must now formulate a discrete-time distributed parameter maximum principle and verify the equivalent of directional convexity for the system Eq. (9-9). Assuming that this principle parallels the ordinary difference equation maximum principle, there will exist (as a necessary condition) a co-state $p_n(\omega)$ which forms a scalar Hamiltonian as follows:

$$H(x_n, p_{n+1}, L_n, C_n, n) = \int_{\omega \in \Omega} p'_{n+1}(\omega)\, A_n(\omega, L_n, C_n)\, x_n(\omega)\, d\omega \tag{9-10}$$

We note that this Hamiltonian is quadratic both in L_n and C_n, so the requirement of minimizing the Hamiltonian with respect to L_n and C_n will always yield unique solutions for L_n and C_n. (The coefficients of L_n^2 and C_n^2 in the Hamiltonian may be interpreted as magnitudes squared of a power flow, and hence are real and positive.) In this case the addition of a term quadratic in the control parameters to avoid the complexities of singular extrema is unnecessary.

It appears that both the necessary theory and the details of an iterative numerical scheme for the necessary conditions (perhaps even sufficient conditions would be available for this problem) are a feasible future development.

If such a solution is feasible, it would be of considerable practical utility because such a matching network would be quite easy to construct. The next obvious extension would be a conversion to filter networks rather than impedance matching networks.

ACKNOWLEDGMENT

I am deeply indebted to my thesis Supervisor, Professor Michael Athans, for his crucial suggestions and patient supervision. Thanks are also extended to Professors Paul Penfield and Richard N. Spann of the M.I.T. Electrical Engineering Department, who acted as readers of the thesis.

Helpful discussion and suggestions were also provided by Dr. Richard P. Wishner and Bliss L. Diamond of the M.I.T. Lincoln Laboratory, and Professor Robert Kyhl of the M.I.T. Electrical Engineering Department.

I wish to express my appreciation to Bolt Beranek and Newman Inc. for providing computer time on their SDS-940 facility; to the M.I.T. Lincoln Laboratory for computer time on their IBM-360 facility, and for financial support during the last phases of this research; and to the National Science Foundation for their financial support during the earlier part of this work.

REFERENCES

1. R.B. Adler, L.J. Chu and R.M. Fano, Electromagnetic Energy Transmission and Radiation (Wiley and Sons, 1960), Chap. III.
2. H.W. Bode, Network Analysis and Feedback Amplifier Design (Van Nostrand, New York, 1945).
3. R.M. Fano, "Theoretical Limitations on the Broadband Matching of Arbitrary Impedances," Technical Report 41, Research Laboratory of Electronics, M.I.T. (January 1948).
4. J.D. Schoeffler, "Impedance Transformation Using Lossless Networks," Sc. D. Thesis, Dept. of Elec. Eng., M.I.T. (1960).
5. A. Vassiliadis, "Impedance Matching Limitations with Application to the Broadband Antenna Problem," Technical Report 60, Stanford Research Institute (January 1957).
6. D. Varon, "Parallel Impedance Voltage Equalization" Microwave Research Institute Report 1036, Polytechnic Institute of Brooklyn (September 1962).
7. G.L. Matthaei, "Synthesis of Chebyshev Impedance Matching Networks, Filters, and Interstages," Electronics Research Laboratory Report 139, University of California (June 1955).
8. B.K. Kinariwala, "Realization of Broadband Matching Networks for Arbitrary Impedances," Institute of Engineering Research Report 176, University of California (February 1957).
9. H.N. Dawirs, H. Tulloss and W. Tulloss, "Impedance Matching of Simple-Stub Transmission Line Filters," Research Foundation Report 667-25, Ohio State University (February 1967).
10. L. Young, "Optimum Quarter-Wave Transformers," IRE Trans. PGMTT MTT-8, 478 – 482 (September 1960).
11. S.B. Cohn, "Optimum Design of Stepped Transmission Line Transformers," IRE Trans. PGMTT MTT-3, 16 – 21 (April 1955).
12. R.M. Fano, "A Note on the Solution of Certain Approximation Problems in Network Synthesis," Technical Report 62, Research Laboratory of Electronics, M.I.T. (April 1948).
13. G.L. Matthaei, "Conformal Mappings for Filter Transfer Function Synthesis," Proc. IRE 41, 1658 – 1664 (November 1953).
14. G.L. Matthaei, L. Young and E.M.T. Jones, Microwave Filters, Impedance-Matching Networks and Coupling Structures (McGraw-Hill, New York, 1964).

15. H. J. Carlin and R. LaRosa, "Broadband Reflectionless Matching With Minimum Insertion Loss," Proc. Symposium on Modern Network Synthesis, Polytechnic Institute of Brooklyn (1952).

16. R. LaRosa and H. J. Carlin, "A General Theory of Wide-Band Matching with Dissipative Four-Poles," Microwave Research Institute Report 247, Polytechnic Institute of Brooklyn (February 1953).

17. P. A. Ligomenides, "A New Design Method for Coupling Networks, With Application to Broadband Transistor Amplifiers and Antenna Matching," IRE WESCON Conv. Record, Pt. 2, 47 – 61 (1958).

18. W. Ku, "Optimum Voltage Transfer Equalization for a Reactive Load and a Finite Generator," Microwave Research Institute Report 606, Polytechnic Institute of Brooklyn (February 1959).

19. P. Sulzer, "Modified Resonant Circuits Match Impedances," Tele-Tech 9, 41 – 42 (November 1950).

20. H. F. Mathis, "Experimental Procedures for Determining the Efficiency of Four-Terminal Network," J. Appl. Phys. 25, 982 – 986 (August 1954).

21. H. M. Allschuler, "Maximum Efficiency of Four-Terminal Networks," Proc. IRE 43, 1016 (August 1955).

22. E. F. Bolinder, "Maximum Efficiency of Four-Terminal Networks," Proc. IRE 44, 941 (July 1956).

23. L. Barter, "Coaxial Line Impedance Transformers," Report TR-5, Electrical Engineering Department, University of Washington (June 1952).

24. E. F. Bolinder, "Impedance and Power Transformations by the Isometric Circle Method and Non-Euclidean Hyperbolic Geometry," Technical Report 132, Research Laboratory of Electronics, M.I.T. (August 1949).

25. R. A. Rohrer, J. A. Resh and R. A. Hoyt, "Distributed Network Synthesis for a Class of Integrated Circuits," IEEE International Convention Record, Pt. 7, p. 100 (1965).

26. R. A. Rohrer, "Synthesis of Arbitrary Tapered Lossy Transmission Lines," Symposium on Generalized Networks, Polytechnic Institute of Brooklyn, p. 115 (April 1966).

27. H. G. Moyer, M. R. Wohlers and R. E. Kopp, "Computational Aspects of the Design of Optimal Distributed Components," Proc. of Electronics Components Conference (1966).

28. M. R. Wohlers, R. E. Kopp and H. G. Moyer, "Computational Aspects for the Synthesis of Optimum Nonuniform Transmission Lines Based on Variational Principles," Proc. Nat. Elec. Conf., XXI, 135 – 140, Chicago, Illinois (October 1965).

29. P. K. C. Wang, "Control of Distributed Parameter Systems," Advances in Control Systems (Ed. C. F. Leondes) (Academic Press, 1964).

30. Adler, Chu and Fano, op. cit., Chap. II.

31. H. J. Kelley, "A Second Variation Test for Singular Extremals," AIAA J. 2, 1380 (August 1964).

32. J. Warga, "Functions of Relaxed Controls, SIAM J. on Control 5, 628 (1967).

APPENDIX A
OPTIMAL CHOICE OF REFLECTION COEFFICIENT

Given the constraint

$$\int_0^\infty \ln 1/|\rho(\omega)|\, d\omega \leq M$$

we wish to demonstrate that a local minimum of the functional

$$J = \int_W |\rho(\omega)|^2\, d\omega$$

is obtained by the strategy

$$|\rho(\omega)| = \begin{cases} \exp[-M/W] & , \quad \omega \epsilon W \\ 1 & , \quad \omega \notin W \end{cases} .$$

Consider a strong first-order variation about this strategy of the following form:

$$|\rho(\omega)| = \begin{cases} \exp[-K/a] & , \quad \omega \epsilon a \\ \exp[-\dfrac{(a+b)M - KW}{bW}] & , \quad \omega \epsilon b \\ \exp[-M/W] & , \quad \omega \epsilon \{W - a - b\} \\ 1 & , \quad \omega \notin W \end{cases}$$

where

$$a \epsilon W \quad , \quad b \epsilon W \quad , \quad a \epsilon b = 0 \quad .$$

It is simple to confirm that this variation satisfies the integral constraint, i.e.,

$$\int_0^\infty \ln 1/|\rho(\omega)|\, d\omega = M$$

and the perturbed cost is

$$\int_W |\rho(\omega)|^2\, d\omega = a \exp[-2K/a] + b \exp\{-[(a+b)M - 2KW]/W\}$$

$$+ (W - a - b) \exp[-2M/W] \quad .$$

Differentiating with respect to K and setting the derivative to zero will give a stationary value for the perturbed cost. This results in

$$K = aM/W$$

which means that the only stationary perturbation in $|\rho(\omega)|$ is the zero perturbation. To show that the unperturbed $|\rho(\omega)|$ characteristic gives not only a stationary cost but a minimal cost, we differentiate again with respect to K

$$\left.\frac{\partial^2 J}{\partial K^2}\right|_{K=(aM/W)} = \frac{4}{a+b} \exp[-\frac{2M}{W}] > 0 \quad .$$

Therefore the unperturbed strategy $|\rho(\omega)| = \exp[-M/W]$, $\omega \epsilon W$ is indeed a strong local minimum.

BLANK PAGE

APPENDIX B

FLOW CHARTS FOR ITERATIVE NUMERICAL PROCEDURE

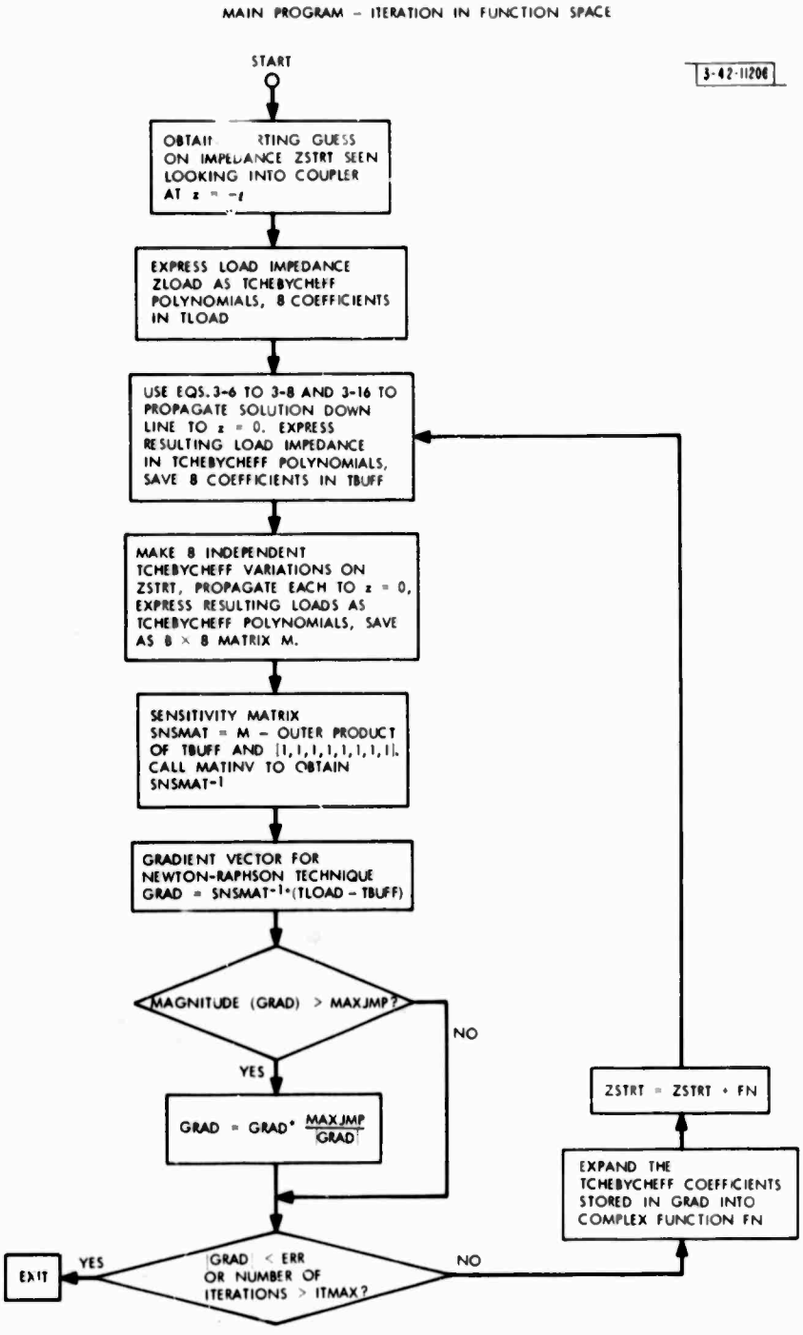

Fig. B-1. Iteration in Tchebycheff space.

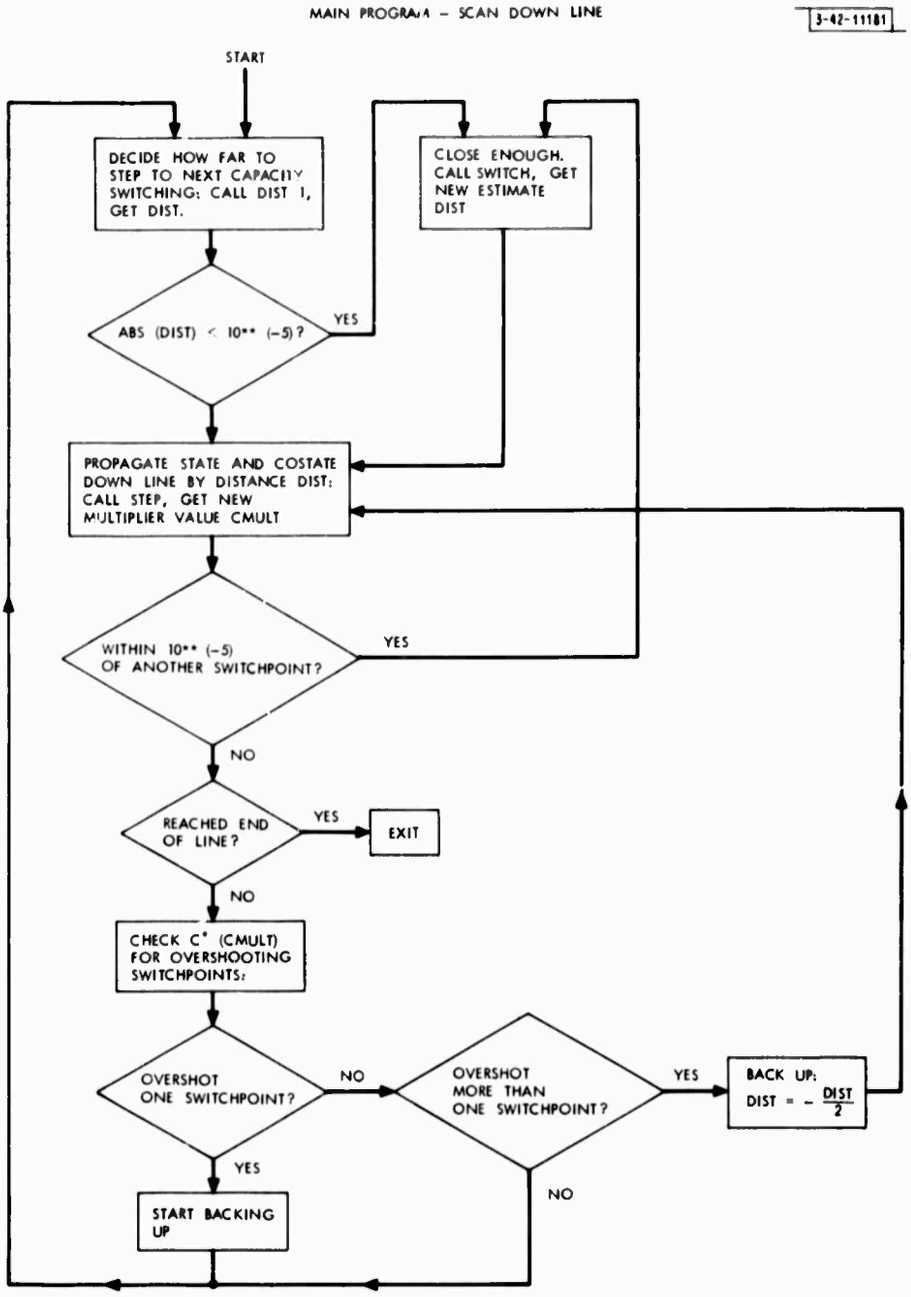

Fig. B-2. Main scan downline.

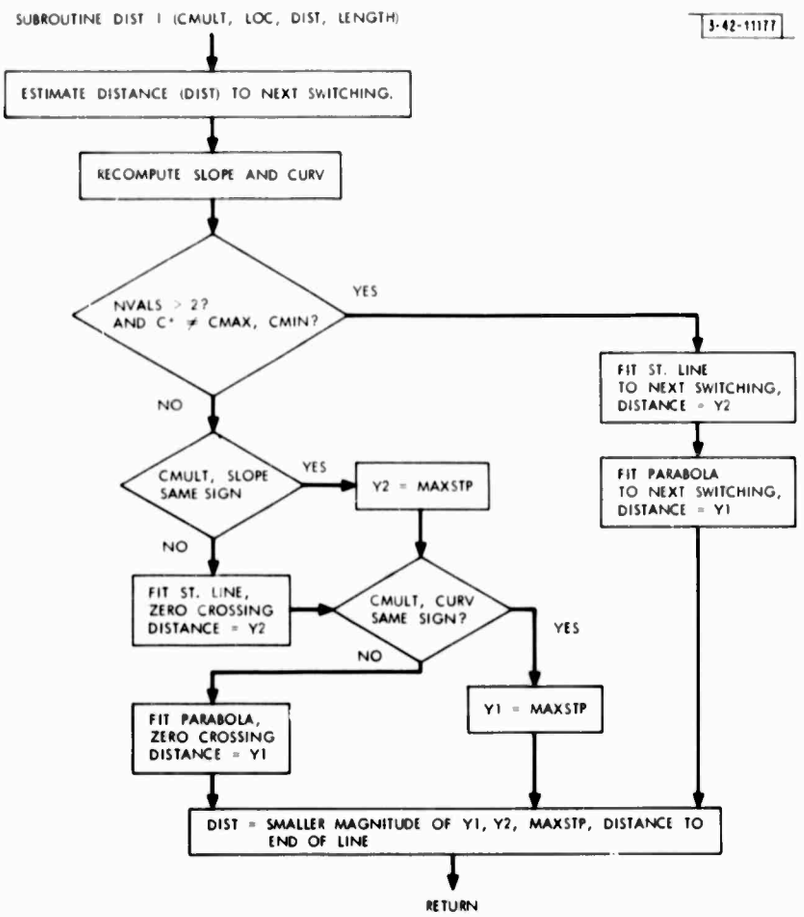

Fig. B-3. Subroutine DIST1.

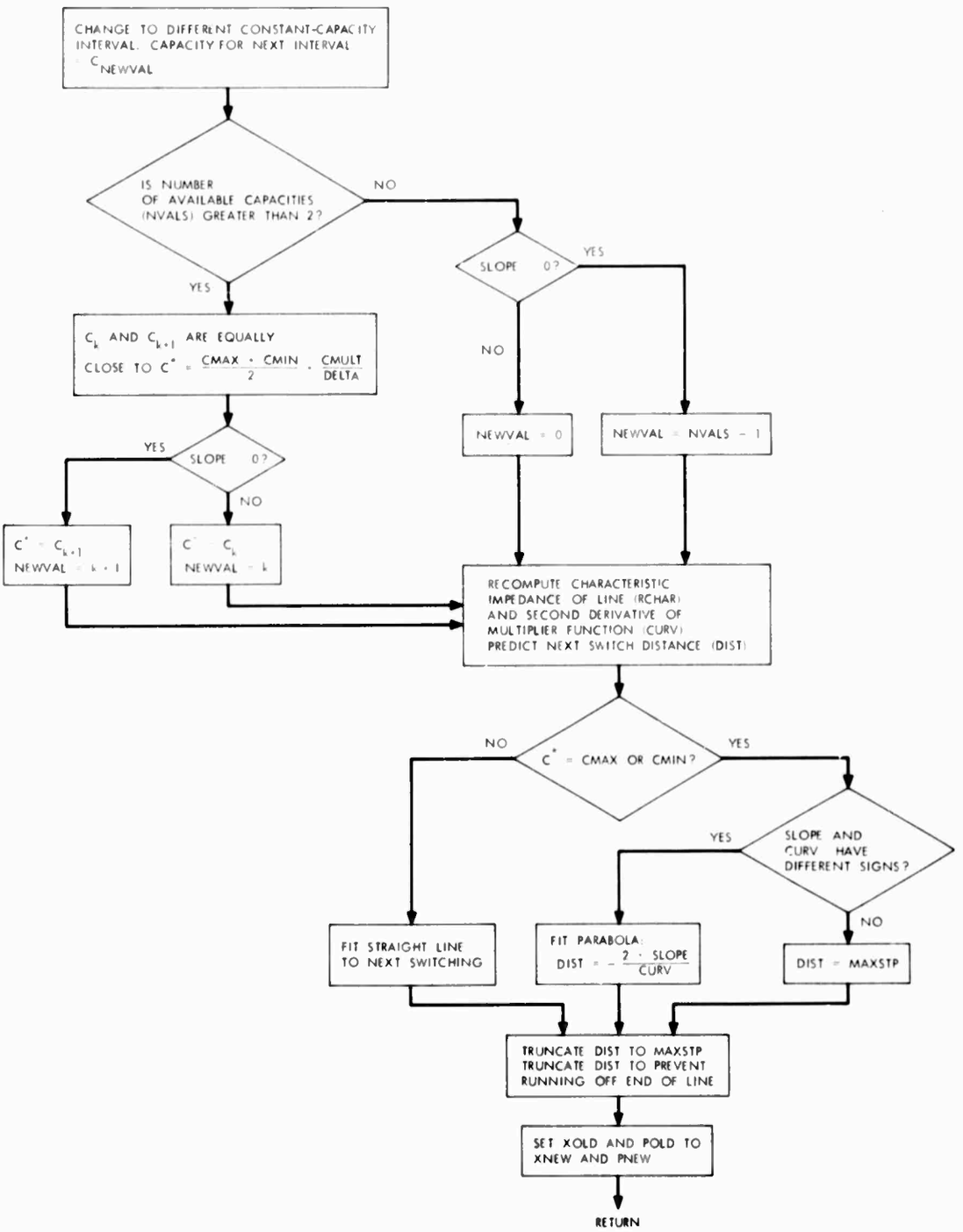

Fig. B-4. Subroutine SWITCH.

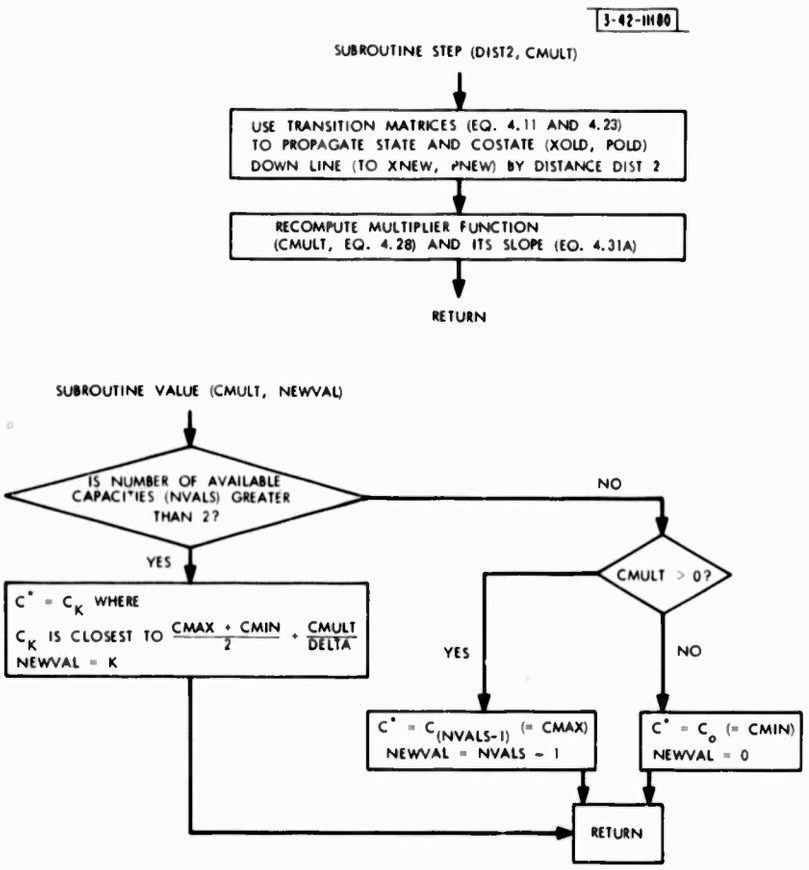

Fig. B-5. Subroutine STEP and VALUE.

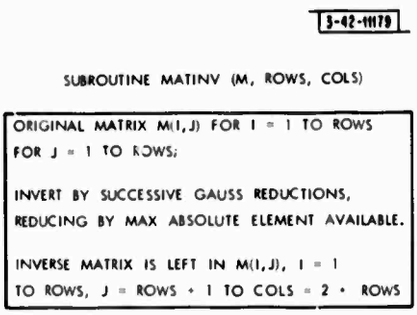

Fig. B-6. Subrautine MATINV.

APPENDIX C

LISTING OF FORTRAN-IV SOURCE PROGRAM

```
C       MAIN PROGRAM
        LOGICAL WAVGDE, FORFLG
        LOGICAL SELFST,CONTIN,TYPOUT,PUNCH
        INTEGER OLDVAL
        INTEGER PASS
        REAL L,LENGTH,LOC,MAXSTP,IMAGPT ,MAXJMP,MAG
        COMPLEX ZSOURC(11),ZLOAD(11),ZSTRT(11),ZEST(11),JJ
        DIMENSION QUAD(4,11),TCHEB(11,4),SNSMAT(8,16),TLOAD(8),TBUFF(8),
       1GRAD(8),PWRDEN(11),SECVAR(200)
        COMMON NVALS,THRESH,L,C,PI,SQRT2,FORFLG,SLOPE,CURV,MAXSTP,
       1FREQ(11),XNEW(11,4),PNEW(11,4),XOLD(11,4),POLD(11,4),RCHAR(11),
       2NSTEPS,DIST2,CMIN,CMAX,WAVGDE,WIDTH,CAP(200),SWCHPT(200)
        NAMELIST/POLY/QUAD,TCHEB
        NAMELIST/CNTRL/SELFST,CONTIN,TYPOUT,MAXJMP,ITMAX,PUNCH
        NAMELIST/PARAMS/ WAVGDE,NVALS,LENGTH,MAXSTP,L,CMIN,CMAX,QCOST,
       1FREQM,BNDWTH,PWRDEN,ZSOURC,ZLOAD,VAR /WIDTH1/WIDTH
        NAMELIST /ZSTART/ZSTRT
        CALL MSGDP
C
C
C
C       SETUP CONSTANTS
        PI=3.141593
        SQRT2=SQRT(2.0)
        JJ=(0.0 , 1.0)
        NERRS=0
C
C
 76     READ(5,POLY,ERR=90)
        WRITE(6,123)
 123    FORMAT('1  QUADRATURE MATRIX = ',/)
        DO 79 I=1,4
 79     WRITE(6,130)(QUAD(I,J),J=1,11)
 130    FORMAT(1X,11F11.4)
        WRITE(6,103)
 103    FORMAT(/,'  SAMPLED TCHEBYCHEFF FUNCTIONS = ',/)
        DO 80 I=1,11
 80     WRITE(6,131)(TCHEB(I,J),J=1,4)
 131    FORMAT(1X,4F11.4)
C
C       BIGGEST LOOP OF ALL
 70     WRITE(6,144)
 144    FORMAT('1   ********  BEGIN NEW PROBLEM ******** ',//)
        READ(5,CNTRL,ERR=91,END=84)
C       READ IN PARAMETERS
 77     READ(5,PARAMS,ERR=92)
 11     WRITE(6,CNTRL)
        WRITE(6,PARAMS)
        IF(.NOT.WAVGDE)GO TO 83
 78     READ(5,WIDTH1)
        WRITE(6,WIDTH1)
        IF(L*CMIN*(2.*WIDTH*(FREQM-BNDWTH/2.))**2.GT.1.)GO TO 83
 55     WRITE(6,139)
 139    FORMAT(///,'  WAVEGUIDE IS TOO NARROW TO PROPAGATE REAL POWER AT
       1YOUR LOWEST FREQUENCY.  CHOOSE WIDER WAVEGUIDE TO GET ABOVE
       2CUTOFF.',//'  PROBLEM IS ABORTED.  WILL TRY NEXT PROBLEM....',///)
        GO TO 70
C
C
 83     DO 56 I=1,11
 56     FREQ(I)=FREQM+BNDWTH*((I-6.0)/10.)
C
C
```

```
      IF(SELFST)GO TO 72
      IF(CONTIN)GO TO 73
 86   READ(5,ZSTART,ERR=93)
 73   CONTINUE
      WRITE(6,ZSTART)
 54   DELTA=8.*QCOST/(LENGTH*(CMAX-CMIN)**2)
      THRESH=DELTA*(CMAX-CMIN)*(NVALS-2.)/(2.*NVALS-2.)
      THRSH2=.05*QCOST/(CMAX-CMIN)
      WRITE(6,143)DELTA,THRESH,THRSH2
 143  FORMAT(/,'  DELTA = ',E15.5,'      THRESH = ',E15.5,
     1'      THRSH2 = ',E15.5,/)
      ITER=0
      DO 30 I=1,4
      TLOAD(I)=0.
      TLOAD(I+4)=0.
      DO 30 J=1,11
      TLOAD(I)=TLOAD(I)+QUAD(I,J)*REAL(ZLOAD(J))
 30   TLOAD(I+4)=TLOAD(I+4)+QUAD(I,J)*AIMAG(ZLOAD(J))
      WRITE(6,110)(TLOAD(I),I=1,8)
 110  FORMAT('  TLOAD = ',8E15.6)
C
C
C
C     VERY BIG LOOP
 51   DO 31 I=1,11
 31   ZEST(I)=ZSTRT(I)
      WRITE(6,113)ITER
 113  FORMAT('1  ITERATION = ',I4)
      CALL TIMHMS(IH,IM,IS)
      IF(TYPOUT)WRITE(6,122)IH,IM,IS
 122  FORMAT('  HOURS = ',I4,3X,'MINUTES = ',I4,3X,'SECONDS = ',I4)
C
C
C     PASS ZERO
C
C
      PASS=0
      IF(TYPOUT)WRITE(6,109)
109   FORMAT(///,'  PASS ZERO',///)
      GO TO 60
 32   DO 33 I=1,4
      TBUFF(I)=0.
      TBUFF(I+4)=0.
      DO 33 J=1,11
      TBUFF(I)=TBUFF(I)+QUAD(I,J)*XNEW(J,4)/(SQRT2*XNEW(J,2))
 33   TBUFF(I+4)=TBUFF(I+4)+QUAD(I,J)*XNEW(J,3)/(SQRT2*XNEW(J,2))
      WRITE(6,111)(TBUFF(I),I=1,8)
 111  FORMAT(///,'  TBUFF = ',8F11.4,//)
C
C
C     PASS ONE
C
C
      DO 34 I=1,11
 34   ZEST(I)=ZSTRT(I)+VAR*TCHEB(I,1)
      IF(TYPOUT)WRITE(6,112)
 112  FORMAT(///,'  PASS ONE',///)
      GO TO 60
C
C
C     PASS TWO
C
C
```

```
 35    DO 36 I=1,11
 36    ZEST(I)=ZSTRT(I)+VAR*TCHEB(I,2)
       IF(TYPOUT)WRITE(6,114)
 114   FORMAT(///,'  PASS TWO',///)
       GO TO 60
C
C
C      PASS THREE
C
C
 37    DO 38 I=1,11
 38    ZEST(I)=ZSTRT(I)+VAR*TCHEB(I,3)
       IF(TYPOUT)WRITE(6,115)
 115   FORMAT(///,'  PASS THREE',///)
       GO TO 60
C
C
C      PASS FOUR
C
 39    DO 40 I=1,11
 40    ZEST(I)=ZSTRT(I)+VAR*TCHEB(I,4)
       IF(TYPOUT)WRITE(6,116)
 116   FORMAT(///,'  PASS FOUR',///)
       GO TO 60
 41    DO 42 I=1,11
 42    ZEST(I)=ZSTRT(I)+JJ*VAR*TCHEB(I,1)
C
C      PASS FIVE
       IF(TYPOUT)WRITE(6,117)
 117   FORMAT(///,'  PASS FIVE',///)
       GO TO 60
 43    DO 44 I=1,11
 44    ZEST(I)=ZSTRT(I)+JJ*VAR*TCHEB(I,2)
C
C      PASS SIX
       IF(TYPOUT)WRITE(6,118)
 118   FORMAT(///,'  PASS SIX',///)
       GO TO 60
 45    DO 46 I=1,11
 46    ZEST(I)=ZSTRT(I)+JJ*VAR*TCHEB(I,3)
C
C      PASS SEVEN
       IF(TYPOUT)WRITE(6,119)
 119   FORMAT(///,'  PASS SEVEN',///)
       GO TO 60
 47    DO 48 I=1,11
 48    ZEST(I)=ZSTRT(I)+JJ*VAR*TCHEB(I,4)
C
C      PASS EIGHT
       IF(TYPOUT)WRITE(6,120)
 120   FORMAT(///,'  PASS EIGHT',///)
       GO TO 60
C
C
C      MAIN SCAN DOWN THE LINE
C
 60    LOC=-LENGTH
       SUBCHPT(1)=LOC
       NSTEPS=1
       ICNT=0
       FORFLG=.TRUE.
       FORSGN=1.0
       CCSTQ=0.
```

```
      CMULT=0.
      DIST2=0.
      DO 1 I=1,11
      POLD(I,1)=1./(8.*REAL(ZSOURC(I)))
      POLD(I,2)=(REAL(ZSOURC(I))**2+AIMAG(ZSOURC(I))**2)/
     1(8.*REAL(ZSOURC(I)))
      POLD(I,3)=SQRT2*AIMAG(ZSOURC(I))/(8.*REAL(ZSOURC(I)))
      POLD(I,4)=-SQRT2/8.
      XOLD(I,4)=SQRT2*8.*PWRDEN(I)*REAL(ZSOURC(I))*REAL(ZEST(I))/
     1((REAL(ZSOURC(I)+ZEST(I)))**2+(AIMAG(ZSOURC(I)+ZEST(I)))**2)
      XOLD(I,3)=XOLD(I,4)*AIMAG(ZEST(I))/REAL(ZEST(I))
      XOLD(I,2)=XOLD(I,4)/(SQRT2*REAL(ZEST(I)))
      XOLD(I,1)=XOLD(I,2)*(REAL(ZEST(I))**2+AIMAG(ZEST(I))**2)
1     CMULT=CMULT+2.0*SQRT2*PI*FREQ(I)*(XOLD(I,3)*POLD(I,2)+
     1XOLD(I,1)*POLD(I,3))
      DO 24 I=1,11
      DO 24 J=1,4
      PNEW(I,J)=POLD(I,J)
24    XNEW(I,J)=XOLD(I,J)
      CALL VALUE(CMULT,NEWVAL)
      C=CMIN+((CMAX-CMIN)/(NVALS-1))*NEWVAL
      CAP(I)=C
      OLDVAL=NEWVAL
      DO 20 I=1,11
      IF(WAVGDE) GO TO 19
      T1=C
      GO TO 20
19    T1=C-1./(L*(2.*WIDTH*FREQ(I))**2)
20    RCHAR(I)=SQRT(L/T1)
      PWRREF=0.
      HAMILT=0.
      PWRNET=0.
      PWRAVL=0.
      DO 3 I=1,11
      DO 2 J=1,4
2     PWRREF=PWRREF+POLD(I,J)*XOLD(I,J)
      PWRAVL=PWRAVL+PWRDEN(I)
      PWRNET=PWRNET+XOLD(I,4)/(2.*SQRT2)
3     HAMILT=HAMILT+(C*(XOLD(I,3)*POLD(I,2)+XOLD(I,1)*POLD(I,3))-
     1L*(XOLD(I,3)*POLD(I,1)+XOLD(I,2)*POLD(I,3)))*FREQ(I)
      VSWR=(1.+SQRT(PWRREF/PWRAVL))/(1.-SQRT(PWRREF/PWRAVL))
      HAMILT=2.*SQRT2*PI*HAMILT-DELTA/2.*(C-CMAX/2.-CMIN/2.)**2
      ATTEN=10.*ALOG10(PWRAVL/PWRNET)
      IF((.NOT.TYPOUT).AND.(PASS.NE.0))GO TO 4
      WRITE(6,100)PWRAVL,PWRREF,PWRNET,VSWR,HAMILT,ATTEN
100   FORMAT(/,'  AVAIL. PWR =',F6.3,'   WATTS   REFLECTED PWR. = ',
     1F6.3,3X,'WATTS',3X,'NET POWER DELIVERED =',F6.3,3X,'WATTS',//,
     2'  EFFECTIVE VSWR = ',F10.4,' TO 1.',5X,'HAMILTONIAN = ',D13.4,3X,
     3'WATTS PER UNIT DISTANCE',//,' NET ATTENUATION = ',F10.4,' DB',/)
      WRITE(6,108)
      DO 18 I=1,11
      REALPT=XNEW(I,4)/(SQRT2*XNEW(I,2))
      IMAGPT=XNEW(I,3)/(SQRT2*XNEW(I,2))
18    WRITE(6,106) FREQ(I),REALPT,IMAGPT
      LOGICAL DUMP
      DOUBLE PRECISION OVAL,DINT
      NAMELIST/BARF/LOC,DIST,DIST2,CMULT,SLOPE,CURV,FORFLG,OLDVAL,
     1NEWVAL,NSTEPS,ICNT,OVAL,DINT,ERR,TOL
      NAMELIST/FRAB/OLDVAL,NEWVAL
      NAMELIST/BLAH/CMULT,SLOPE,CURV,DIST,LOC,NSTEPS,OLDVAL,NEWVAL,
     1DIST2,ICNT,OVAL,DINT,ERR,TOL,FORFLG
C
C
```

```
C
C      MAIN LOOP
C      DECIDE HOW FAR TO STEP
 4     CALL DIST1(CMULT,LOC,DIST,LENGTH)
       IF(CAP(NSTEPS).EQ.CAP(NSTEPS-1))WRITE(6,BLAH)
       IF(ABS(DIST)-10.**(-5))5,5,6
C      SWITCH TO DIFFERENT CAPACITY INTERVAL
 5     CALL SWITCH(CMULT,LOC,DIST,NEWVAL)
       IF(LOC.EQ.0.)GO TO 10
       FORSGN=1.D
       IF(NSTEPS.LT.200)GO TO 59
       WRITE(6,147)
 147   FORMAT(/,'  YOU HAVE MORE THAN 200 SWITCHINGS IN THE LINE AND
      1ARRAYS ARE OVERFLOWING.',/,' DECLARE A COARSER GRID ON AVAILABLE
      2CAPACITIES.',//,' PROBLEM IS ABORTED. WILL READ NEXT PROBLEM.',//)
       GO TO 70
 59    VAR2=0.
       DUMP=.FALSE.
       DO 16 I=1,11
 16    VAR2=VAR2+(FREQ(I)**3*(XNEW(I,1)*PNEW(I,3)+XNEW(I,3)*PNEW(I,2)))
       SECVAR(NSTEPS)=-16*SQRT2*PI**3*L*VAR2
       COSTQ=COSTQ+(SWCHPT(NSTEPS)-SWCHPT(NSTEPS-1))*DELTA/2.*
      1(CAP(NSTEPS-1)-CMAX/2.-CMIN/2.)**2
       OLDVAL=NEWVAL
       ICNT=0
       IF(ABS(SLOPE)-.01*THRESH/LENGTH)57,57,69
 69    IF((THRESH.NE.0).OR.(ABS(SLOPE).GT.THRSH2/LENGTH))GO TO 6
 57    WRITE(6,140)
 140   FORMAT(///,'  YOU ARE ATTEMPTING TO ITERATE ALONG A SINGULAR
      1EXTREMAL TRAJECTORY.IT IS UNSTABLE AND YOU HAVE ',/,'  NO HOPE OF
      2CONVERGENCE.  CHANGE YOUR CAPACITY CONSTRAINT SET AND TRY AGAIN.',
      3//,'  PROBLEM IS ABORTED. WILL TRY NEXT PROBLEM.... ',///)
       GO TO 70
 6     LOC=LOC+DIST
       DIST2=DIST2+DIST
C      PROPAGATE STATE AND COSTATE DOWN LINE BY DISTANCE 'DIST'
 9     CALL STEP(DIST2,CMULT)
       ICNT=ICNT+1
       IF(ICNT.GT.20)DUMP=.TRUE.
       IF(ICNT.GT.30)WRITE(6,148)
 148   FORMAT(/,' HANGUP - MORE THAN 30 ITERATIONS ON A SINGLE
      1SWITCHPOINT.',/)
       IF(ICNT.GT.30)GO TO 70
       IF(THRESH.NE.0)GO TO 88
       IF((ABS(CMULT).LE.THRSH2).AND.(ABS(CMULT+SLOPE*LENGTH).LE.THRSH2))
      1GO TO 5
       IF((-CMULT*FORSGN/SLOPE).LT.0)GO TO 58
       IF(-CMULT*FORSGN/SLOPE-1DE-5)5,5,58
 88    DVAL=1.0D0+(-1.0D0+NVALS/2.0D0)*(1.0D0+(DBLE(CMULT)+10.D0-5*
      1ABS(SLOPE))/THRESH)
       IF(DVAL.LT.1.0D0)GO TO 58
       IF(DVAL.GT.(NVALS-.5D0))GO TO 58
       DINT=IDINT(DVAL)
       ERR=DVAL-DINT
       TOL=(NVALS-2.D)*10.0E-5*ABS(SLOPE)/THRESH
       IF(ERR.LE.TOL)GO TO 5
 58    IF(DUMP)WRITE(6,BARF)
       CALL VALUE(CMULT,NEWVAL)
C      CHECK FOR END OF LINE
       IF((LOC .EQ. 0.) .AND. (NEWVAL .EQ. OLDVAL)) GO TO 10
       IF(IABS(NEWVAL-OLDVAL)-1) 7,7,8
C      OVERSHOT TWO OR MORE SWITCHPOINTS-BACK UP
 8     DIST=DIST/2.
```

```
      LCC=LOC-DIST
      DIST2=DIST2-DIST
      GO TO 9
C     IF NEWVAL .NE. OLDVAL, OVERSHOT SHITCHPT-START BACK
 7    IF(NEWVAL.EQ.OLDVAL)GO TO 89
      FORFLG=.NOT.FORFLG
      FORSGN=-FORSGN
 89   IF(DUMP)WRITE(6,FRAB)
      OLDVAL=NEWVAL
      GO TO 4
C
C
C     FINISHED WITH A SCAN DOWN THE LINE
C
 10   IF(.NOT.TYPOUT)GO TO 75
      WRITE(6,107)
 107  FORMAT(/,'  LOCATION              CAPACITY',/)
      DO 12 I=1,NSTEPS
 12   WRITE(6,105)SWCHPT(I),CAP(I)
 105  FORMAT(1X,F10.6,8X,E15.4)
      HAMILT=0.
      DO 74 I=1,11
 74   HAMILT=HAMILT+(C*(XNEW(I,3)*PNEW(I,2)+XNEW(I,1)*PNEW(I,3))-
     1L*(XNEW(I,3)*PNEW(I,1)+XNEW(I,2)*PNEW(I,3)))*FREQ(I)
      HAMILT=2.*SQRT2*PI*HAMILT-DELTA/2.*(C-CMAX/2.-CMIN/2.)**2
      WRITE(6,128)HAMILT
 128  FORMAT('  HAMILTONIAN = ',E10.5)
      WRITE(6,108)
 108  FORMAT(3X,'FREQUENCY',10X,'REAL PT.',8X,'IMAG. PT.',/)
      DO 17 I=1,11
      REALPT=XNEW(I,4)/(SQRT2*XNEW(I,2))
      IMAGPT=XNEW(I,3)/(SQRT2*XNEW(I,2))
 17   WRITE(6,106) FREQ(I),REALPT,IMAGPT
 106  FORMAT(1X,E12.4,8X,F10.5,6X,F10.5)
 75   COSTQ=COSTQ-SWCHPT(NSTEPS)*DELTA/2.*(CAP(NSTEPS)-CMAX/2.-CMIN/2.)
     1**2
      IF(TYPOUT.OR.(PASS.EQ.0))WRITE(6,124)COSTQ
 124  FORMAT(/,'  COST ASSOCIATED WITH QUADRATIC CAPACITY TERM = ',
     1F8.4,'   WATTS',/)
      IF(PASS)63,62,63
 63   DO 65 I=1,4
      SNSMAT(I,PASS)=0.
      SNSMAT(I+4,PASS)=0.
      DO 61 J=1,11
      SNSMAT(I,PASS)=SNSMAT(I,PASS)+QUAD(I,J)*XNEW(J,4)/(SQRT2*XNEW(J,2)
     1)
 61   SNSMAT(I+4,PASS)=SNSMAT(I+4,PASS)+QUAD(I,J)*XNEW(J,3)/(SQRT2*
     1XNEW(J,2))
 65   CONTINUE
      IF(TYPOUT)WRITE(6,121)(SNSMAT(I,PASS),I=1,8)
 121  FORMAT(//'  TEST = ',8F11.5,//)
      DO 64 I=1,4
      SNSMAT(I,PASS)=(SNSMAT(I,PASS)-TBUFF(I))/VAR
 64   SNSMAT(I+4,PASS)=(SNSMAT(I+4,PASS)-TBUFF(I+4))/VAR
      IF(.NOT.TYPOUT)GO TO 62
      WRITE(6,133)PASS,(SNSMAT(I,PASS),I=1,8)
 133  FORMAT('  SENSMAT(I,',I2,') = ',8F11.5)
 62   PASS=PASS+1
      GO TO (32,35,37,39,41,43,45,47,53),PASS
C
C
C     FINISHED WITH AN ENTIRE 9-PASS ITERATION
C
```

```
 53   CONTINUE
      WRITE(6,134)
 134  FORMAT(//,'  SENSMAT = ',/)
      DO 66 I=1,8
 66   WRITE(6,104)(SNSMAT(I,J),J=1,8)
 104  FORMAT(1X,8F11.5)
      CALL MATINV(SNSMAT,8,16)
      WRITE(6,135)
 135  FORMAT(/,'  (SENSMAT)**-1 = ',/)
      DO 67 I=1,8
 67   WRITE(6,104)(SNSMAT(I,J),J=9,16)
      DO 49 I=1,8
      GRAD(I)=0.
      DO 49 J=1,8
 49   GRAD(I)=GRAD(I)+SNSMAT(I,J+8)*(TLOAD(J)-TBUFF(J))
      WRITE(6,136)
 136  FORMAT(/,'  GRADIENT VECTOR = ',/)
      WRITE(6,104)(GRAD(I),I=1,8)
      ITER=ITER+1
      MAG=0.
      DO 87 I=1,8
 87   MAG=MAG+GRAD(I)**2
      MAG=SQRT(MAG)
      IF(MAG.GT.MAXJMP)STPSZE=MAXJMP/MAG
      IF(MAG.LE.MAXJMP)STPSZE=1.0
      DO 50 I=1,11
      DO 50 J=1,4
 50   ZSTRT(I)=ZSTRT(I)+(GRAD(J)*TCHEB(I,J)+JJ*GRAD(J+4)*TCHEB(I,J))*
     1STPSZE
      WRITE(6,137) STPSZE
 137  FORMAT(/,'  STEPSIZE MULTIPLIER = ',F8.4)
      WRITE(6,101)
 101  FORMAT(/,'  LOCATION            CAPACITY           2ND VARIATION',/)
      WRITE(6,102)(SWCHPT(I),CAP(I),SECVAR(I),I=1,NSTEPS)
 102  FORMAT(1X,F10.6,8X,E15.4,5X,E15.4)
      IF(MAG.LT.10.E-2*MAXJMP)GO TO 27
      IF(ITER.LE.ITMAX) GO TO 51
C
C
C     DONE WITH THE ENTIRE PROBLEM-PUNCH,THEN READ ANOTHER.
C
C
 52   CONTINUE
      WRITE(6,145)
 145  FORMAT(//,'  THIS PROBLEM IS FINISHED ... WILL READ THE NEXT
     1PROBLEM ... ',//)
      IF(.NOT.PUNCH) GO TO 70
      SELFST=.FALSE.
      CONTIN=.FALSE.
      WRITE(7,CNTRL)
      WRITE(7,PARAMS)
      IF(WAVGDE)WRITE(7,WIDTH1)
      WRITE(7,ZSTART)
      GO TO 70
C
C
C     ITERATION HAS CONVERGED
C
 27   WRITE(6,146)
 146  FORMAT(//,'  THIS ITERATION HAS CONVERGED... WILL READ THE NEXT
     1PROBLEM ... ',//)
      GO TO 70
C
```

```
C
C       SELF-STARTUP PROCEDURE
 72     CONTINUE
        C=CMIN
        DO 13 I=1,11
        XOLD(I,4)=1.
        XOLD(I,3)=AIMAG(ZLOAD(I))/REAL(ZLOAD(I))
        XOLD(I,2)=1./(SQRT2*REAL(ZLOAD(I)))
        XOLD(I,1)=XOLD(I,2)*(REAL(ZLOAD(I))**2+AIMAG(ZLOAD(I))**2)
        IF(WAVGDE) GO TO 14
        T1=C
        GO TO 13
 14     T1=C-1./(L*(2.*WIDTH*FREQ(I))**2)
 13     RCHAR(I)=SQRT(L/T1)
        DIST2=-LENGTH
        CALL STEP(DIST2,CMULT)
        DO 15 I=1,11
 15     ZSTRT(I)=(1.D+JJ*XNEW(I,3))/(SQRT2*XNEW(I,2))
        GO TO 73
C
C
C       ERROR DIAGNOSTICS FOR READ
C
 90     WRITE(6,129)
 129    FORMAT('  ERROR WHILE READING DATASET /POLY/')
        GO TO 71
 91     WRITE(6,125)
 125    FORMAT('  ERROR WHILE READING DATASET /CNTRL/')
        READ(6,PARAMS,ERR=92)
        NERRS=NERRS+1
        IF(NERRS.GE.4)GO TO 71
        GO TO 70
 92     WRITE(6,126)
 126    FORMAT('  ERROR WHILE READING DATASET /PARAMS/')
        NERRS=NERRS+1
        IF(NERRS.GE.4)GO TO 71
        GO TO 70
 93     WRITE(6,127)
 127    FORMAT('  ERROR WHILE READING DATASET /ZSTART/')
        NERRS=NERRS+1
        IF(NERRS.GE.4)GO TO 71
        GO TO 70
C
C
C       FINAL EXIT
C
 71     CONTINUE
 84     WRITE(6,138)
 138    FORMAT(///,'   ******      THATS ALL FOLKS    *****',///)
C
C
C
        STOP
        END
```

```
      SUBROUTINE DIST1(CMULT,LOC,DIST,LENGTH)
      COMMON NVALS,THRESH,L,C,PI,SQRT2,FORFLG,SLOPE,CURV,MAXSTP,
     1FREQ(11),XNEW(11,4),PNEW(11,4)
      REAL L,LENGTH,LOC,MAXSTP
      LOGICAL FORFLG
C     FLAG TO SCAN FORWARD
      IF(FORFLG) FORSGN=1.
C     ELSE SCAN BACKWARD
      IF(.NOT. FORFLG) FORSGN=-1.
      SLOPE=0.
      CURV=0.
      Y5=0.
      Y6=0.
      DO 1 I=1,11
      SLOPE=SLOPE+(XNEW(I,1)*PNEW(I,1)-XNEW(I,2)*PNEW(I,2))*FREQ(I)**2
    1 CURV=CURV+(L*(XNEW(I,2)*PNEW(I,3)+XNEW(I,3)*PNEW(I,1))+C*
     1(XNEW(I,1)*PNEW(I,3)+XNEW(I,3)*PNEW(I,2)))*FREQ(I)**3
      SLOPE=8.*PI**2*L*SLOPE
      CURV=-16*PI**3*L*SQRT2*CURV
C
C
C
      IF(NVALS.LT.3 .OR. THRESH.EQ.0.0) GO TO 12
      IF(CMULT-THRESH) 2,2,3
C     CMULT ABOVE THRESHOLD REGION
    3 Y7=CMULT-THRESH
      GO TO 5
    2 IF(CMULT+THRESH)18,7,7
C     CMULT BELOW THRESH. REGION
   18 Y7=CMULT+THRESH
      GO TO 5
C     CMULT INSIDE THRESH REGION
C
C
C
    7 Y7=0.
      T3=2.*THRESH/(NVALS-2.)
      T2=CMULT*(NVALS-2.)/(2.*THRESH)+NVALS/2.0-INT(CMULT*(NVALS-2.)/
     1(2.*THRESH)+NVALS/2.0)
      IF(SLOPE*FORSGN)22,23,23
   22 Y5=T2*T3
      GO TO 24
   23 Y5=(1.0-T2)*T3
   24 IF(CURV)25,26,26
   25 Y6=T2*T3
      GO TO 27
   26 Y6=(1.0-T2)*T3
   27 CONTINUE
      T1=Y6
C     LINEAR EXTRAPOLATION
      Y2=FORSGN*Y5/ABS(SLOPE)
      GO TO 13
C
C
C
C     ONLY TWO CAPACITY VALUES
   12 Y7=CMULT
    5 T1=ABS(Y7)
      IF(Y7*SLOPE*FORSGN)8,10,10
   10 Y2=FORSGN*MAXSTP
      GO TO 9
C     LINEAR EXTRAPOLATION
    8 Y2=-Y7/SLOPE
```

```
 9     IF(Y7*CURV)13,11,11
 11    Y1=FORSGN*MAXSTP
       GO TO 14
C      QUADRATIC EXTRAPOLATION
 13    Y1=-SLOPE/CURV+FORSGN/ABS(CURV)*SQRT(SLOPE**2+2.*ABS(CURV)*T1)
C      PICK SMALLER OF TWO STEPS
 14    IF(ABS(Y1)-ABS(Y2))15,15,16
 16    DIST=Y2
       GO TO 17
 15    DIST=Y1
C      TRUNCATE IF STEP IS TOO LARGE
 17    IF(ABS(DIST).GT.MAXSTP) DIST=FORSGN*MAXSTP
C      TRUNCATE IF ROUNDOFF ERRORS GIVE WRONG SIGN
       IF(FORSGN*DIST.LT. 0.0) DIST=0.0
C      CHECK FOR RUNNING OFF END OF LINE
       IF((LOC+DIST .GT. 0.0).AND.FORFLG) DIST=-LOC
C      CHECK FOR RUNNING OFF BEGINNING OF LINE
       IF((LOC+DIST .LT. -LENGTH).AND..NOT.FORFLG) DIST=-LENGTH-LOC
C
C
C
       RETURN
       END




       SUBROUTINE STEP(DIST2,CMULT)
       COMMON NVALS,THRESH,L,C,PI,SQRT2,FORFLG,SLOPE,CURV,MAXSTP,
      1FREQ(11),XNEW(11,4),PNEW(11,4),XOLD(11,4),POLD(11,4),RCHAR(11)
       DOUBLE PRECISION TD1,TD2,TD3,TD4,THETA
       LOGICAL FORFLG
       REAL L,MAXSTP
       CMULT=0.
       SLOPE=0.
       DO 1 I=1,11
       THETA=4.*PI*DIST2*L*FREQ(I)/RCHAR(I)
       TD1=DSIN(THETA)
       TD2=DCOS(THETA)
       TD3=1.+TD2
       TD4=1.-TD2
       TS2=RCHAR(I)/SQRT2
       TS1=TS2**2
       TS4=1./(RCHAR(I)*SQRT2)
       TS3=TS4**2
       XNEW(I,1)=.5*TD3*XOLD(I,1)+TS1*TD4*XOLD(I,2)-TS2*TD1*XOLD(I,3)
       XNEW(I,2)=TS3*TD4*XOLD(I,1)+.5*TD3*XOLD(I,2)+TS4*TD1*XOLD(I,3)
       XNEW(I,3)=TS4*TD1*XOLD(I,1)-TS2*TD1*XOLD(I,2)+TD2*XOLD(I,3)
       PNEW(I,1)=.5*TD3*POLD(I,1)+TS3*TD4*POLD(I,2)-TS4*TD1*POLD(I,3)
       PNEW(I,2)=TS1*TD4*POLD(I,1)+.5*TD3*POLD(I,2)+TS2*TD1*POLD(I,3)
       PNEW(I,3)=TS2*TD1*POLD(I,1)-TS4*TD1*POLD(I,2)+TD2*POLD(I,3)
       SLOPE=SLOPE+(XNEW(I,1)*PNEW(I,1)-XNEW(I,2)*PNEW(I,2))*FREQ(I)**2
 1     CMULT=CMULT+2.*SQRT2*PI*FREQ(I)*(XNEW(I,3)*PNEW(I,2)+
      1XNEW(I,1)*PNEW(I,3))
       SLOPE=8.*PI**2*L*SLOPE
C
C
C
       RETURN
       END
```

```
      SUBROUTINE SWITCH(CMULT,LOC,DIST,NEWVAL)
      COMMON NVALS,THRESH,L,C,PI,SQRT2,FORFLG,SLOPE,CURV,MAXSTP,
     1FREQ(11),XNEW(11,4),PNEW(11,4),XOLD(11,4),POLD(11,4),RCHAR(11),
     2NSTEPS,DIST2,CMIN,CMAX,WAVGDE,WIDTH,CAP(200),SWCHPT(200)
      NAMELIST/FOOVAR/SLOPE,CURV,DIST,NEWVAL,T1,NSTEPS,LOC,C,CMULT
      REAL L,LOC,MAXSTP
      LOGICAL WAVGDE,FORFLG
      IF(THRESH*(NVALS-2))1,1,2
    1 IF(SLOPE)3,3,4
    3 NEWVAL=0
      GO TO 5
    4 NEWVAL=NVALS-1
      GO TO 5
C     MAP THRESHOLD REGION INTO (0,1)
    2 T1=(CMULT/THRESH+1.)/2.
      NEWVAL=INT(1.+(NVALS-2)*T1+.5*SIGN(1.0,SLOPE))
      IF(NEWVAL.LT.0)NEWVAL=0
      IF(NEWVAL.GT.NVALS-1)NEWVAL=NVALS-1
    5 NSTEPS=NSTEPS+1
      SWCHPT(NSTEPS)=LOC
      FORFLG=.TRUE.
      DIST2=0.
      C=CMIN+((CMAX-CMIN)/(NVALS-1))*NEWVAL
      CAP(NSTEPS)=C
      CURV=0.
      DO 8 I=1,11
      IF(WAVGDE) GO TO 6
      T2=C
      GO TO 7
    6 T2=C-1./(L*(2.*WIDTH*FREQ(I))**2)
    7 RCHAR(I)=SQRT(L/T2)
    8 CURV=CURV+(L*(XNEW(I,2)*PNEW(I,3)+XNEW(I,3)*PNEW(I,1))+C*
     1(XNEW(I,1)*PNEW(I,3)+XNEW(I,3)*PNEW(I,2)))*FREQ(I)**3
      CURV=-16.*PI**3*L*SQRT2*CURV
C
C
C
      IF(THRESH*(NVALS-2).EQ.0.0) GO TO 13
      IF(NEWVAL*(NEWVAL+1-NVALS))9,13,13
C     OUTSIDE THRESHOLD REGION
   13 IF(SLOPE*CURV)10,11,11
   10 DIST=-2.*SLOPE/CURV
      GO TO 12
   11 DIST=MAXSTP
      GO TO 12
C     INSIDE THRESHOLD REGION
    9 DIST=2.0*THRESH/((NVALS-2)*ABS(SLOPE))
   12 IF(ABS(DIST).GT.MAXSTP) DIST=MAXSTP
      IF((LOC+DIST).GT. 0.0) DIST=-LOC
      DO 14 I=1,11
      DO 14 J=1,4
      XOLD(I,J)=XNEW(I,J)
   14 POLD(I,J)=PNEW(I,J)
      IF(CAP(NSTEPS).EQ.CAP(NSTEPS-1))WRITE(6,FOOVAR)
      RETURN
      END
```

```
      SUBROUTINE VALUE(CMULT,NEWVAL)
      COMMON NVALS,THRESH
      IF(THRESH*(NVALS-2))6,6,7
 7    T1=(CMULT/THRESH+1.)/2.
      GO TO 8
 6    T1=SIGN(2.0,CMULT)
 8    IF(T1)1,1,2
 1    NEWVAL=0
      GO TO 3
 2    IF(T1-1.)4,4,5
 5    NEWVAL=NVALS-1
      GO TO 3
 4    NEWVAL=INT((NVALS-2)*T1+1.)
 3    CONTINUE
C
C
C
      RETURN
      END
```

```
      SUBROUTINE MATINV(M,ROWS,COLS)
      INTEGER ROWS,COLS
      INTEGER C(11)
      REAL M(ROWS,COLS),T2(22)
C     ENTER WITH M(I,J),I=1 TO ROWS, J=1 TO ROWS
      DO 1 I=1,ROWS
C     ADJOIN IDENTITY MATRIX
      C(I)=I
      IRP1=ROWS+1
      DO 1 J=IRP1,COLS
      IF(J-I-ROWS)2,3,2
 2    M(I,J)=0.
      GO TO 1
 3    M(I,J)=1.
 1    CONTINUE
C
C
C
C     GAUSS REDUCTION ON EACH ROW
      DO 10 K=1,ROWS
C     FIND MAX ABS ELEMENT AVAILABLE FOR REDUCTION
      ABSMAX=0.
      DO 5 I=1,ROWS
      DO 5 J=1,ROWS
      IF(C(I))5,5,6
 6    IF(C(J))5,5,7
 7    IF(ABS(M(I,J))-ABSMAX)5,5,8
 8    ABSMAX=ABS(M(I,J))
      IMAX=I
      JMAX=J
 5    CONTINUE
C
C
C
      C(JMAX)=0
      T1=M(IMAX,JMAX)
C     SWAP ROWS-MAX ABS. ELEMENT ONTO DIAGONAL
      DO 9 J=1,COLS
      T2(J)=M(IMAX,J)
      M(IMAX,J)=M(JMAX,J)
 9    M(JMAX,J)=T2(J)/T1
C     GAUSS REDUCTION ON COLUMN JMAX
      DO 10 I=1,ROWS
      IF(I-JMAX)11,10,11
 11   T1=M(I,JMAX)
      DO 10 J=1,COLS
      M(I,J)=M(I,J)-T1*M(JMAX,J)
 10   CONTINUE
C
C
C
      RETURN
C     LEAVE WITH M(I,J),I=1 TO ROWS, J=ROWS+1 TO COLS
C
C
C
      END
```

DOCUMENT CONTROL DATA - R&D

(Security classification of title, body of abstract and indexing annotation must be entered when the overall report is classified)

1. ORIGINATING ACTIVITY (Corporate author)	2a. REPORT SECURITY CLASSIFICATION
Lincoln Laboratory, M.I.T.	Unclassified
	2b. GROUP: None

3. REPORT TITLE

Design of Transmission Lines and Waveguide Structures Using the Maximum Principle

4. DESCRIPTIVE NOTES (Type of report and inclusive dates)

Technical Report

5. AUTHOR(S) (Last name, first name, initial)

Burchfiel, Jerry

6. REPORT DATE	7a. TOTAL NO. OF PAGES	7b. NO. OF REFS
6 June 1968	114	32

8a. CONTRACT OR GRANT NO.	9a. ORIGINATOR'S REPORT NUMBER(S)
AF 19(628)-5167	Technical Report 440
b. PROJECT NO. ARPA Order 198	
c.	9b. OTHER REPORT NO(S) (Any other numbers that may be assigned this report)
d.	ESD-TR-68-177

10. AVAILABILITY/LIMITATION NOTICES

This document has been approved for public release and sale; its distribution is unlimited

11. SUPPLEMENTARY NOTES	12. SPONSORING MILITARY ACTIVITY
None	Advanced Research Projects Agency, Department of Defense

13. ABSTRACT

A distributed parameter maximum principle provides the basis for design of optimal lossless impedance matching structures. Given an arbitrary (wide-band) source at $z = -\ell$ and an arbitrary load at $z = 0$, the optimization procedure synthesizes a uniform cross section, dielectric loaded waveguide or transmission line of length ℓ which maximizes the real power delivered to the load.

This optimization is performed subject to constraints on the filler material: $\mu(z) \equiv \mu_0$ and $\epsilon(z)$ is in $\{\epsilon_1, \epsilon_2, \ldots \epsilon_n\}$. The solution is easily implemented, as the filler consists of successive intervals of readily available dielectric materials.

An iterative numerical procedure for solving the (split-boundary function) necessary conditions is given, and a number of typical solutions for transmission line and waveguide couplers are presented. In the examples studied, the performance obtained using only ϵ_{MIN} and ϵ_{MAX} was within 0.2 percent of that obtained using a continuum of dielectric constants $[\epsilon_{MIN}, \epsilon_{MAX}]$.

14. KEY WORDS

transmission lines
waveguide structures
distributed parameter maximum principle
phased arrays
Maximum Principle of Pontryagin